Report Rapport

Atomic Energy
Control Board

Commission de contrôle
de l'énergie atomique

Atomic Energy Control Board
P.O. Box 1046
Ottawa, Canada
K1P 5S9

Commission de contrôle de l'énergie atomique
C.P. 1046
Ottawa, Canada
K1P 5S9

RESEARCH REPORT

INFO-0111

THE PERMEABILITY OF CONCRETE FOR REACTOR CONTAINMENT VESSELS

by

R.H. Mills
University of Toronto

A research report prepared for the
Atomic Energy Control Board
Ottawa, Canada

July 1983

THE PERMEABILITY OF CONCRETE FOR REACTOR CONTAINMENT VESSELS

ABSTRACT

Review of the literature pertaining to water, water vapour and gas transmission through concrete revealed conflicting views on the mechanisms involved and the influence of mix design parameters such as initial porosities and water/cement ratio. Consideration of the effects of ageing and of construction defects in field concrete were totally neglected in published work.

Permeability data from three published papers were compared with permeability calculated according to Powers [Ref. 1]. The ratio of calculated to observed permeability varied from 40×10^{-3} to 860×10^{-3} for one group; from 0.17×10^{3} to 8.6×10^{3} in the second; and from 24×10^{3} to 142×10^{3} for the third. There were therefore wide discrepancies within each group of data and between groups.

A bibliography was prepared and an exploratory experimental programme was mounted to determine the relative importance of key parameters such as cement type, porosity and water/cement ratio.

Contrary to frequently cited references it was found that permeability of concrete was not significantly influenced by water/cement ratio when the starting porosity was constant. If water/cement ratio was held constant, however, the permeability was strongly influenced by starting porosity. It was also found that with constant water/cement ratio permeability increased with cement content.

The value of Fly Ash and Blastfurnace slag in partial substitution for Portland cement is neglected in the literature but it is important since such substitutions alleviate alkali-silicate reactions. Permeability of concrete was significantly decreased by partial substitution of Portland cement with Fly Ash but there was no benefit in the use of Blastfurnace slag.

DISCLAIMER

'The Atomic Energy Control Board is not responsible for the accuracy of the statements made or opinions expressed in this publication and neither the Board nor the author assume liability with respect to any damage or loss incurred as a result of the use made of the information contained in this publication'.

PERMÉABILITÉ DU BÉTON POUR ENCEINTE DE CONFINEMENT DU RÉACTEUR

RÉSUMÉ

L'examen de la documentation concernant la transmission d'eau, de vapeur d'eau et de gaz à travers le béton a fait ressortir des opinions contradictoires quant aux mécanismes en cause et à l'influence des paramètres de formule de mélange, tels que les porosités initiales et le rapport entre l'eau et le ciment. Dans les ouvranges publiés, on n'a pas tenu compte des effets du vieillissement et des défauts de construction relatifs au béton coulé in situ.

On a comparé les données liées à la perméabilité recueillies dans trois études publiées à la perméabilité calculée selon Powers [ref. 1]. Le rapport entre perméabilité calculée et perméabilité observée variait entre 40×10^{-3} et 860×10^{-3} pour un groupe; entre $0,17 \times 10^{3}$ et $8,6 \times 10^{3}$ pour un autre; et entre 24×10^{3} et 142×10^{3} pour un troisième. On a donc observé des écarts importants à l'intérieur de chaque groupe de données ainsi qu'entre les groupes.

On a alors préparé une bibliographie et mis sur pied un programme expérimental d'exploration afin de déterminer l'importance relative des paramètres clefs tels que le type de ciment, la porosité et le rapport entre l'eau et le ciment.

On a trouvé que la perméabilité du béton n'était pas influencée de manière importante par le rapport entre l'eau et le ciment lorsque la porosité de départ était constante, bien que des références fréquemment citées contredisent cette affirmation. Si, toutefois, le rapport entre l'eau et le ciment était constant, la perméabilité était fortement influencée par la porosité initiale. On a trouvé, en outre, qu'avec un rapport entre l'eau et le ciment constant, la perméabilité augmentait avec la teneur en ciment.

L'utilité de cendres volantes et de scories de haut fourneau substituées partiellement au ciment de Portland, a été ignorée dans la documentation disponible, mais il faut en tenir compte étant donné que de telles substitutions diminuent les réactions alcali-silicate. On a pu diminuer de beaucoup la perméabilité du béton en substituant partiellement des cendres volantes au ciment de Portland, mais on n'a trouvé aucun avantage à utiliser des scories de haut fourneau.

TABLE OF CONTENTS

ABSTRACT.. i

RÉSUMÉ.. ii

TABLE OF CONTENTS... iii

LIST OF TABLES.. v

LIST OF FIGURES... vi

LIST OF MICROGRAPHS... vii

LIST OF SYMBOLS... x

1. INTRODUCTION... 1

2. THE NATURE OF CONCRETE....................................... 4

2.1 Porosity and Pore Size Distribution......................... 5

2.2 Mass Transfer Across a Concrete Barrier..................... 6

2.3 Models for Mass Transfer.................................... 8

2.3.1 Water... 8

2.3.2 Water vapour.. 8

2.4 The Barrier in a Reactor Building........................... 11

3. EXPERIMENTAL WORK.. 12

3.1 Concrete Mixes.. 12

3.2 Cement Paste Specimens...................................... 13

3.3 Water Permeability.. 13

3.3.1 Results of water permeability tests....................... 15

3.3.2 Discussion of water permeability tests.................... 19

3.3.3 Porosity.. 19

3.4 Water Vapour Permeance and Diffusion........................ 20

3.4.1 Specimen conditioning..................................... 22

3.4.2 Simulated mass curing treatment (a)....................... 23

3.4.3 Simulated mass curing after 24 hours (b).................. 25

3.4.4 Variable free water content............................... 27

TABLE OF CONTENTS

3.4.5 Blank tests.. 29

3.5 Gas Permeation.. 29

3.6 Cementing Properties of Blastfurnace Slag and Fly Ash....... 29

4. MICROSCOPIC EXAMINATION.................................. 30

4.1 Pore Structure from Micrographs............................. 30

4.2 The Present Study.. 31

4.3 Discussion.. 32

5. DISCUSSION.. 70

5.1 General.. 70

5.2 Tentative Conclusions.. 70

6. REFERENCES.. 72

APPENDICES:

VOLUME DISTRIBUTION OF PHASES IN CONCRETE APPENDIX A

ESTIMATION OF WATER PERMEABILITY OF CONCRETE APPENDIX B

DRYING AS A DIFFUSION-CONTROLLED PROCESS APPENDIX C

BIBLIOGRAPHY APPENDIX D

LIST OF TABLES

Table	Subject	Page
1	Perspective on widely quoted data from Technical Memorandum No. 6-380 of the U.S. Waterways Experimental Station	2
2	Isolation of Mix Design Parameters in Concrete Mixes	13
3	Summary of Water Permeability Tests	15
4	Comparison of Various Equations for Water Permeability Coefficient K	18
5	Differential Absorption of Methanol and Water	20
6	Schedule of Treatments	22
7	WVT of Mass Cured Specimens with Variable Porosity	23
8	Specimens with Variable water:cement ratio	24
9	Specimens with Fixed Initial Porosity and Variable Blastfurnace Slag Content	25
10	Specimens with Constant Porosity and Variable Fly Ash Content	25
11	Specimens with Constant Water:cement Ratio = 0.42	26
12	Constant Initial Porosity $\varepsilon = 0.230$ and Variable Water:cement Ratio w_o	26
13	Specimens with Blastfurance Slag	27
14	Specimens with Fly Ash Substitution for Portland Cement	27
15	Permeability with Variable Water Content	28
16	Hydraulic Factor	30
16	Pore radii as Determined by Electron Microscopy and Mercury Intrusion Porosimetry	31

LIST OF FIGURES

Figure	Title	Page
1	Distribution of solids and mobile water at terminal hydration, $\alpha = \alpha_\infty$.	6
2	Variation in pressure across a concrete barrier separating liquid water under pressure with air at relative humidity less than 100 per cent.	7
3	Model pore system	9
4	Water Permeability Apparatus	14
5	Results of water permeability tests for flow parallel to and at right angles to the direction of bleeding	16
6	Permeability as a function of confining stress for porosity $\varepsilon = 0.15$	17
7	Two part dry cup apparatus for water vapour transmission	21
8	Mass transfer of water by drying of specimen (lower curve) and by condensation and evaporation (upper curve)	21

LIST OF MICROGRAPHS

PORTLAND CEMENT SPECIMENS

Figure	Series	Caption	Page
9	A	09 05 01 Low magnification view of fracture surface* showing bleeding cavity partly filled with Calcium Hydroxide precipitated out of solution.	33
10	A	09 05 03 Close-up of bleeding cavity.	34
11	A	09 05 05 Close-up of Calcium Hydroxide precipitated out of solution.	35
12	A	09 05 11 Low magnification of fracture surface showing shrinkage crack.	36
13	A	09 05 12 Ettringite crystals on crack walls.	37
14	A	09 05 08 Ettringite crystals.	38
15	A	09 19 43 Typical fracture surface showing heavy precipitations of Calcium Hydroxide and cement grain remnants.	39
16	A	09 19 44 Selected area of Fig. 11 showing Calcium Hydroxide.	40
17	A	09 19 42 Selected area of Fig. 11 showing cement grain remnants.	41
18	A	09 19 21 General view of fracture surface.	42
19	A	09 19 22 Selected area of Fig. 14.	43
20	A	09 19 25 Selected area of Fig. 14.	44
21	A	10 11 03 General view.	45
22	A	10 11 02 Selected area showing massive Calcium Hydroxide and cement grain remnants.	46
23	A	10 11 01 Cement grain remnant.	47
24	B_2	09 26 07 General view of specimen containing Silica flour having w_o=0.64. Note porous matrix.	48
25	B_2	09 26 10 Selected area of Fig. 20 showing Silica particle.	49

* The plane of each photograph is perpendicular to the direction of casting.

Figure	Series	Caption	Page

SPECIMENS CONTAINING BLAST FURNACE SLAG

26	C	10 01 03 Low magnification view of fracture surface showing unhydrated Blastfurnace slag (BFS) particles.	50
27	C	10 01 01 Vitreous Blastfurnace slag particle and surrounding matrix of Calcium Silicate hydrate.	51
28	C	10 01 09 Interface of BFS particle and hydrate CSH.	52

SPECIMENS CONTAINING FLY ASH

29	D^1	10 02 05 Low magnification view of work area.	53
30	D^1	10 02 12 Siliceous Fly Ash particle (FAP) with adhering shell of hydrate.	54
31	D^1	10 02 16 Siliceous (Si) FAP with Calcium Silicate Hydrate (CSH) and Calcium Hydroxide (CH) matrix.	55
32	D^1	10 02 17 CH with hollow left by unhydrated nucleus of FAP and surrounding shell of CSH hydrate.	56
33	D^1	10 02 18 Hollow FAP with strongly oriented CH.	57
34	D^1	10 02 21 Large FAP with high Si and Al almost totally consumed. Smaller FAP with shell of hydrate.	58
35	D^1	10 02 22 FAP with strongly oriented CH.	59
36	D^1	10 02 20 General view of work area.	60
37	D^2	09 26 17 Typical Fe particle upper left with hollow Si-Al particle and 3 Si particles.	61
38	D^3	09 26 48 General view of work area.	62
39	D^3	09 26 49 Hollow FAP split by fracture plane.	63
40	D^3	09 26 47 Hollow FAP with Fe particle and Hydrate shell.	64
41	D^3	10 08 04 General view of work area.	65
42	D^3	10 08 07 Hollow FAP.	66

Figure	Series	Caption	Page
43	D^3	10 08 08 Hollow FAP's.	67
44	D^3	10 17 01 FAP about 10 μm diameter with hydrate shell about 1 μm thick.	68
45	D^3	10 17 02 Strongly oriented CH matrix.	69

LIST OF SYMBOLS

A	area in m^2
D*	average coefficient of diffusivity
C	mass of cement kgm^{-3}
Q	Quantity of water or water vapour passing through barrier
V	Volume
V_{cap}	$V_w - V_{gel}$
V_{gel}	water held in gel = 3 monolayers = 3 V_m
V_w	volume of evaporable water and air per unit volume of concrete
V_L	volume of large molecular fluid in pore space
V_m	monolayer capacity of cement paste per unit mass of cement
W	mass of mixing water Kg per m^3 of concrete
p	partial pressure of water vapour
ps	saturation pressure of water vapour
p/ps	relative vapour pressure
r	radius of curvature of water meniscus
1-u*	average mositure loss as a fraction of the moisture loss at time = ∞
v*	coefficient of variation
w_o	mass ratio of water per unit of cement
w_e	mass ratio of evaporable water per unit of cement
w_n	non-evaporable water, mass per unit of cement retained at 110°C but lost at 1050°C
w_n^0	wn for unit mass of completely hydrated cement
x	dimensions in metres
α	mass fraction of cement which has hydrated = w_n/w_n^0
α_∞, α^*	the value of α when hdyration ceases
ε	volume fraction of void space containing air and evaporable water

ε_e	effective void space = ε minus space occupied by strongly adsorbed water
θ	relative humidity = p/ps x 100 per cent
σ	strength MPa. σ_A = strength of A. Surface area m^2 per unit mass of cement
σ_1	axial stress
σ_3	uniform transverse stress
τ	(time in hours)$^{1/2}$

1. INTRODUCTION

In the event of a loss of coolant accident (LOCA) the function of the concrete containment building is to contain a mixture of hot air, water vapour and radioactive products to specified release rates.

The present design of the 600 MW(e) units such as Gentilly-2 and Pt. Lepreau relies on:

(a) a primary barrier of epoxy resin which is applied to the inner surface of the concrete barrier; and

(b) a 1 m thickness of prestressed concrete.

The design of the Ontario Hydro units, which is based on vacuum containment, employs elements of reinforced concrete, steel-lined concrete and prestressed concrete as seepage barriers.

In Ontario, and elsewhere, estimates of permeability have been based on the air permeability tests reported by Loughborough [Ref. 2]. Experience has shown that the permeability of concrete placed on site exceeds estimates based on such laboratory tests and that an important source of leakage is through gross defects in the concrete.

Most of the data referred to in recent publications [Ref. 3, 4] was generated between 1929 and 1950 [Ref. 5, 6] and was concerned with properties of unreinforced mass concrete rather than structural concrete.

This study revealed logical flaws and conflicting statements as to the influence of conventional mix design parameters, such as water:cement ratio and cement factor, on permeability. For example Griffin and Henry [Ref. 7] state that water vapour transmission (WVT) increases with increase in water:cement ratio. This statement is meaningless unless the corresponding cement factor or volume concentration of mixing water is specified. The same authors stated that WVT was independent of relative humidity. This conclusion violates common sense and is also contrary to the findings of Henry and Kurz [Ref. 8]. Griffin and Henry also state that WVT decreases with the presence of 1.5 per cent NaCl in the concrete. This quantity of NaCl could lead to serious alkali-aggregate reaction and possible failure of the concrete.

Neville [Ref. 3] and Butler [Ref. 4] cite censored values from Technical Memorandum No. 6-380 published by the Waterways Experimental Station [Ref. 6] which is widely quoted in the literature. Table 1 lists the original data [Ref. 6 page 28] together with calculated standard deviations for mean permeability values and calculated water content.

TABLE 1

Perspective on widely quoted data from Technical Memorandum No. 6-380 of the U.S. Waterways Experimental Station [Ref. 6].

	Report Data			Calculated	
No. of Observations	Water:Cement ratio	Cement kgm^{-3}	Permeability $10^{-12} ms^{-1}$	Standard Deviation $10^{-12} ms^{-1}$	Water* kgm^{-3}
5	0.60	223	48	32	134
2	0.86	112	84	27	96
3	0.65	140	49	17	91
5	0.69	156	8	10	108
5	0.75	140	34	12	105
5	0.74	153	24	5	113
4	0.58	168	41	50	97
1	0.46	223	27	-	103

*Conflicting values are obtained if calculated from Neville [Ref. 3] or from Butler [Ref. 4].

The scatter in the results inhibits any firm conclusions as to the influence of mix design parameters and since the standard deviation is large compared with or even exceeds the mean value, casts doubt on the value of this data when it is presented without the relevant mix characteristics.

For 20 mm aggregate and for the class of concrete used for containment buildings the lowest permissible cement factor is 320 kgm^{-3} according to National Standard of Canada CAN3-A23.1-M77 Clause 14 and 310 kgm^{-3}

according to the British Code of Practice CP110:1972. Furthermore, even the best available commercial concrete is unlikely to have a water content below 180 kgm^{-3}, and therefore the mix properties given in Table 1 are thus outside normal limits for structural concrete.

Current thinking on the subject of air permeability of concrete relies heavily on ad hoc tests reported by Loughborough [Ref. 2]. These tests were limited in scope and did not include the influence of key variables such as water:cement ratio and cement or water content. The finding that permeance of concrete to air is 'minimal' is at variance with common experience of field concrete. A more recent paper by Figg [Ref. 9] suggested a type of 'rising head' test in which the time taken to dissipate a vacuum applied to a small cavity in the concrete is taken as a measure of the permeability to air. The test is only useful as a basis of comparison between one concrete and another since it does not produce absolute values of permeability. This author also states: 'There is a large accumulation of experience which has shown that strength and water/cement ratio can be related to the behaviour of concrete in practice and hence it can be expected that the new tests will give reasonable predictions for likely performance of concrete'. The value of the test method is therefore related to the correlation between strength and water cement ratio on one hand and permeability number on the other. No correlation between real permeability and permeability number is given. Both strength and water/cement ratio can be held constant over a wide range of porosities and therefore the claim made for the test that it is a measure of performance is, in the present context, false.

Figg also states that there is a linear relationship for air and water permeability with moisture content of the concrete. The implication of this statement is that there is no possibility that the permeance of concrete to gas can be described by a single valued constant.

Rose's work [Ref. 10] also leads to the same conclusion on the basis of an essentially non-linear variation of permeance with moisture content and complete inhibition of gas flow in areas of high relative humidity.

Feldman in his helium inflow experiments found that partial drying was necessary to establish measureable inflow of helium [Ref. 11]. Lawrence [Ref. 13] found it necessary to dry his concrete specimens at Relative Humidity = 50 per cent in order to establish gas flow. It seems clear that gas transfer through a porous barrier containing water meniscii must take place mainly by diffusion rather than flow and, if flow is to occur, the concrete must be dried.

The present work was intended to develop information which is needed to characterise concrete in terms of its performance as a barrier to the passage of gas, water vapour and water and which is not readily available in the literature.

The capacity of concrete itself to survive in an aggressive environment and also its capacity to protect steel against corrosion depends on it having low permeability. In some cases, for example gravity dams [Ref. 14] and barrier plugs in rock [Ref. 15], structural stability is influenced by uplift pressure which is a function of permeability.

This work is therefore of interest to a wider field outside the nuclear power industry. To the industry itself with existing structures fast approaching the 25 year critical aging period, improved knowledge is vitally important for the assessment of useful service life.

This report is presented within the framework of Section 5 of the writer's proposal which was the basis for contract OSU82-00099 and the work described herein was performed during the period 1 May 1982 to 31 March 1983.

2. THE NATURE OF CONCRETE AND THE PROCESS OF MASS TRANSFER

Permeance of a porous solid is clearly determined by the volume ratio of voids. In concrete technology this is defined as the ratio of the volume of air and the volume of evaporable water to total volume of concrete and is denoted by ε. The volume ratio of solid material is therefore $(1-\varepsilon)$. The minimum void ratio of cement hydrate is about $\varepsilon = 0.28$ and this translates into a minimum attainable void ratio in the final concrete of about $\varepsilon = 0.07$. At this value, the permeance of concrete is only about one fiftieth of that of natural rock having the same void ratio. In other words, for an equal volume of solids per unit volume, concrete is fifty times more effective as a barrier than natural rock [Ref. 5]. The special character of concrete derives from its pore size distribution and the fact that a significant amount of pore water is strongly attracted to the solid.

2.1 Porosity and Pore Size Distribution

The porosity of concrete changes with water content according to whether hydration of the cement continues, is hindered or stops; whether the concrete is shrinking due to partial drying or swelling due to re-wetting; whether microcracking occurs as a result of internal stresses; or whether the pore size distribution is affected by aging.

Cement hydration results in reduction of pore volume: this is the fundamental process which determines the degree of hardening of concrete. At terminal hydration the chemical reaction stops because there is insufficient space to accommodate the products of hydration or because the water is unable to reach the cement-grain remnant because it is coated by an impervious shell of hydrate or because the concrete is dry and no water is available to react with cement.

In Nature, the degree of hydration and therefore porosity is influenced by all of these factors in a mathematically unpredictable manner. When hydration reaches a terminal value the total porosity is fixed but the pore size distribution varies due to ageing and this increases the proportion of coarse pores [Ref. 16, 17]. There is thus no way in which porosity and pore size distribution can be accurately predicted while hydration is proceeding.

It is possible to estimate the porosity and the permeability of cement paste when hydration has reached a terminal value [Ref. 18, 19]. At this stage about 3 'monolayers' of water are strongly attracted to the solid [Ref. 20, page 399]. This water was regarded by Feldman and Sereda as part of the solid [Ref. 21] and by Powers as adsorbed water [Ref. 18]. It seems safe to classify it as water of infinite viscosity in the present context and the remaining free water as mobile under the influence of pressure gradients across the concrete barrier. Powers [Ref. 20] states that the mean activation energy for flow in mature cement pastes is from 1.5 to 2.8 times the normal value for water at the same temperature.

Assuming that concrete reaches terminal hydration, the space occupied by unhydrated cement, bulk cement hydrate and free water may be computed as shown in Appendix A and illustrated below for unit volume of cement paste having various water:cement ratios. For unit volume of concrete the paste occupies about 30 per cent of the total volume and this leads to values shown on the right hand scale.

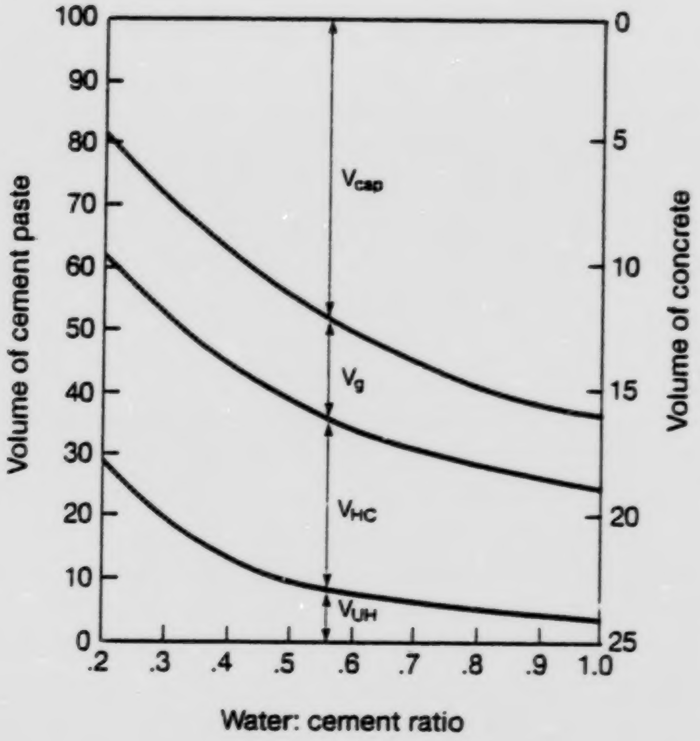

Figure 1. Distribution of solids and mobile water at terminal hydration, $\alpha = \alpha_\infty$ [Ref. 22].

In the present study, performance was related to initial porosity computed as the sum of the volume concentration of air and water in the fresh mix at the time of compaction. The permeability may thus be related to parameters which are controlled by the Engineer and capable of formal definition in contract documents.

2.2 Mass Transfer Across a Concrete Barrier

Mass transfer of liquid water, water vapour and gas through a microporous material like concrete takes place by different mechanisms. Concrete will rarely be saturated even when one face is in contact with liquid water unless it is under hydrostatic pressure on both sides. Even if it is perfectly sealed against gain or loss of moisture, it will undergo self-dessication due to chemical reaction of water and cement. In the context of the present project, concrete will generally be partially saturated or, in rare cases, dry when it is exposed to a permeant.

In the case of a concrete barrier having liquid water on one face and air on the other, transfer of water on the air side must be by evaporation. At some position in the barrier there must be a phase change from liquid water under pressure upstream to water under tension downstream as illustrated in Figure 2.

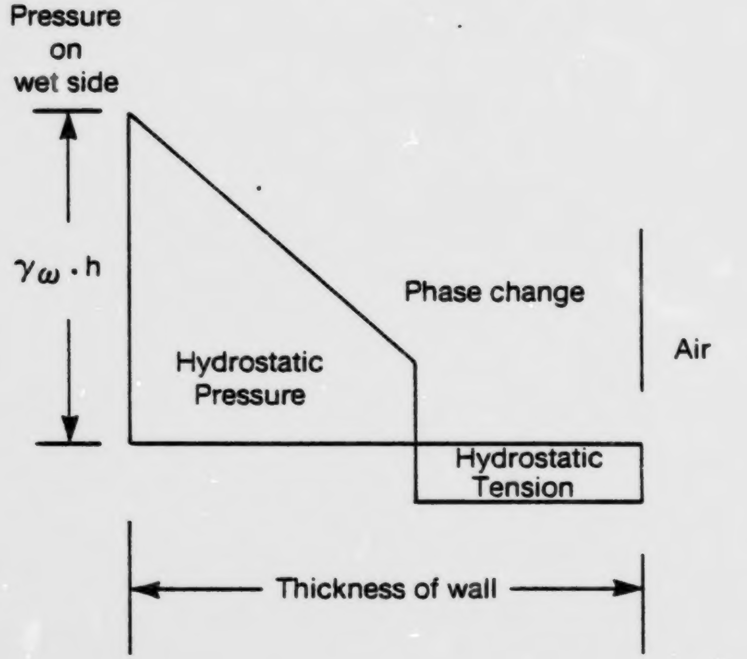

Figure 2. Variation in pressure across a concrete barrier separating liquid water under pressure with air at relative humidity less than 100 per cent.

If both faces are exposed to less than 100 per cent relative humidity, mass transfer can only take place if there is a difference in relative humidity. The mechanism will be one of condensation at the upstream side and evaporation at the downstream side.

Gas permeation will be maximum when the concrete is dry and water vapour transfer will be maximum when the surface areas subject to condensation at the high pressure side and evaporation at the low pressure side are maximum. Gas permeation is through interconnected empty pores and is therefore governed by the interplay of pore size distribution and relative humidity. The pores in concrete are extremely fine and the dimensions are usually given in nanometers (1 nanometer = 10 E-09 metres). Because the solid surfaces are separated by such small spaces, surface tension cannot be measured directly and must be estimated by the Kelvin equation [Ref. 23]. At 96 per cent relative humidity, it may be estimated that all pores having a diameter of 35 nm and less are filled with water under hydrostatic tension of 57 atmospheres [Ref. 18]. At 50 per cent relative humidity the corresponding values are 3 nm diameter and 963 atmospheres. For small laboratory samples of mature concrete without substantial flaws, only 10 per cent of the pores are greater than 100 nm but 90 per cent are greater than 10 nm [Ref. 23].

2.3 Models for Mass Transfer

2.3.1 Water

Powers [Ref. 18, 24] gives the permeability of cement paste as a function of porosity, temperature, fluid viscosity, particle shape, Stokes diameter of particles, Kozeny-Carman tortuosity factor k_1 etc. Appendix B gives an adaptation of this approach to concrete together with a comparison of estimated and observed permeability for three groups of published data. It is clear from these comparisons that the model fails in its purpose. The root of the deficiency rests with the failure of the model to take account of imperfections due to internal bleeding and sources of leakage at the cement paste - aggregate interface. Fagerlund [Ref. 25] distinguished between mobile and immobile water in his model for the conduction of water in concrete.

2.3.2 Water vapour

The theoretical part of the work done to date has been an attempt to model the most common mechanism of mass transfer i.e. by condensation and evaporation of water vapour.

The model pore system depicted in Figure 3b has the following characteristics:

(i) When the model pore is saturated and subjected to unequal hydrostatic pressure on both sides coherent flow of liquid water takes place and the rate of mass exchange is determined by the pressure gradient and the volume and length of pores of molecular dimensions in the neck.

(ii) When the upstream pores are filled and the sink side is in contact with air at relative vapour pressure less than unity mass transfer is by evaporation from a curved water surface at the downstream side. Flow on the upstream side is coherent and on the downstream side it is diffuse.

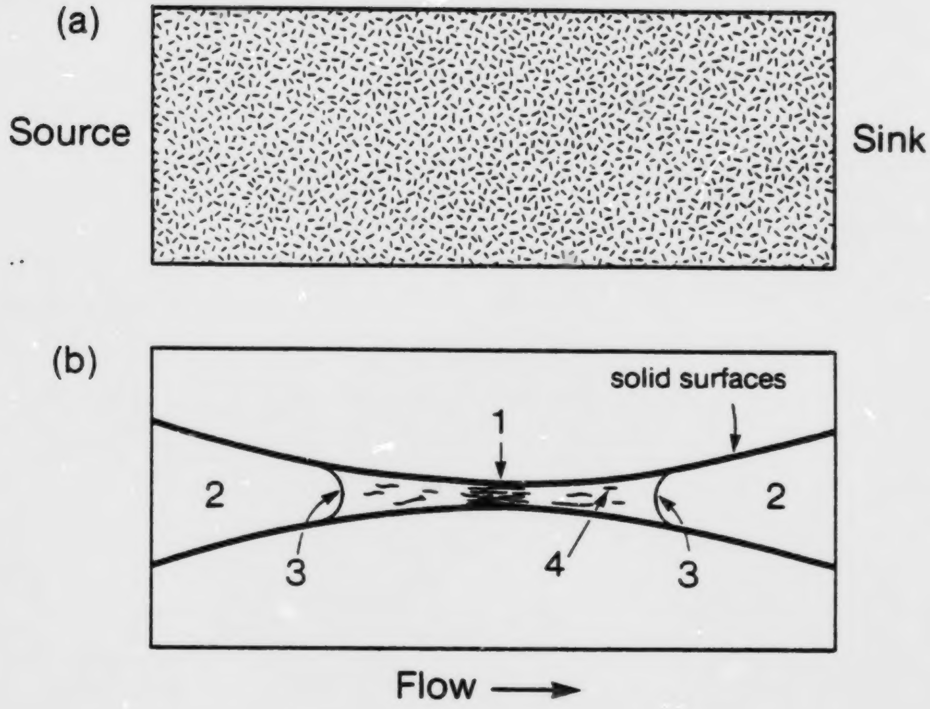

Figure 3. Model pore system (a) pores in three-dimensional random array. (b) Idealized single pore with (1) fine pores containing adsorbed water. Mass transfer occurs by condensation and evaporation of water (2) from liquid surface (3). Liquid water (4) communicates pressure changes from one side to the other.

(iii) When both surfaces are exposed to air such that, in each case $0.45 < p/ps < 1$, transfer is by condensation at the high pressure side and evaporation at the low pressure side. Under these conditions the system is impervious to gas and as Rose has said 'pervious to water only by a process of distillation in which the necks act as short circuits for vapour movement. The process might be described as liquid-assisted vapour transfer, the assistance arising because the liquid shortens the effective path length for vapour diffusion [Ref. 10].

(iv) When $0 < p/ps < 0.45$ a meniscus cannot be sustained because surface tension exceeds the fracture strength of water and the only water in the system is adsorbed and of very high effective viscosity since it is strongly attracted to the solid phase. Mass transfer is by molecular diffusion. The system is pervious to gas.

(v) When p/ps approaches zero there is no condensed water and little adsorbed water. Gas transfer is maximum and any water vapour from an external source is first absorbed before transfer can take place according to (iv) above.

According to the Kelvin equation, the radius of curvature of the meniscus - r is given by:

$$r = (b)/(\ln(p/ps) \qquad (1)$$

Assuming values of 40, 140 and 450 nm, respectively, for the neck mean and maximum dimensions of the bell shape and a repeat distance for the neck = 400 nm, the following equations were derived:

$$\text{Pore radius } y = [e^{x-10}/1 + (e)^{x-10}]20.5 + 2, \qquad (2)$$

where x = distance from neck,

and y = pore radius.

Putting $u = e^{x-10}$;

$$dy/dx = \left(\frac{u}{1 + 2u + u^2}\right) \cdot 20.5 \qquad (3)$$

Assuming the existence of a spherical bubble of radius r, in each wide part of the pore, the quantity of liquid water contained in each neck is obtained when the slope of the surface of the solid = the slope of the bubble surface.

Thus

$$20.5 \cdot u/(1 + 2u + u^2) - (r^2 - \bar{y}^2/\bar{y} = 0 \qquad (4)$$

where $\bar{y}$ is the radius of the solid at the point where the bubble contacts the surface and r = the radius of the bubble.

The volume of water contained in the neck was therefore:

$$V_w = 2\pi[\sum_{o-\bar{x}} (dx/8(y_1 + y_2)^2) - \sum_{(\bar{x}-\Delta x)-\bar{x}} (dx/18(y'_1 + 2y'_2))] \qquad (5)$$

where $\bar{x}$ = the x coordinate of the contact surface;
y_1, y_2 = coordinates of the wetted surface separation by Δx;
y'_1, y'_2 = coordinates of the bubble surface.

This model needs further refinement and calibration to include the effects of film transfer at low vapour pressures, and the effect of surface energy which may vary with different cements and aggregates. Work is proceeding in this direction.

2.4 The Barrier in a Reactor Building

In a reactor building it may be expected that the inside face is saturated under positive or negative transient pressure above the water line of pooled water and under hydrostatic head plus pressure head transients below this level. Outside the building the outside surface is at the ambient relative humidity. Thus, if we assume a temperature of 20°C throughout, the pressure drop across the wall will be from P_i to P_o; where:

$P_i = (0.238 + h)$ m of water; and

$P_o = \frac{\theta}{100}(0.238)$ m; where

θ = relative humidity per cent.

Above the level of condensed water on the floor of the building, mass transfer is determined by disequilibrium at curved water surfaces near the inner and outer faces of the concrete barrier.

Below the water surface, transfer is determined by a pressure of liquid water at the inner face and evaporation at the outer face and in between there will be a phase change from water in compression to water in tension.

It is to be expected that condensed water will be present at all times in the wall of a reactor building so that transfer of gas will be by diffusion through micropores or by permeation through gross defects in the concrete. Although the words diffusion and permeation are often used interchangeably, in the present context the former is used to describe incoherent flow where the diffusing species is dispersed, whereas permeation refers to the passage of a continuum without dispersion.

3. EXPERIMENTAL WORK

The experimental work, exploratory in nature, was designed to provide insight into the rates of transfer through concrete of water - in the vapour and in the liquid phase - and gas as influenced by controllable characteristics of the concrete. In order to keep the programme within manageable limits, the pressure gradient for water vapour transfer was fixed between the limits of saturation and zero relative humidity. The ASTM C355-64 wet cup method was modified so that the weight change of the specimen could be monitored. Water transmission in the liquid phase was carried out in a triaxial cell with various values of confining pressure. Air permeability was determined by observing air flow at constant pressure in a purpose-made cell.

3.1 Concrete Mixes. Four series of concrete mixes were prepared:

Series A: Portland cement concrete with constant water:cement ratio = 0.42 and variable water and cement contents to give 4 different values of initial porosity, respectively, 29, 23, 17 and 14 per cent by volume. The workability was maintained constant by adding small quantities of Lomar-D superplasticiser, respectively 0, 2.7, 4.1 and 7.1 kgm^{-3}. The corresponding cement contents were 695, 548, 412 and 357 kgm^{-3}.

Series B: Concrete having 23 volume per cent of mixing water, 2.7 kgm^{-3} of Lomar-D and the following combinations of Portland cement/Silica flour: 412/136, 357/191, 300/248 kgm^{-3}. The effective water:cement ratios were: 0.42, 0.56, 0.64 and 0.77.

Series C: Instead of the Silica flour in Series B, Blastfurnace slag was added to give Portland cement/Blastfurnace slag ratios = 412/136, 357/191 and 300/248 kgm^{-3}.

Series D: Instead of Silica flour in series B, Fly Ash was added to give Portland cement/Fly Ash ratios = 412/136, 357/181 and 300/248 kgm^{-3}.

The mixes were designed to yield data on the influence of characteristic mix parameters on concrete strength, water vapour transmission and water permeability as follows:

TABLE 2. Isolation of mix design parameters in concrete mixes.

Mix Series	Main Variables	Constant
A_1 to A_4	Initial porosity	Water:cement
A_2, B_1 to B_3	Water:cement	Initial porosity
A_2, C_1 to C_3	Blastfurnace slag substitution	Initial porosity
A_2, D_1 to D_3	Fly Ash substitution	Initial porosity
A_2B_1, A_3B_2, A_4B_3	Figures of merit for	Water:cementitious
A_2C_1, A_3C_2, A_4C_3	Blastfurnace slag and Fly Ash	material
A_2D_1, A_3D_2, A_4D_3	as cement substitutes	Initial porosity

3.2 Cement Paste Specimens.

Samples of all mixes in the ABC and D series without fine or coarse aggregate were prepared for microscopic examination.

3.3 Water Permeability

At 24 hours age cores were drilled out of concrete prisms parallel and transverse to the direction of casting. The ends of the cores were finished plane and parallel and they were then surface dried and stored in sealed plastic bags to simulate mass curing in the field. After 14 days the cores were sealed in a rubber membrane and placed in a triaxial cell. The cell was placed in a testing frame and hydrostatic compression $\sigma_2 = \sigma_3$ applied in the lateral direction together with a constant effective longitudinal stress σ_1.

The stainless steel platen through which the σ_1 stress was applied were connected to a water system allowing the axial flow of water through the specimen to be determined with a precision of 10^{-3}gm. Water permeation was

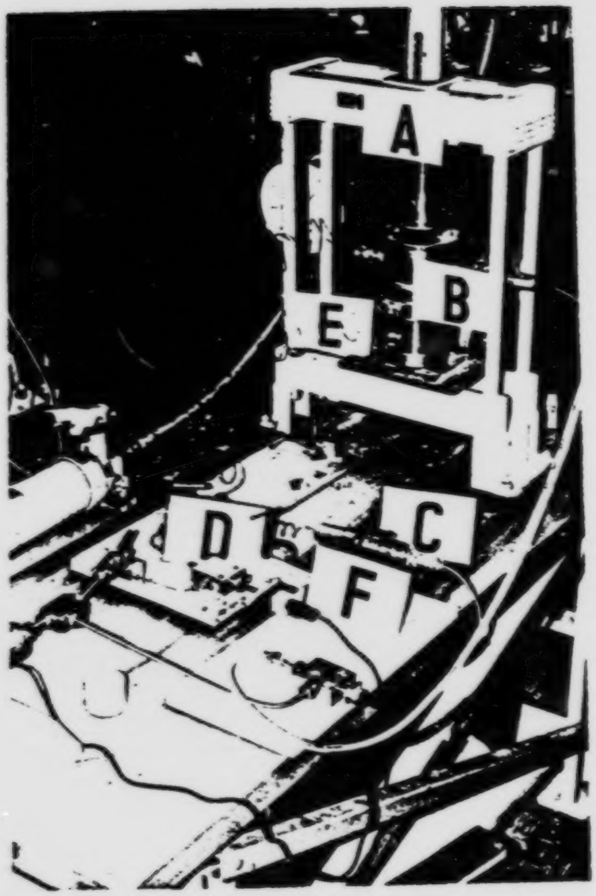

4(a) General View. A = loading frame, B = triaxial cell, C = Pressure transducers, D = screw pump E = Stainless steel loading head.

4(b) specimen on stainless steel loading head E.

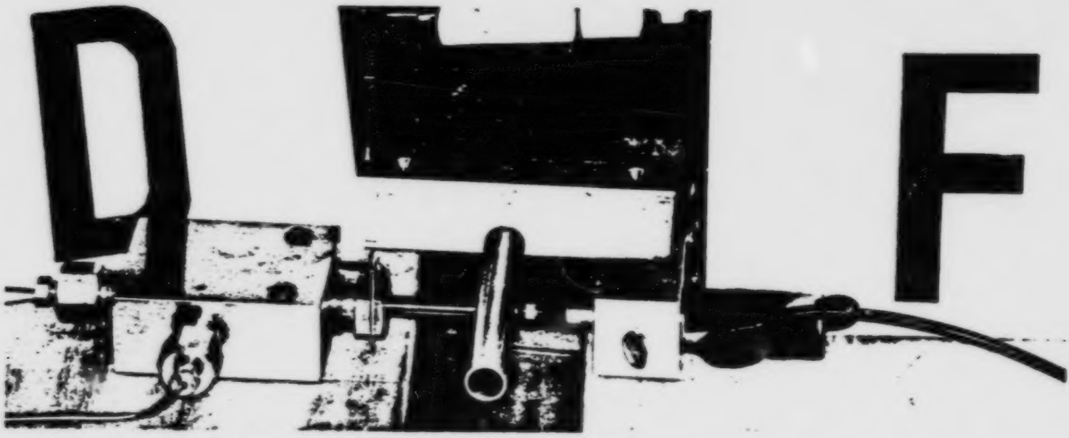

4(c) Screw pump D with LVDT sensor F

Figure 4 Water Permeability Apparatus

measured for values of the σ_3 confining stress = 10, 15 and 20 MPa respectively. The apparatus is shown in Figure 4.

3.3.1 Results of Water Permeability Tests

Data from these tests was fitted to Power curves as shown in Figure 5. The coefficients of the empirical curves and the coefficients of variation of the ratio of observed to calculated permeability coefficient are shown in Table 3. The influence of lateral confining pressure for porosity $\varepsilon = 0.15$ is shown in Fig. 6.

TABLE 3. Summary of Water Permeability Tests

Least square fit of experimental data to curve of the form.
Permeability $K/10^{-12} = A\varepsilon^B$ ms^{-1}, where ε = porosity. v* is coefficient of variation (percent) in the ratio of observed to calculated permeability, and N is the number of determinations.

Flow Direction	Confining Pressure MPa	Coefficients A	B	N	v*
Parallel to bleeding	10	82.6	2.0	8	15
	15	51.6	1.9	8	24
	20	40.0	1.8	8	22
Perpendicular to bleeding	10	4419	4.8	7	18
	15	1415	4.3	8	19
	20	974	4.2	8	30

N = number of determinations
v* = coefficient of variation per cent in the ratio of observed to calculated coefficient of permeability

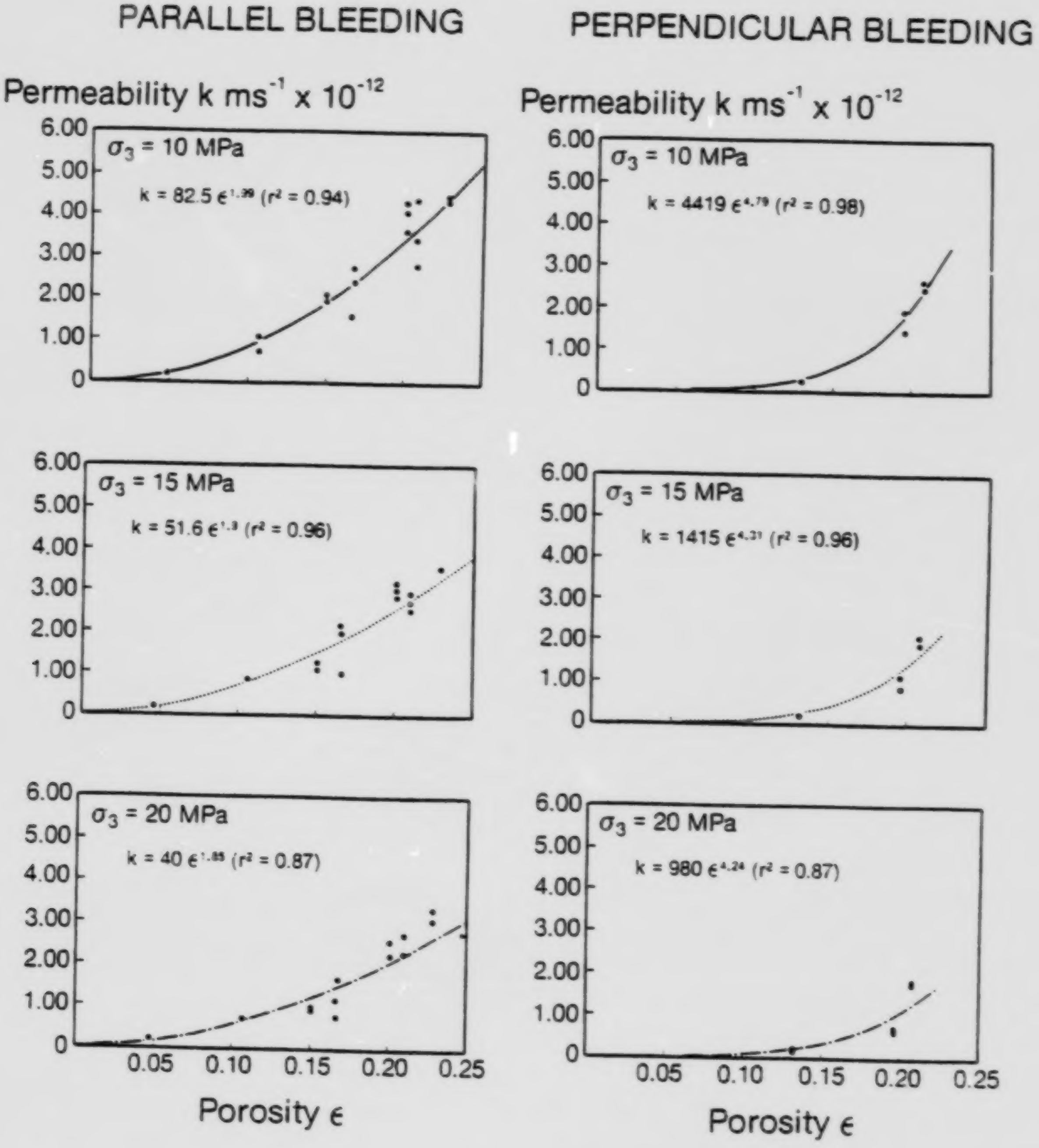

Figure 5. Results of water permeability tests for flow parallel to and at right angles to the direction of bleeding.

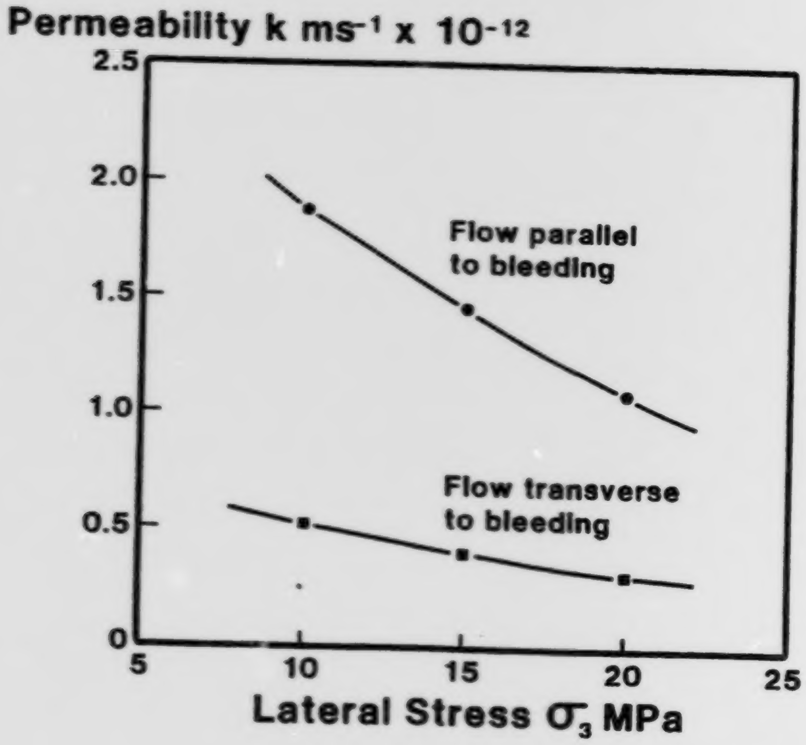

Figure 6. Permeability as a function of confining stress for porosity ε - 0.15.

$$K^* = \phi \{ \frac{\varepsilon^2}{1-\varepsilon} \exp - 4.19 (\frac{1-\varepsilon}{\varepsilon}) \} \tag{55}$$

$$K^{**} = \chi . \frac{1}{K' \sigma^2} . \frac{(\varepsilon_e)^3}{(1-\varepsilon_e)^2} \tag{53}$$

$$K^{***} = \Psi \cdot \frac{\varepsilon^{1.5}}{K'\sigma^2} \cdot \frac{(\varepsilon_e)^3}{(1-\varepsilon_e)^2} \qquad 53a$$

TABLE 4. Comparison of various equations for water permeability coefficient K

				[Ref. 18] Eq. 55		[Ref. 18] Eq. 53		This investigation Eq. 53a	
Source	Direction	σ_3(MPa)	N	ϕ	v*	χ	v*	Ψ	v*
This Investigation	Parallel	10	8	16.2 E 23	283	128 E 6	34	1.7 E 9	14
		15	8	13.2 E 21	264	85 E 6	52	1.3 E 9	21
		20	8	12.7 E 21	283	86 E 6	53	1.1 E 9	23
	Perp.	10	7	7.2	128	54 E 6	85	0.9 E 9	43
		15	8	6.8 E-3	108	39 E 6	88	0.5 E 9	56
		20	8	5.6 E-3	116	32 E 6	96	0.4 E 9	63
US WES [Ref. 6]	Unknown	0	75	1.8 E-7	54	374 E 6	100	360 E 6	87
Reuttgers et al. [Ref. 5]	Parallel	0	20	1.6 E 3	200	6.1 E 3	110	8.8 E 9	124
McMillan and Lyse [Ref. 27]	Parallel	0	20	24.6 E 3	150	148 E 9	72	1731	35
	Parallel	0	20	57.6 E 3	198	118 E 9	28	1468	31
	Perp.	0	20	24.6 E 3	145	112 E 9	33	1571	34

3.3.2 Discussion of Water Permeability Tests

The most striking feature of these tests was the strong dependence of permeability on confining pressure as shown in Figure 6. It appeared that this effect was weaker when the direction of flow was at right angles to the direction of casting.

Data from this investigation and from three other investigations was fitted to theoretical models attributed to Powers [Ref. 18] and to Carman [Ref. 26]. The Powers model gave unsatisfactory correlation with the data. The Carman model was better, but the modified Carman model gave the best fit to the available data as shown in Table 5. Values of v* in the final column are of the same order as experimental error.

An important factor which requires definition is the least dimension and volume of the smallest 'statistically uniform' sample. Clearly this is some function of maximum aggregate size but it is also a function of the significance, size and spacing of construction defects.

3.3.3 Porosity

After completion of the permeability test, porosity was determined by evaporation of free water at 110°C. Some specimens were re-saturated with Methanol in an attempt to distinguish pore space containing relatively mobile water - roughly proportional to the Methanol volume - and that containing water strongly attracted to solid surfaces - the difference between water volume and solid volume.

In this investigation the original water:cement ratio was = 0.42. If it is assumed that terminal hydration was reached, the ratio of 3 mono-layers of gel water to total evaporable water is computed as 0.191 to 0.394 = 0.48 for the past. In the Methanol Sorption tests this quantity should be close to $(V_w - V_m)/V_w$. The actual values follow in Table 5.

TABLE 5. Differential absorption of Methanol and water.

Mix	Pore Volume ε	$(V_w - V_m)/V_w$
A_1	0.205	0.8
A_2	0.164	0.8
A_3	0.137	0.9
A_4	0.107	0.9

V_w = volume of evaporable water
V_m = volume of Methanol

It was decided to use the calculated values of ε and ε_e, where $\varepsilon_e = \varepsilon - 3V_m$ for subsequent work.

3.4 Water vapour permeance and diffusion.

These tests followed ASTM C355-64 except that provision was made for monitoring weight change in the specimen and in the dessicant. The concrete specimen was cast in the upper part of a two-part container (Figure 7) which could be hermetically sealed to the bottom part containing solid calcium chloride.

The advantage of this system was that both transient and steady state conditions of the specimen could be monitored.

During the initial drying period, the rate of moisture loss from the concrete was linear with respect to the square root of time [Appendix C]. A diffusion constant D* was calculated from:

$$D^* = 218.7(10^{-6})\left(\frac{d.b^*}{M_{ew}}\right)^2 \ m^2s^{-1} \quad \text{where}$$

d = the thickness of concrete
b^* = the slope of the moisture loss versus square root of time curve; and
M_{ew} = the mass of total evaporable water.

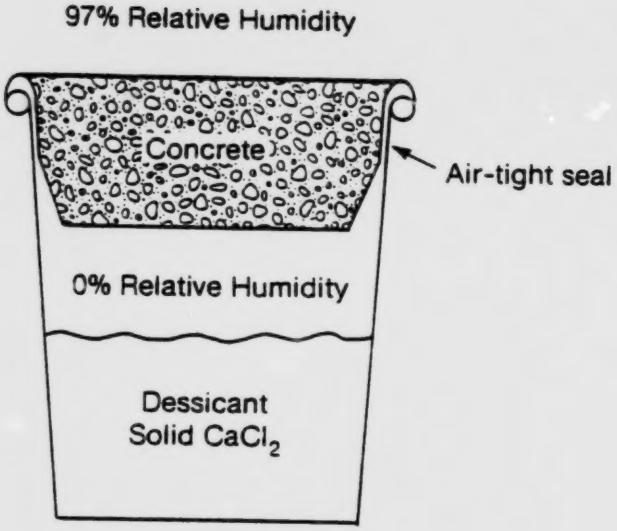
97% Relative Humidity
Concrete
Air-tight seal
0% Relative Humidity
Dessicant
Solid $CaCl_2$

Figure 7. Two part dry cup apparatus for Water Vapour Transmission

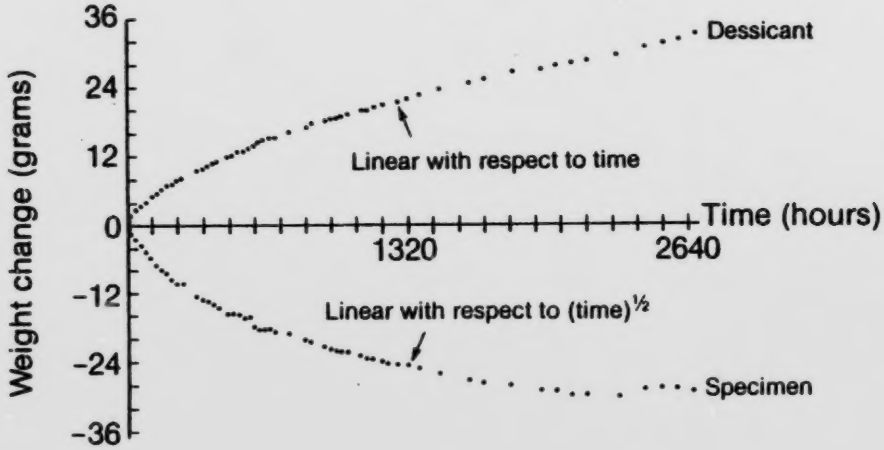

Figure 8. Mass transfer of water by drying of specimen (lower curve) and by condensation and evaporation (upper curve).

After the concrete reached constant mass, the time rate of change in the mass of water collected at the sink was related to a pseudo coefficient of permeability K as follows:

$$K = \frac{(277.8 \times 10^{-12})}{Ai} \cdot \frac{dw}{dt} \text{ metres per second; where}$$

$\frac{dw}{dt}$ = mass collected in grams/hour;
A = area of cross section in m^2;
i = pressure ratio between source and sink divided by the thickness of concrete.

3.4.1 Specimen Conditioning

The specimens were subjected to the following treatment before testing:

TABLE 6. Schedule of treatments

	Treatment	Specimens	No. of Replicates
(a)	Sealed against gain or loss of water	All of A B C D	3
(b)	Moist cured for 24 hours and then sealed as above	All of A B C D	3
(c)	Treated as (a) above and oven-dried	A_2, B_1, B_2, B_3	3
(d)	Treated as in (c) above and re-saturated to 50 per cent of initial moisture content	A_2, B_1, B_2, B_3	3
(e)	Treated as in (c) above and re-saturated to 75 per cent of initial moisture content	A_2, B_1, B_2, B_3	3
(f)	Treated as in (a) above but initial concrete mix modified with the brands of latex polymer added at 1/2, 1x and 2x the recommended dosage	A_1, A_2, A_3, A_4, A_2, D_1, D_2, D_3	2

3.4.2 Simulated Mass Curing Treatment (a)

3.4.2.1 Specimens with constant water:cement ratio

TABLE 7. WVT of mass cured specimens with variable porosity

Specimen	Porosity ε litres per cubic metre When mixed ε	 As tested ε'	$K/10^{-12}$ ms^{-1}	Correlation Coefficient r^2
A_1	290	204	48.4	0.99
A_2	230	173	39.0	1.00
A_3	170	127	25.9	1.00
A_4	140	102	21.9	1.00

The coefficient of permeability k varies linearly with total porosity according to the empirical equation

$$K = 0.25\,\varepsilon' - 6.34$$

with correlation coefficient $r^2 = 0.99$.

Bearing in mind that the water:cement ratio was held constant, and therefore strength was constant, the coefficient of permeability was found to depend on porosity and it reduced with both cement and water content. This is a matter of some importance since it means that the lowest permeability will result from the smallest quantity of cement which will achieve a given strength.

3.4.2.2 Specimens with constant porosity

TABLE 8. Specimens with variable water:cement ratio

Specimen	Water Cement Ratio w_o	Porosity ε litres per cubic metre When mixed	As tested	$K/10^{-12}$ ms^{-1}	Correlation Coefficent r^2
A_2	0.42	230	173	39.0	1.00
B_1	0.56	230	157	46.5	0.99
B_2	0.64	230	159	45.1	1.00
B_3	0.77	230	168	49.9	1.00

The above results yield the following correlation:

$$K = 27.9 + 28.8\ w_o \text{ with } r^2 = 0.86.$$

The correlation is poor and suggests that permeability of concrete of constant initial porosity was relatively insensitive to wide variations of water:cement ratio. Thus strength, which is often accepted as a measure of all the desirable properties of concrete, is probably not a reliable index of permeability.

3.4.2.3 Specimens containing substitutes for Portland cement

In these specimens Blastfurnace slag and Fly Ash was substituted for Portland cement in such a way as to maintain constant initial porosity and constant ratio of water to cement and substitute.

TABLE 9. Specimens with fixed initial porosity and variable Blastfurnace slag content

		Porosity ε litres per cubic metre			Correlation
Specimen	PC/BFS	Initial Nominal	As Tested	$K/10^{-12}$ ms^{-1}	Coefficient r^2
A_2	100/0	230	173	39.0	0.99
C_1	75/25	230	129	46.0	0.99
C_2	65/35	230	131	42.8	0.99
C_3	55/45	230	135	43.8	0.99

TABLE 10 Specimens with constant porosity and variable Fly Ash content

	PC/FA				
D_1	75/25	230	147	35.6	0.99
D_2	65/35	230	165	43.1	0.99
D_3	55/45	230	169	35.9	0.99

Within the limits of experimental variations there appeared to be no correlation between k values and porosity or the mass ratio of Portland cement substituted by the alternate materials.

3.4.3 Simulated Mass Curing after 24 hours - Treatment (b)

Water vapour permeability k and diffusion constant D* for concrete cured at 99 per cent relative humidity for 24 hours then sealed for 6 days against gain or loss of moisture before test. The purpose was to simulate mass curing after an initial period of moist curing.

TABLE 11 Specimens with Constant water:cement ratio = 0.42

Specimen	Porosity ε litres per cubic metre When mixed ε'	 As Tested ε"	$K/10^{-12}$ ms^{-1}	r^2	$D^*/10^{-12}$ m^2s^{-1}	r^2
A_1	290	149	50.0	1.00	78.4	0.99
A_2	230	147	46.4	1.00	78.1	1.00
A_3	170	85	28.4	0.99	76.2	0.97
A_4	140	68	33.8	1.00	63.4	0.99

The following regression equations were calculated:

$$K = 11.16 + 0.14\,\varepsilon' \quad (r^2 = 0.80)$$
$$D^* = 57.01 + 0.08\,\varepsilon'' \quad (r^2 = 0.58)$$
$$K = 14.45 + 0.22\,\varepsilon' \quad (r^2 = 0.85)$$
$$D^* = 58.00 + 0.14\,\varepsilon'' \quad (r^2 = 0.63)$$

It is clear that only the relationship between k and ε' showed poor to fair correlation. All the other regression equations had unsatisfactory correlations.

TABLE 12 Constant initial porosity ε = 0.230 and variable water:cement ratio w_o

Specimen	w_o	Porosity ε litres per cubic metre When mixed	 As tested	$K/10^{-12}$ ms^{-1}	r^2	$D^*/10^{-12}$ m^2s^{-1}	r^2
A_2	0.42	230	147	46.4	1.00	78.1	1.00
B_1	0.56	230	157	37.8	0.99	71.6	0.97
B_2	0.64	230	159	38.7	0.99	73.7	0.95
B_3	0.77	230	169	47.0	0.97	77.0	0.92

There was no correlation between water:cement ratio or porosity when tested against either K or D*.

TABLE 13 Specimens with Blastfurnace slag

Specimen	PC/BFS	Porosity ε litres per cubic metre		$K/10^{-12}$ ms^{-1}	r^2	$D^*/10^{-12}$ m^2s^{-1}	r^2
		When mixed	As tested				
A_2	100/0	230	147	37.8	0.99	78.1	0.97
C_1	75/25	230	129	37.2	0.97	79.9	0.98
C_2	65/35	230	131	39.9	0.99	62.8	0.99
C_3	55/45	230	135	45.0	1.00	75.5	0.99

TABLE 14 Specimens with Fly Ash substitution for Portland cement

	PC/FA						
D_1	75/25	230	147	42.4	0.99	37.9	0.98
D_2	65/35	230	165	43.5	0.96	50.1	0.98
D_3	55/45	230	169	47.2	0.99	43.7	0.99

No formal correlation was found between PC/BFS or PC/FA ratio and either K or D*. In respect of fly ash, the diffusion coefficient D* appeared low in relation to the Portland cement control, A_2, and the Blastfurnace slag mixes C_1, C_2 and C_3.

3.4.4 Variable Free Water Content

Water vapour permeability of concrete with variable free water content was determined by firstly drying specimens from each mix to constant weight at 110°C to determine total evaporable water then drying companion specimens under vacuum at moderate temperatures (50°C) to moisture levels corresponding to 25, 50 and 75 per cent of the evaporable water. The results follow: Water vapour permeability k for specimens having various free water contents at the start of test.

TABLE 15 Permeability with Variable Water Content

Specimen	w_o	Free water content W_e kgm^{-3}	$K/10^{12}$ ms^{-1}	r^2
A_2	0.42	0	7.7	0.84
		28.4	24.3	0.95
		56.9	34.3	0.97
		85.5	53.1	0.98
B_1	0.56	0	1.7	0.17*
		55.5	38.5	0.95
B_2	0.64	0	9.4	0.78
		55.5	43.7	1.00
B_3	0.77	0	16.3	0.86
		58.4	48.0	1.00

*unreliable correlation

For the A series:

$$K/10^{-12}\ \mathrm{ms}^{-1} = 7.94 + 0.51\ W_e \qquad r^2 = 0.99;\ \text{where}$$

W_e = evaporable water litres per cubic metre

For the A and B series and about 50 per cent evaporable water

$$K/10^{-12}\ \mathrm{ms}^{-1} = 17.0 + 40.4\ w_o \qquad r^2 = 0.98;\ \text{where}$$

w_o = water:cement ratio.

It is clear that pore water acts as a'short circuit' for vapour transfer - the condensed water in pores effectively shortens the path length for vapour. It is not yet known what is the effect on transfer of radioactive water vapour. The results are consistent with Roses's model [Ref. 10]. Water condensing at the wet side changes the surface curvature of condensed water at the dry side. The resulting disequilibrium at the water surface-air interface causes water molecules to escape into the atmosphere. Transfer of radioactive water would, it is believed, be much slower since this would proceed by molecular diffusion. Thus, if an active silica gel capsule were hermetically sealed to the downstream face it would take up water vapour in measureable quantities but this water would not necessarily be radioactive.

3.4.5 Blank Tests

Blank tests were mounted to determine the extent of both leakage and evaporation from the surface at the high pressure side. Both leakage and evaporation were insignificantly small.

3.5 Gas Permeation

Specimen B_2, initial porosity = 0.23 and w_o = 0.64, was selected for gas transmission tests. The specimen was sealed into a two part container so as to separate the lower part under vacuum from the upper part under atmospheric pressure of dry air.

It was necessary to dry the specimen before a measurable flow of air passed through the specimen. In the case of a specimen dried to approximately 5 per cent of its saturated moisture content, the flow of dry air stabilised after 6 hours and has remained constant for the past 6 months at a value of 99.8×10^{-6} gs^{-1}.

The corresponding diffusion coefficient D* was calculated on the assumption that formal solution of Fick's equation (see appendix C) includes terms in t/x^2 or $t^{1/2}/x$; where t is time and x is distance from source or sink. For specimens of fixed dimensions, moisture loss is a linear function of $t^{1/2}$. The diffusion coefficient D* is given by the slope w t of the moisture loss versus t curve.

This may be compared with Oxygen diffusion values obtained by Lawrence (2) which ranged from 20 to 184×10^{-9} m^2s^{-1} for Portland cement concrete made with w_o = 0.7 and initial voids ratio $\simeq$ 0.19.

3.6 Cementing Properties of Blastfurnace Slag and Fly Ash

Hydraulicity factor H for Blastfurnace slag and Fly Ash determined according to Lea and Desch (5).

TABLE 16 Hydraulicity Factor

$$H_1 = \frac{\sigma_C - \sigma_B}{\sigma_A - \sigma_B} .$$

Mix	PC/BFS	28 days	90 days
C_1	75/25	0.76	0.66
C_2	65/35	0.71	0.51
C_3	55/45	0.55	0.51

$$H_2 = \frac{\sigma_D - \sigma_B}{\sigma_A - \sigma_B} .$$

Mix	PC/FA		
D_1	75/25	0.79	1.02
D_2	65/35	0.46	0.73
D_3	55/45	0.35	0.61

When $H = 0$; the material has the same cementitious value as silica powder i.e. zero. When $H = 1$, it has the same value as Portland cement, and when $H > 1$, it is superior to Portland cement.

The values of H listed above are much lower then would be expected from continuous moist curing; but they are not unreasonable for concrete which is deprived of water from an external source.

4. MICROSCOPIC EXAMINATION

4.1 Pore Structure from Micrographs

Determination of pore structure from micrographs has been discussed by Haynes [Ref. 28] and Midgley and Illston [Ref. 23]. The latter [Ref. 23] found a strong correlation between pore radii as determined by electron microscopy and those determined by Mercury porosimetry.

Table 17 Pore radii as determined by electron microscopy and mercury intrusion porosimetry (After Midgley and Illston [Ref. 23]).

Pore radius in nanometers Electron Microscopy	 Mercury porosimetry
490	500
300	300
200	200
140	150
50	50
30	30
18.5	15
13	10
5.2	5.0

4.2 The Present Study

In the present investigation it was decided to examine representative samples in the electron microscope to determine whether physical behaviour in other tests could be correlated with readily observed microstructure. This was considered to be important both as an aid to understanding the process of mass transfer and as a possible means of rapid classification of hardened concrete.

An important feature of this part of the investigation was to observe the extent and morphology of Calcium Hydroxide in coarse pores since this is one microstructural component which is profoundly modified by additions of Blastfurnace slag and Fly Ash. For these purposes Energy Dispersive X Ray Analysis was used to identify significant structural features.

The last fraction of each mix, i.e. Portland cement + water or Portland cement + Silica flour, Blastfurnace slag or Fly ash substitute + water was prepared in a form suitable for examination by Scanning Electron Microscopy (SEM) and Energy-dispersive X-ray analysis (EDX). The objective was to characterise microstructure and seek correlation with tests described in section 3 above.

The study generally included four stages:

(a) Low magnification of an area about 3 mm square to determine the nature and extent of shrinkage cracking and the occurrence of gross defects such as bleeding cavities, air bubbles etc.

(b) Moderate magnifications of areas 0.03 mm square between unhydrated nuclei of cement and at the interface with other matrices to assess microstructural features of zones in which cement hydrate is laid down.

(c) Moderate magnifications of areas 0.03 mm square bordering cracks.

(d) Close examination of prominent structural features such as Calcium Hydroxide crystals and Etteringite crystals.

4.3 Discussion

A representative collection of micrographs is attached as Figures 9 to 45. The following statements are based on study of the SEM and EDR data:

4.3.1 Mixes made with Portland cement, Series A and B showed increasing voids and visible crystalline products, such as Ettringite, as water: cement w_0 was increased from 0.42 to 0.77. Fig. 18 shows a typical example of Calcium Hydroxide plates together with Calcium Sulpho-Aluminate (Ettringite) rods.

4.3.2 Mixes made with Blastfurnace slag were characterised by relatively high Mg contents and the presence of vitroous slag as shown in figures 22 to 24. The matrix was essentially similar in appearance to the A and B series.

4.3.3 Mixes made with Fly Ash (FA) showed massive deposits of Calcium Hydroxide (CH) around FAP particles. The micrographs suggest that this preferential precipitation of CH in what was originally water filled space separating FA is the reason why the C mixes showed reduced permeance.

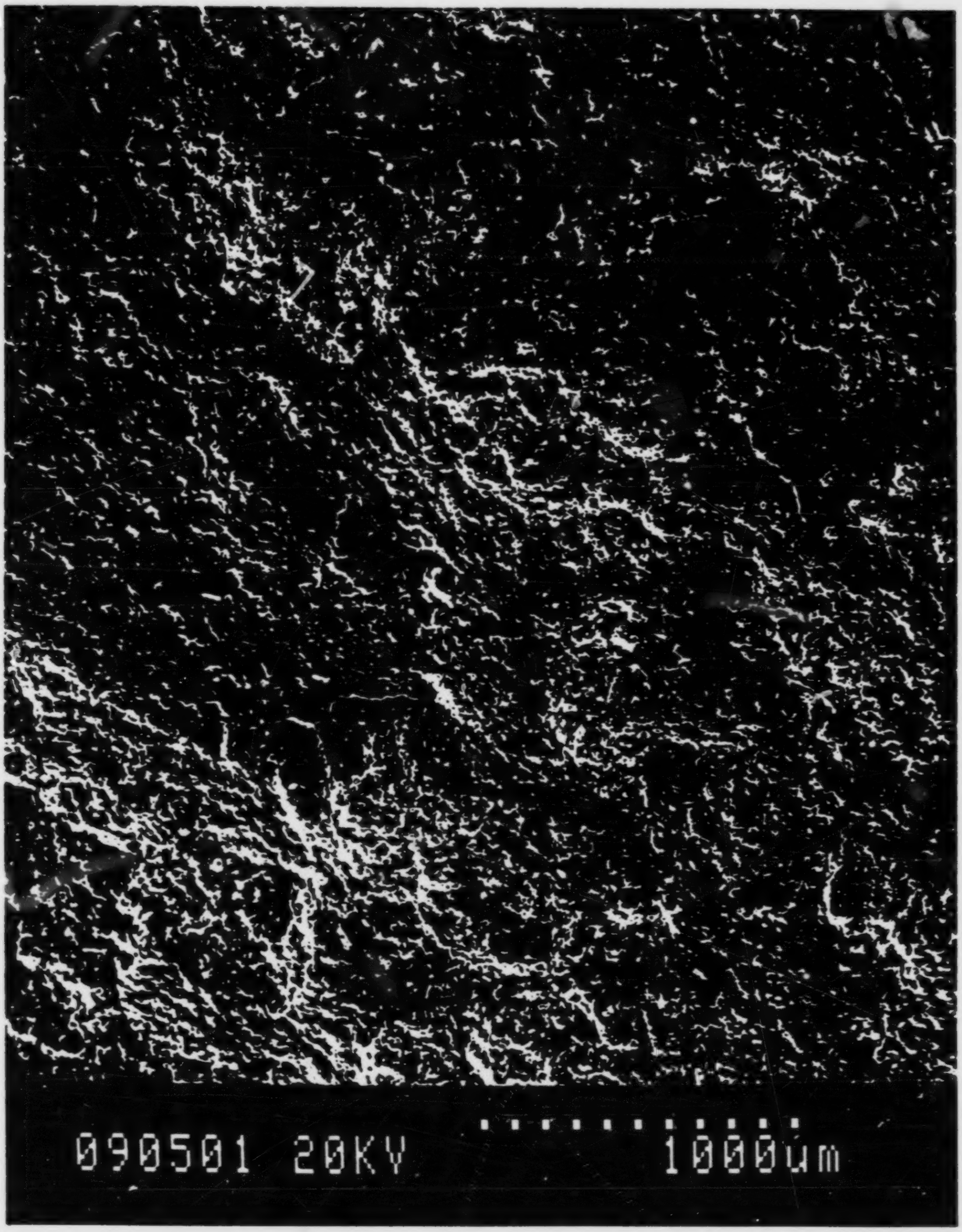
090501 20KV
1000um

Figure 9. Low magnification view of fracture surface* showing bleeding cavity partly filled with Calcium Hydroxide precipitated out of solution.

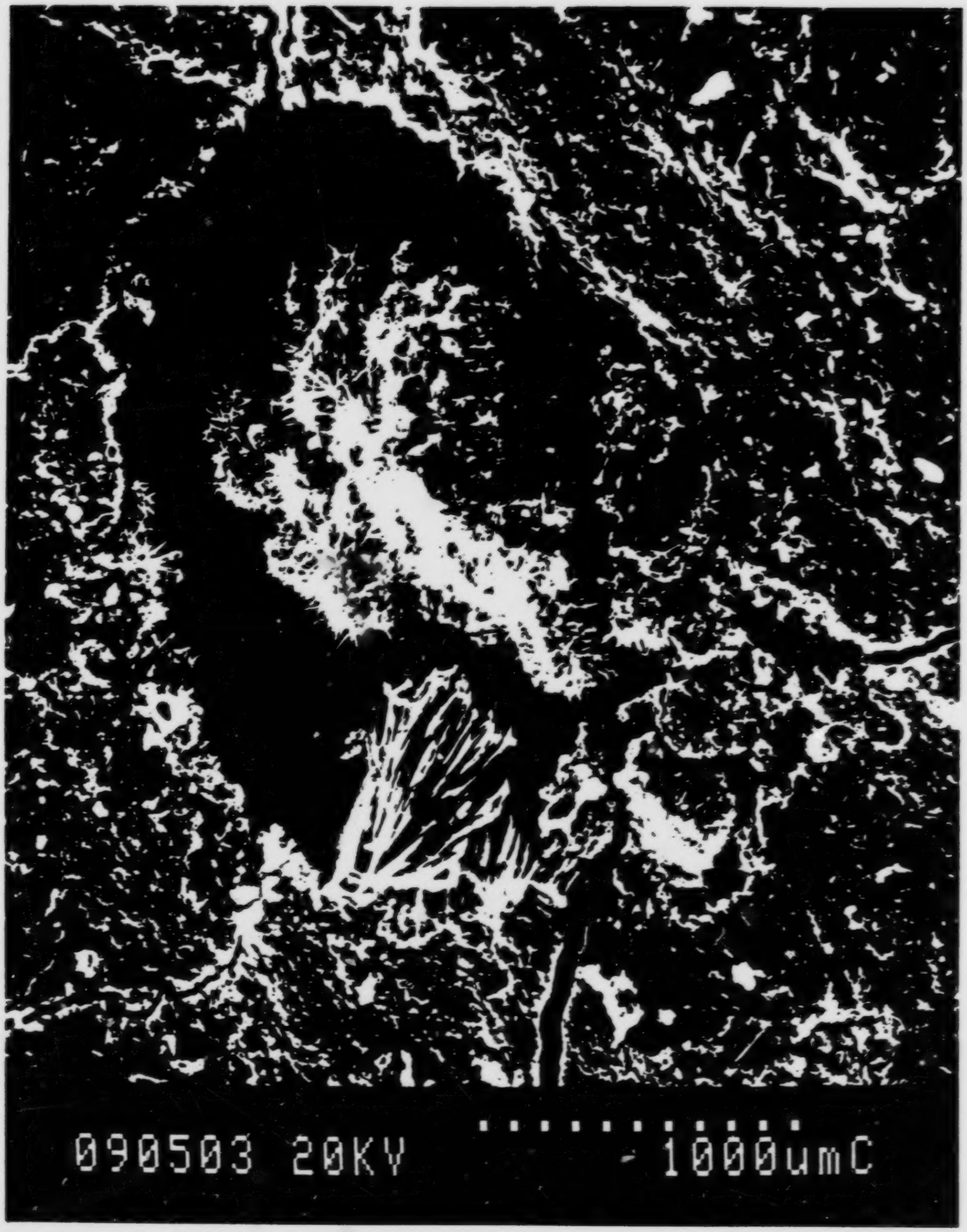
090503 20KV
1000umC

Figure 10. Close-up of continuous bleeding cavity partially filled with glassy Calcium Hydroxide and acicular Ettringite.

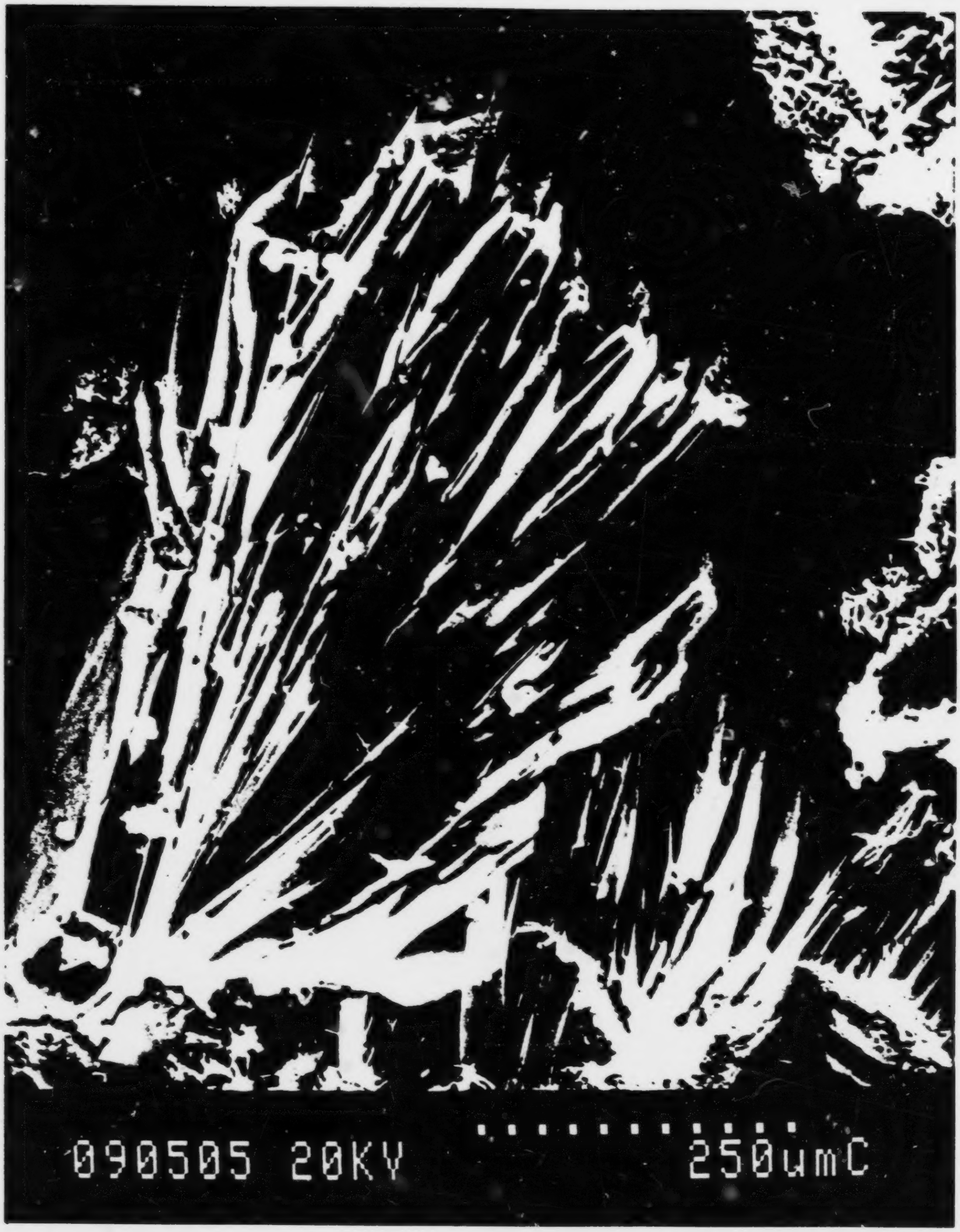
090505 20KV
250umC

Figure 11. Close-up of Calcium Hydroxide precipitated out of solution and partially filling bleeding cavity.

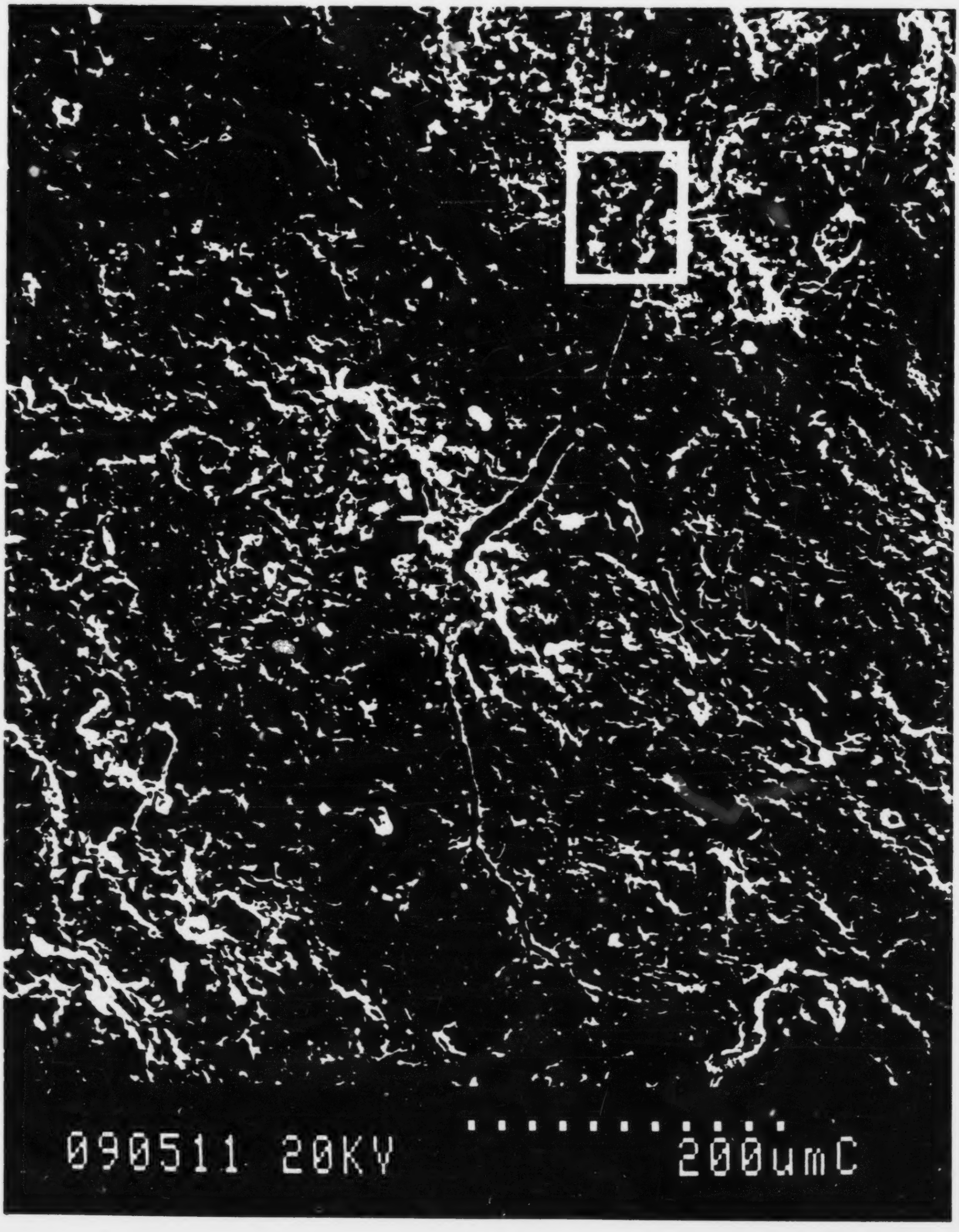
090511 20KV
200umC

Figure 12. Low magnification of fracture surface showing drying shrinkage cracks.

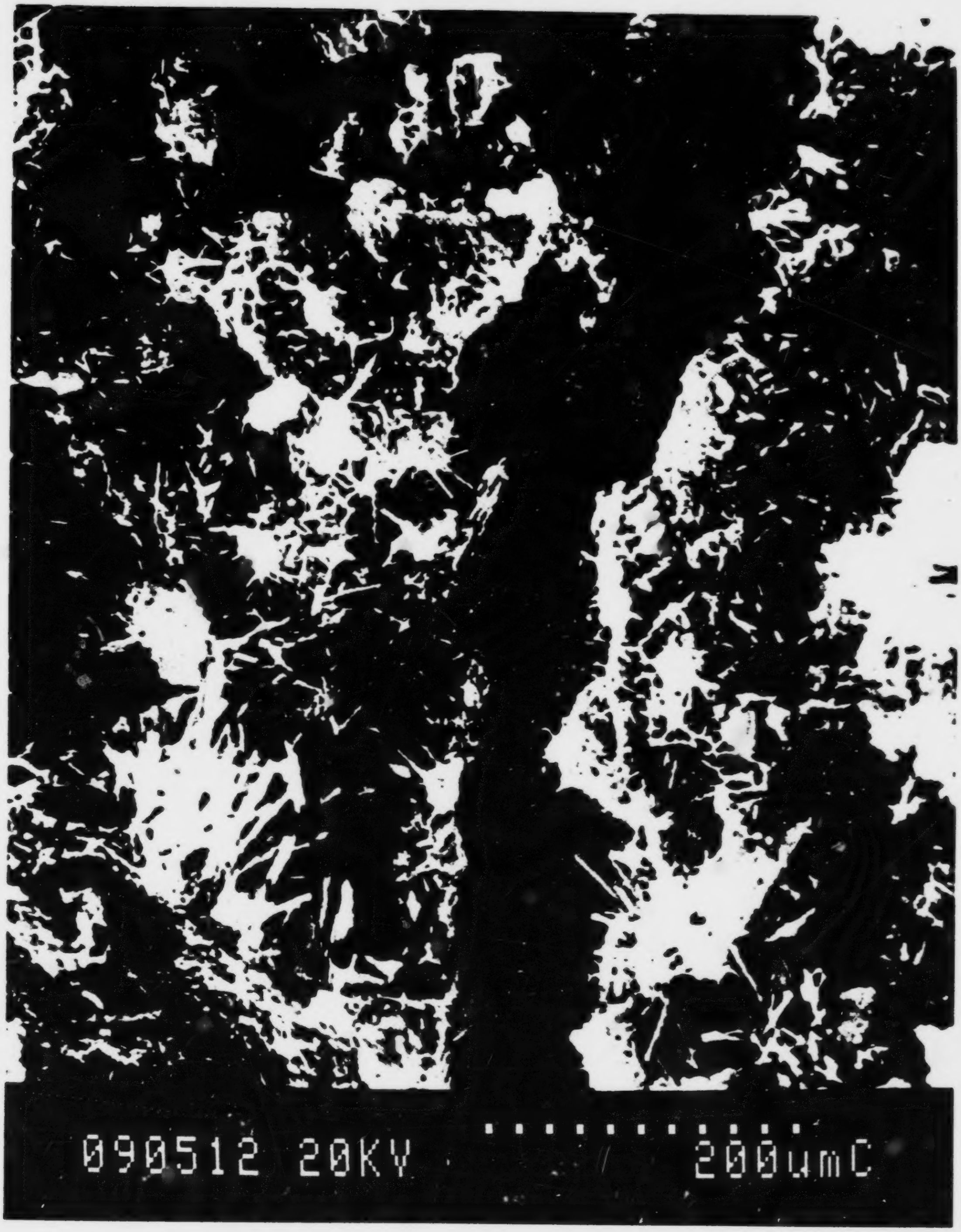
090512 20KV
200umC

Figure 13. Ettringite crystals on walls of shrinkage crack. Note that the crack is orders of magnitude larger than other natural cavities.

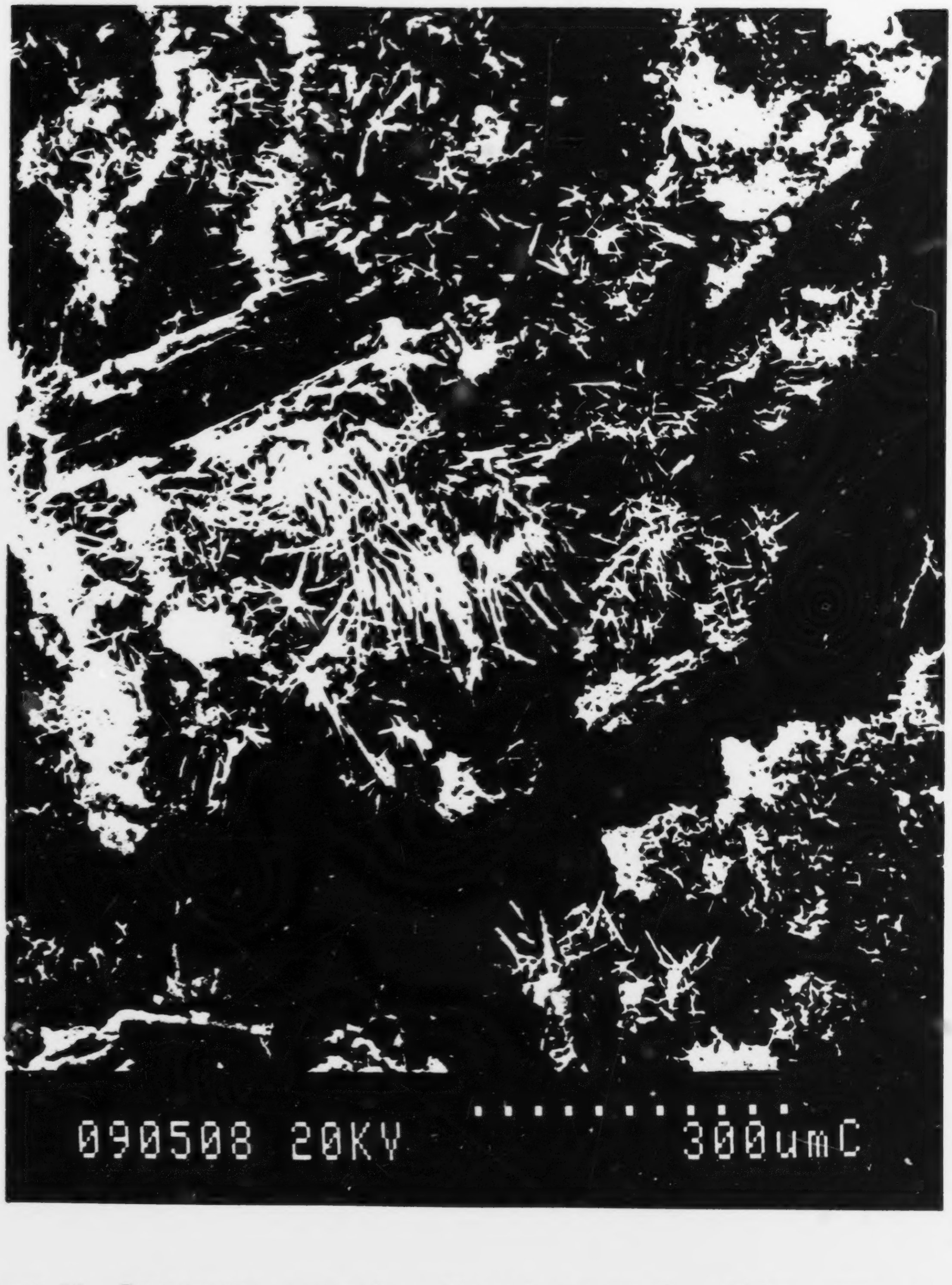
090508 20KV
300umC

Figure 14. Ettringite crystals adjacent to crack. Under some cricumstances formation of Ettringite causes cracking.

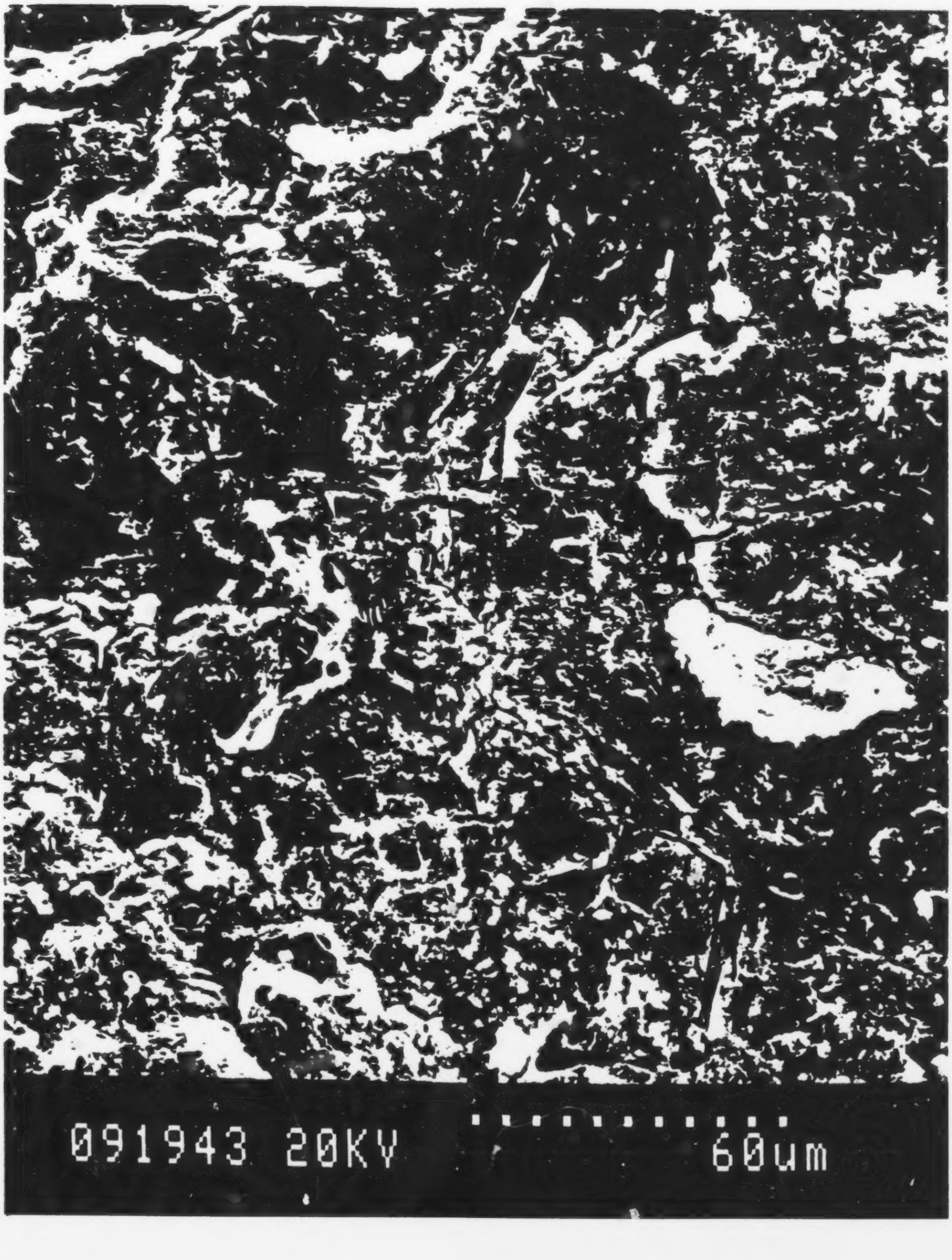
091943 20KV
60um

Figure 15. Typical fracture surface showing heavy precipitations of Calcium Hydroxide and cement grain remnants. Note shrinkage cracks.

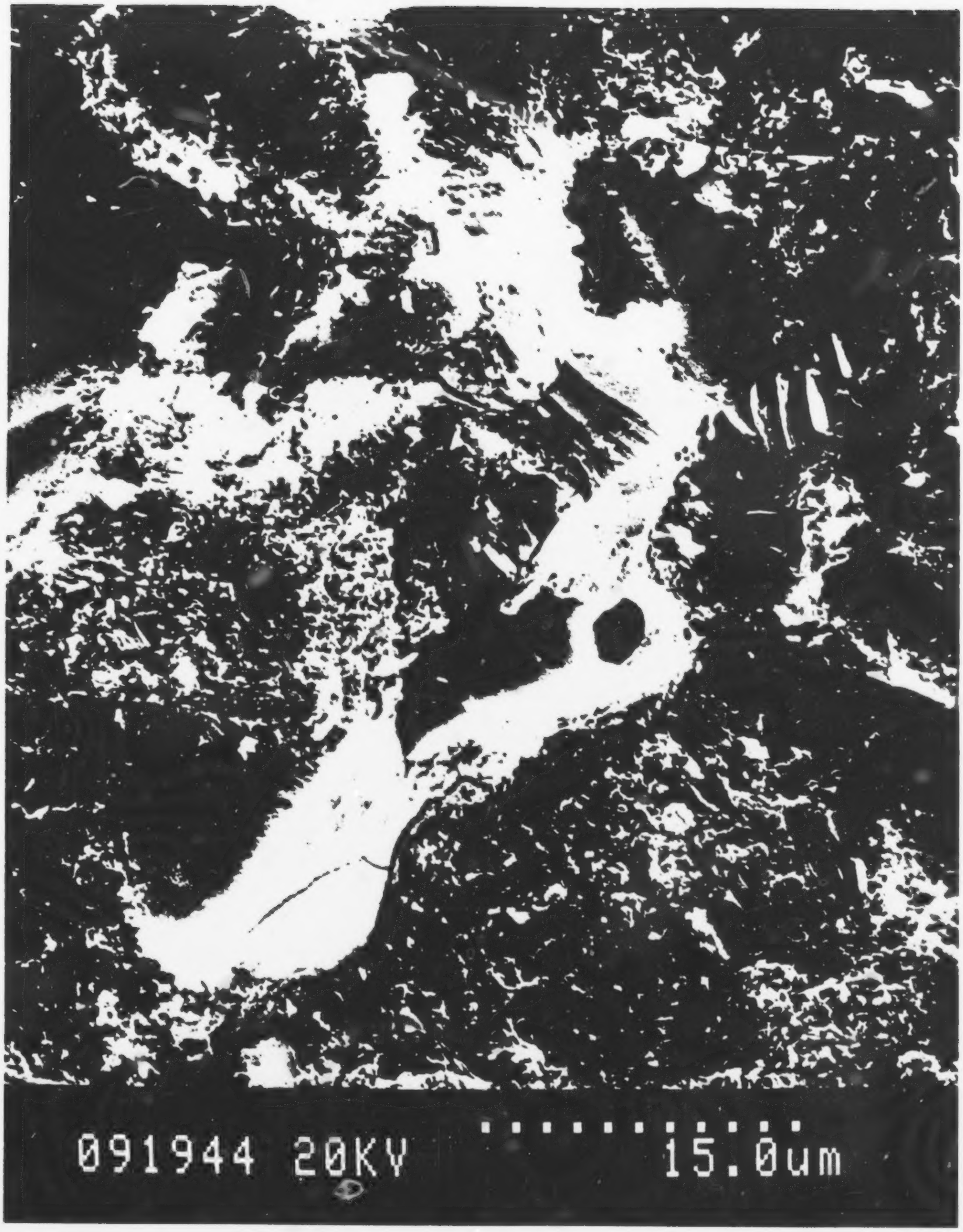
091944 20KV
15.0um

Figure 16. Selected area of Fig. 11 showing massive depositions of Calcium Hydroxide.

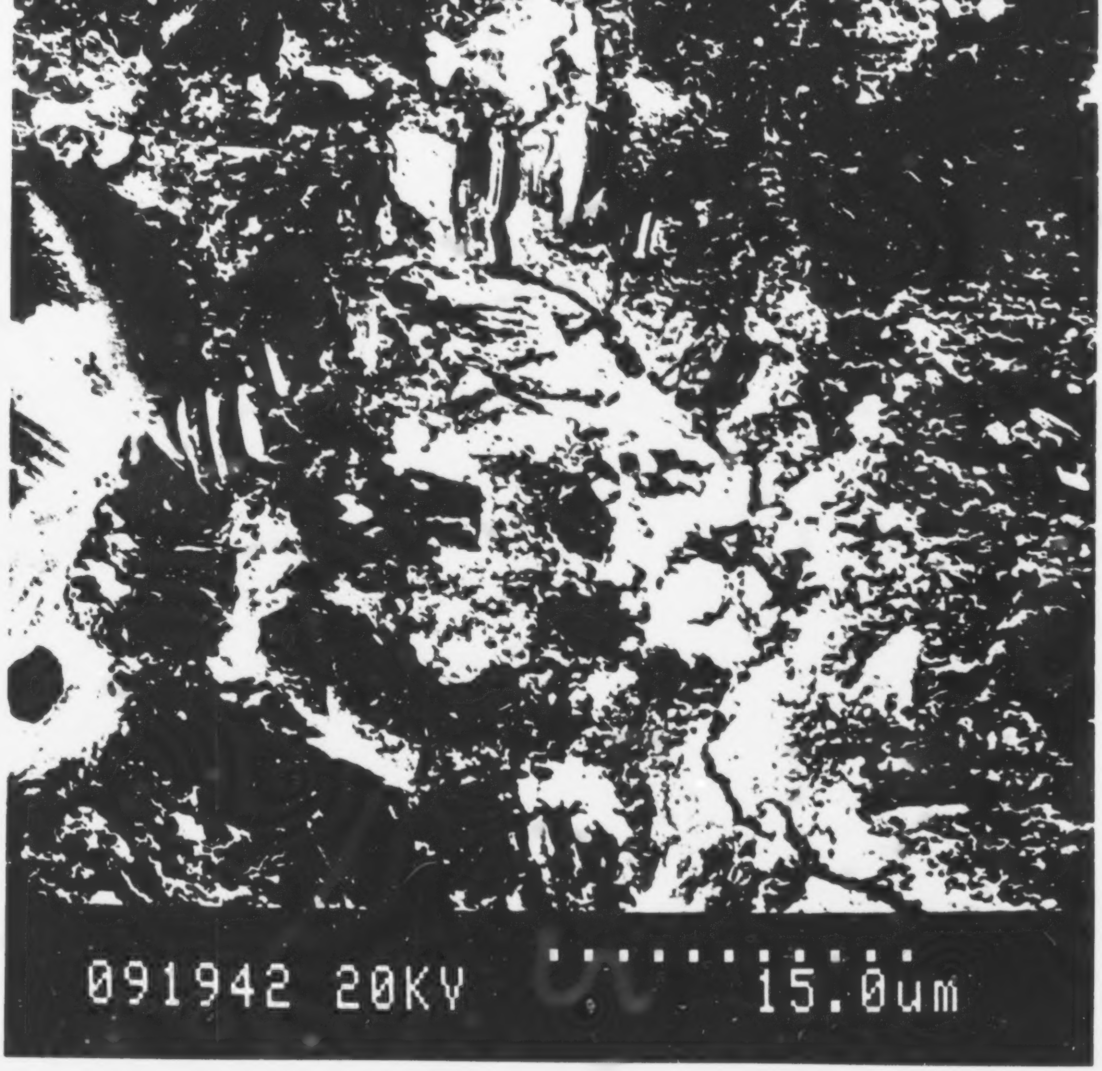
091942 20KV
15.0um

Figure 17. Selected area of Figure 15 showing cement grain remnants.

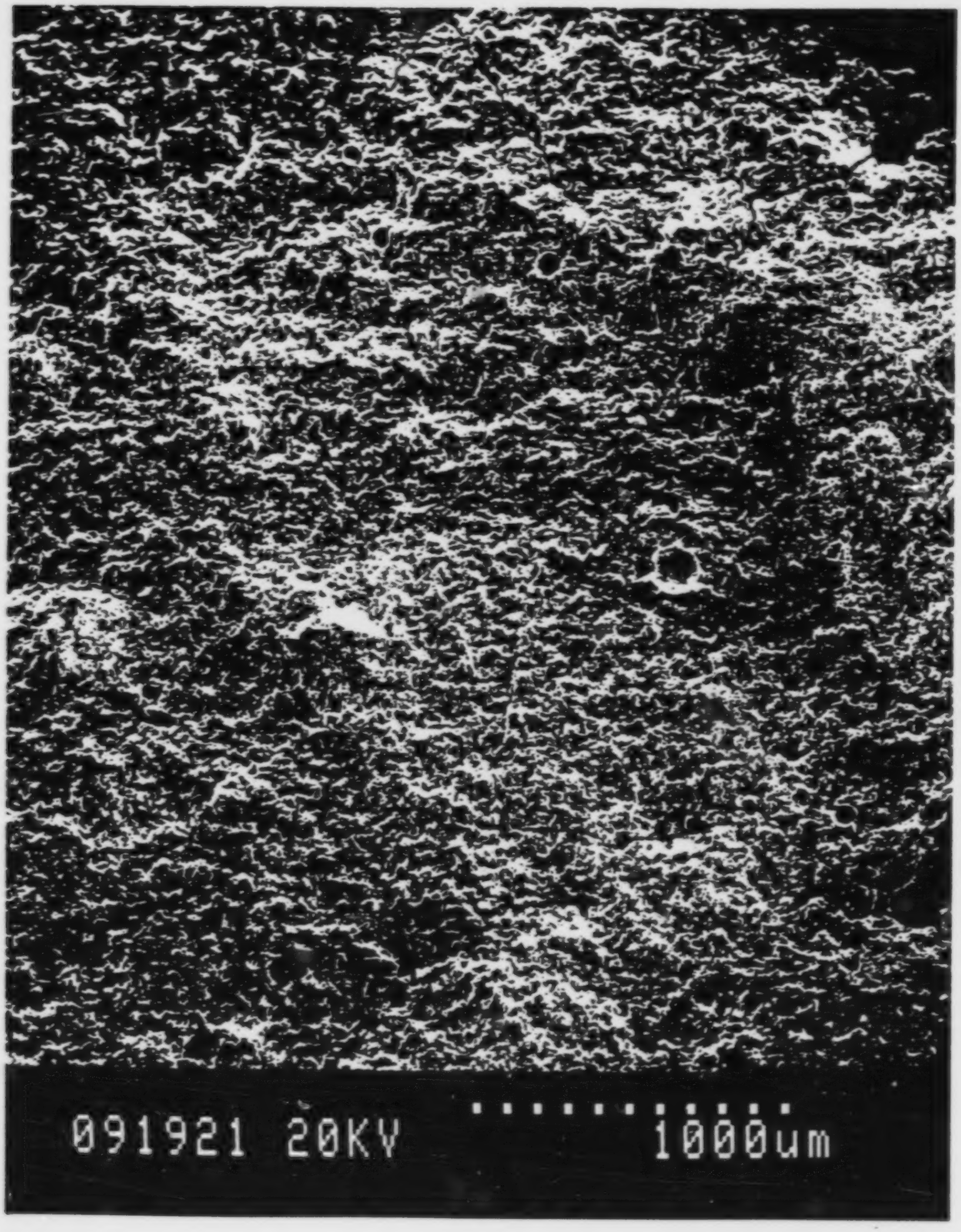
091921 20KV
1000um

Figure 18. General view of fracture surface. Note shrinkage cracks, bleeding cavity upper right and 3 small air bubbles.

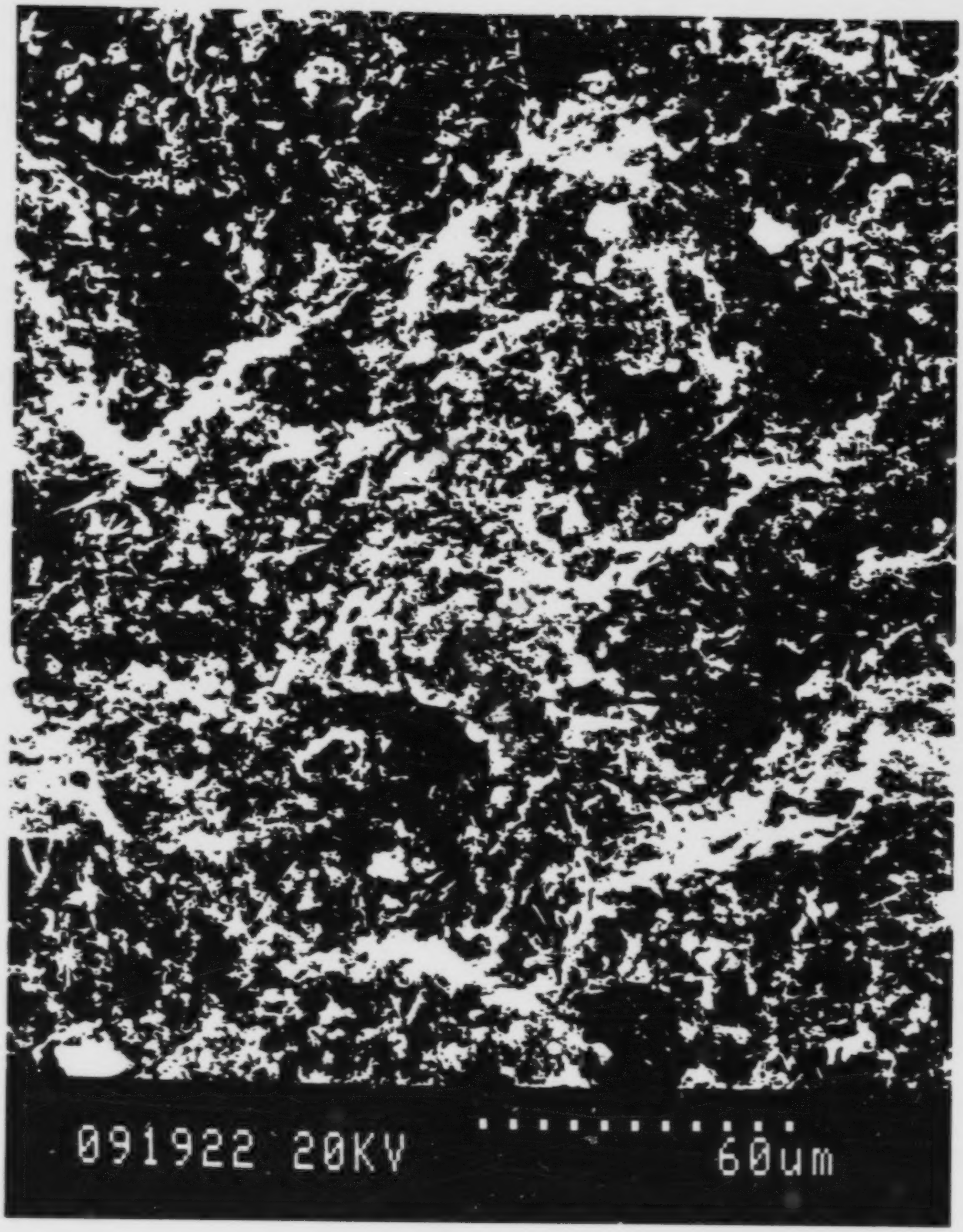
091922 20KV
60um

Figure 19. Selected area of Fig. 18. Showing extensive growth of acicular crystals.

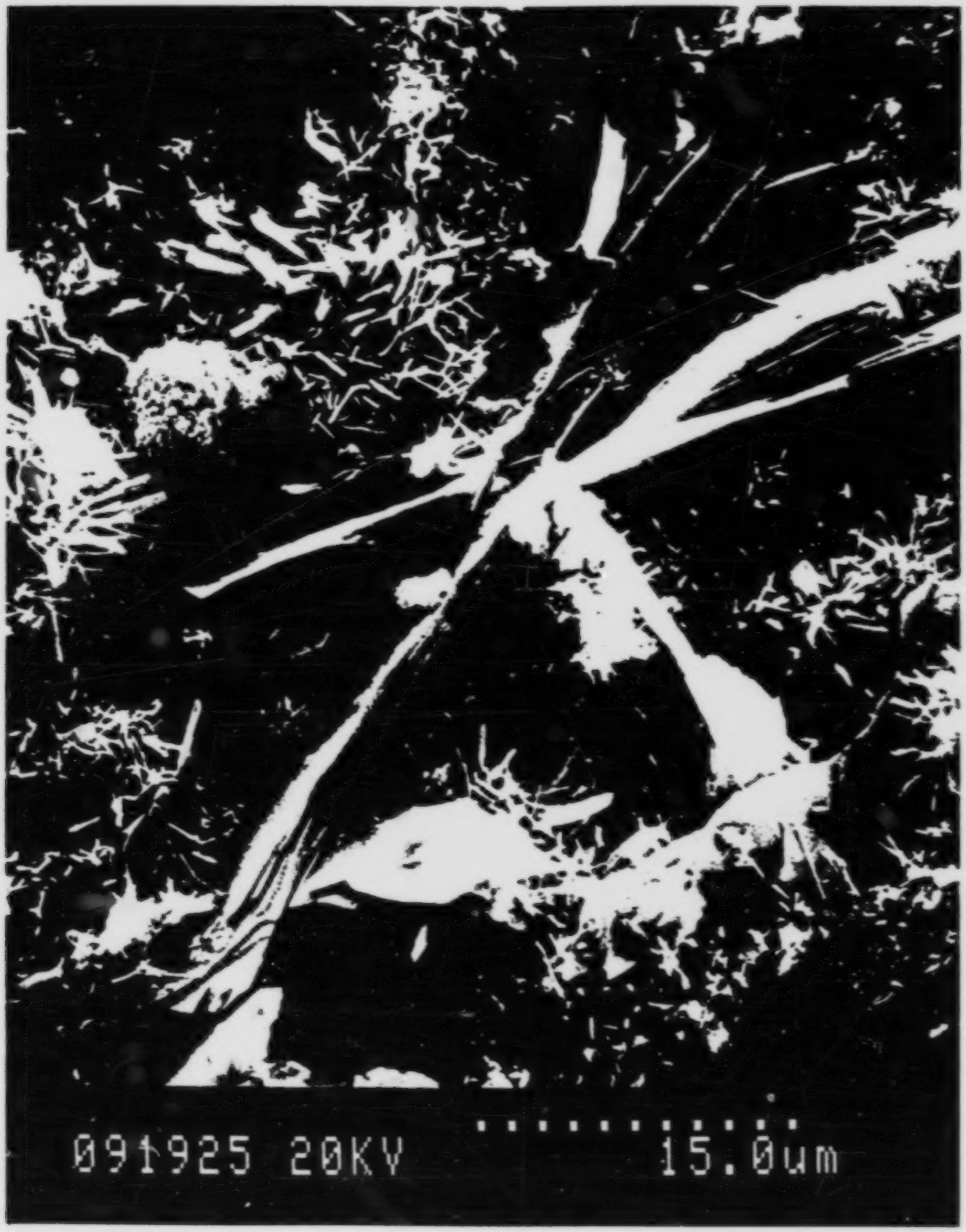

Figure 20. Selected area of Fig. 18. Showing layered Calcium Hydroxide (CH) and hexagonal crystals of Ettringite (CSH). CH is precipitated out of solution while CAH grows from clinker surfaces.

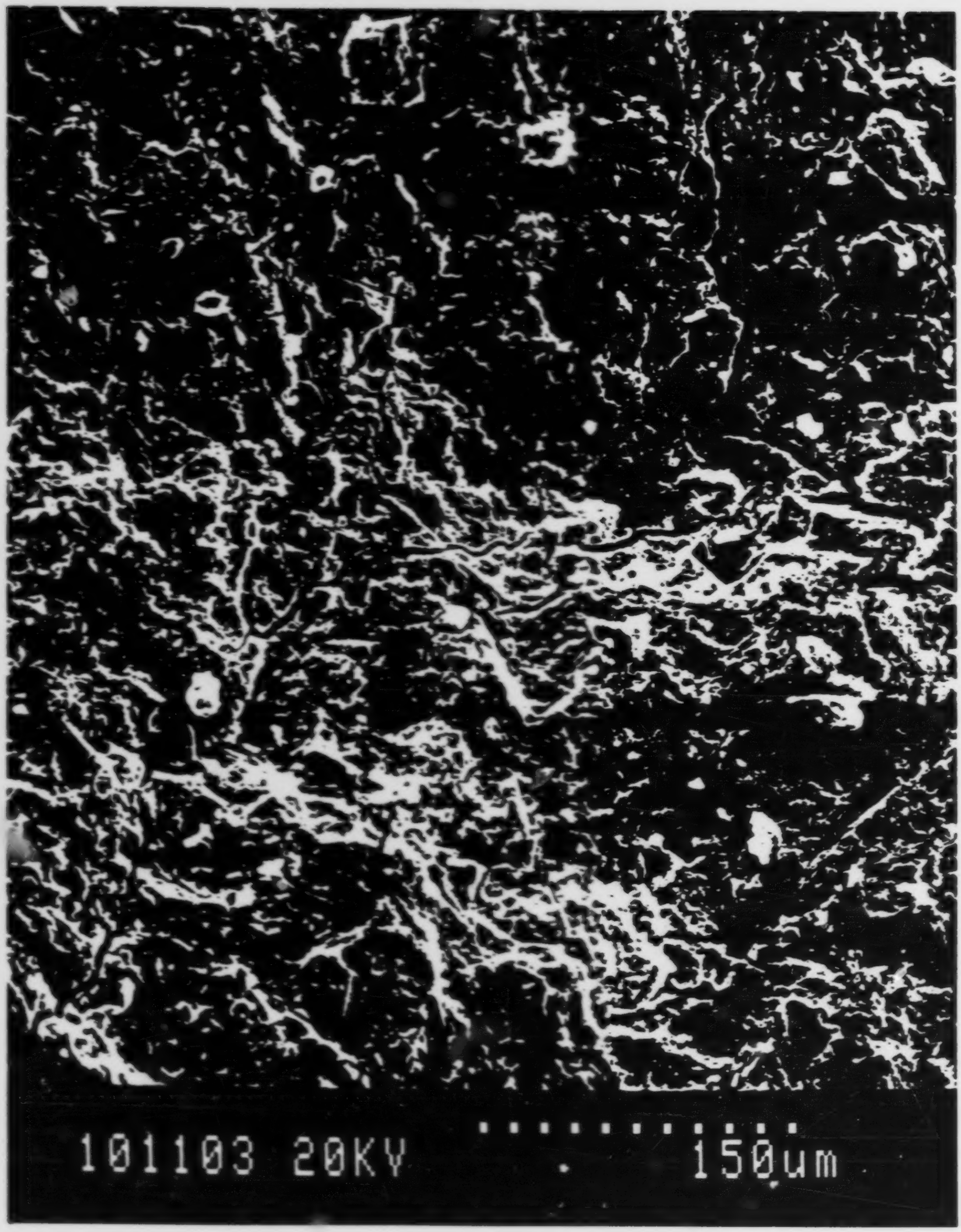
101103 20KV
150um

Figure 21. General view of Portland cement specimen showing shrinkage cracks, massive depositions of Calcium Hydroxide (CH) and cement clinker remnants.

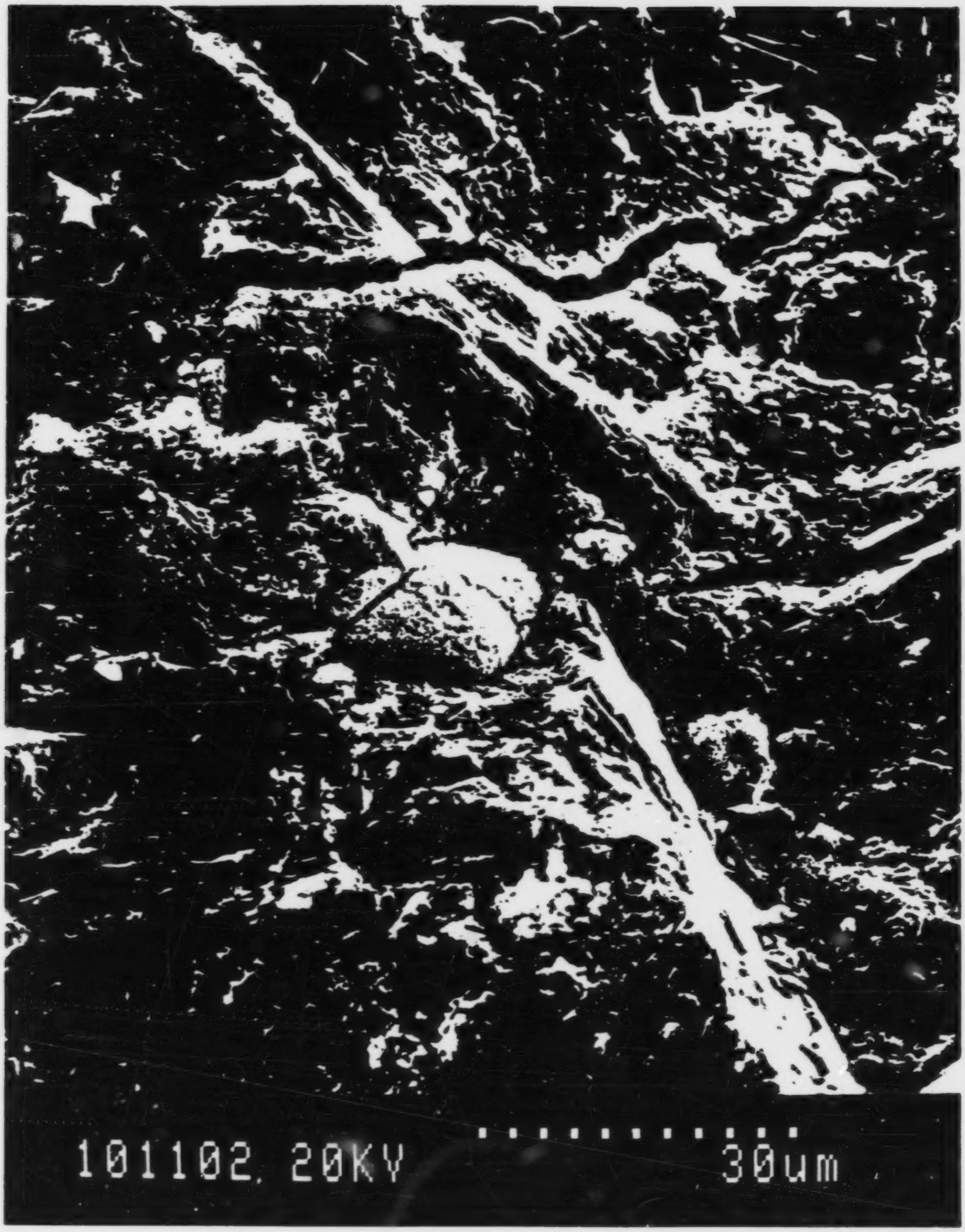
101102 20KV
30um

Figure 22. Selected area showing massive Calcium Hydroxide and cement clinker remnant in centre field.

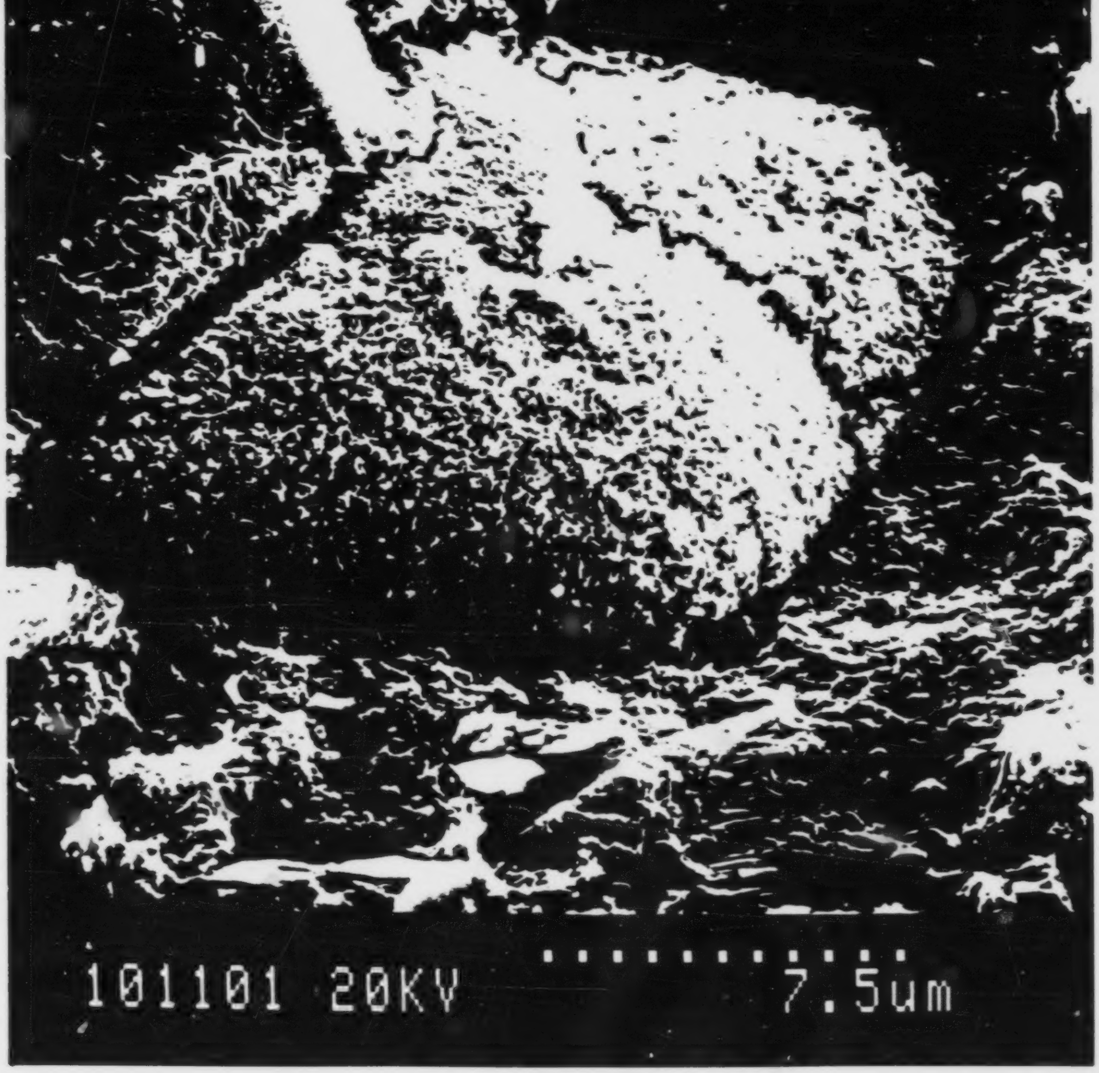
101101 20KV
7.5um

Figure 23. Cement grain remnant of Figure 22 separated on boundary from surrounding hydrate material by a peripheral shrinkage crack.

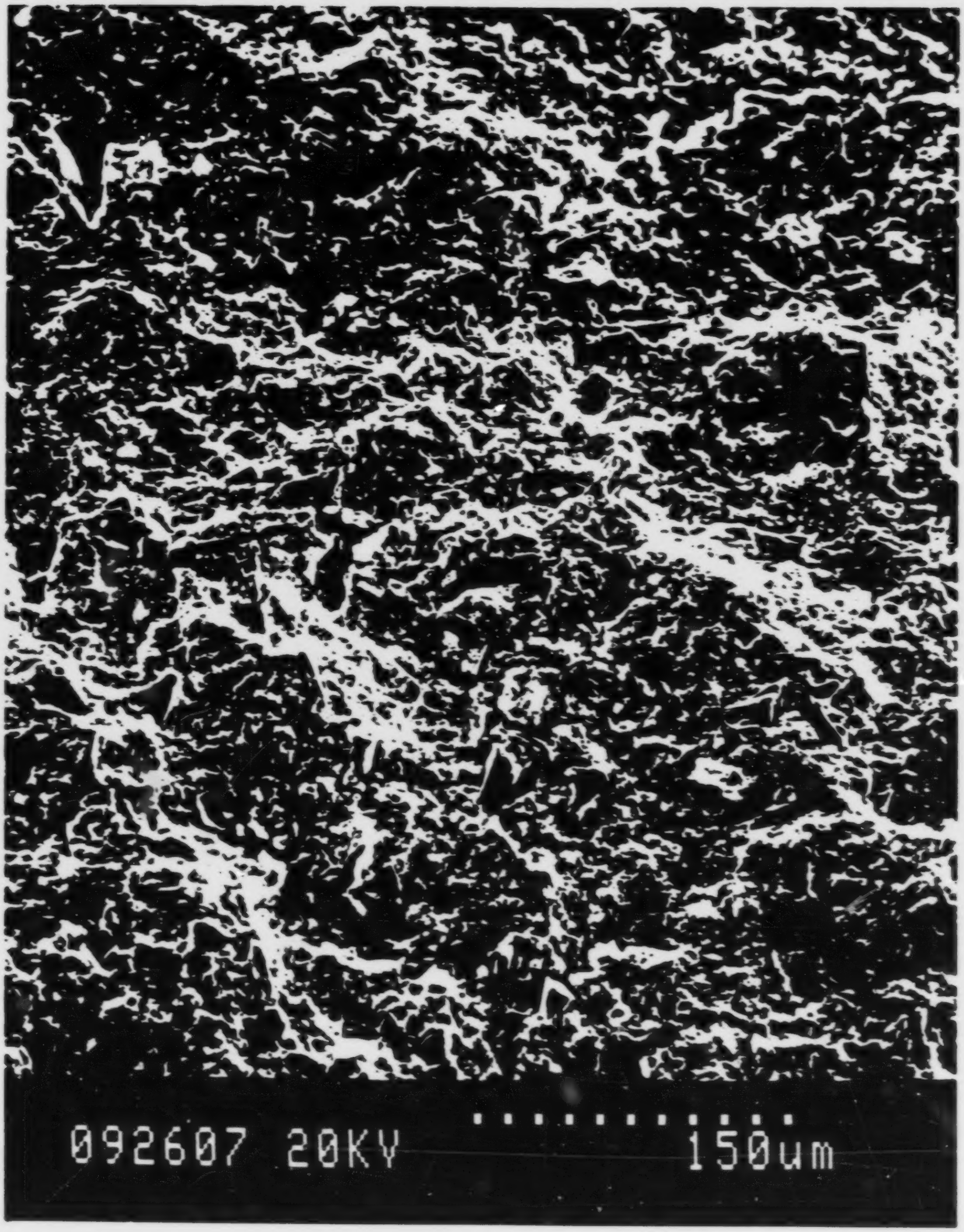
092607 20KV
150um

Figure 24. General view of specimen containing Silica flour having w_c=0.64. Note porous nature of matrix compared with Figure 21.

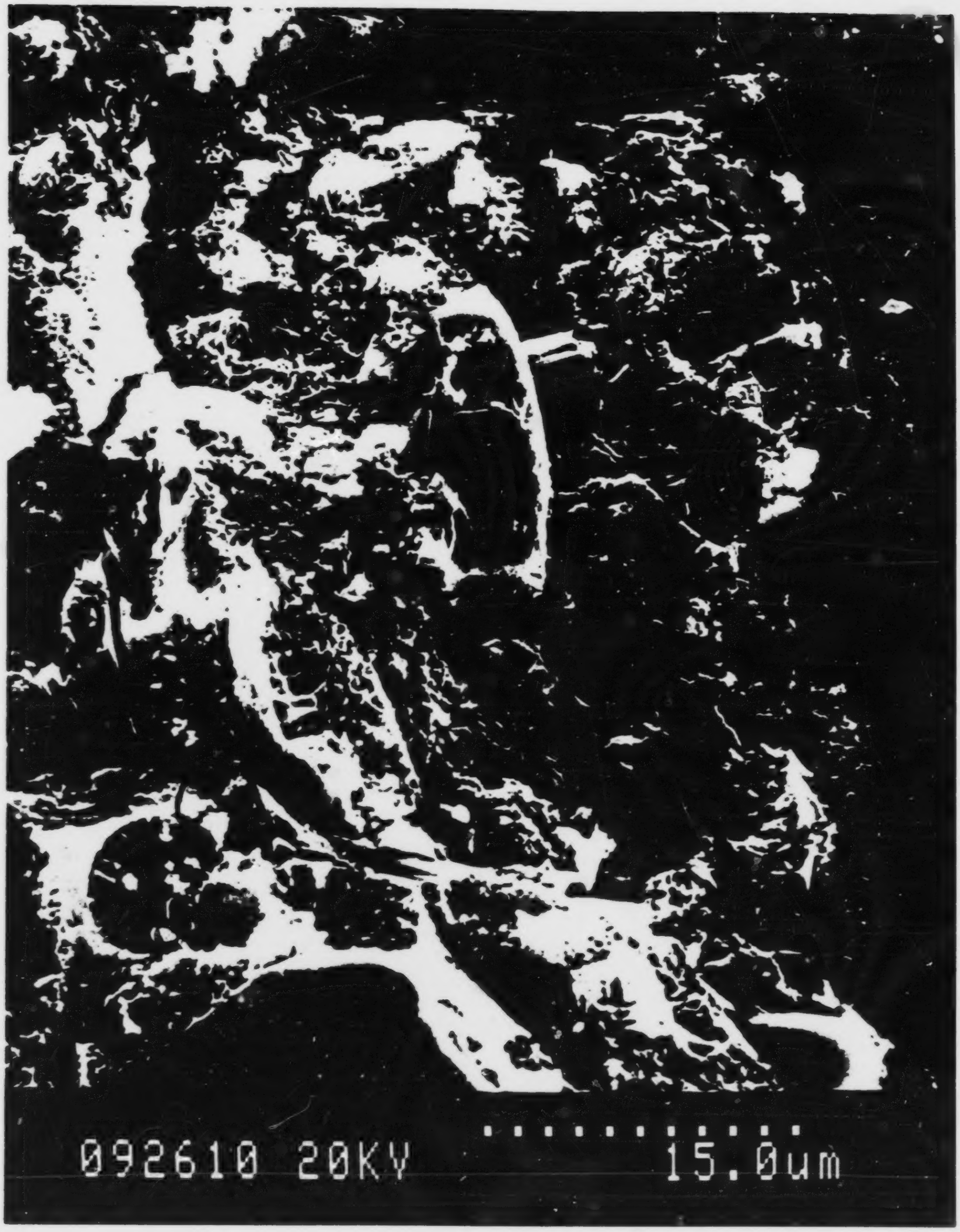
092610 20KV
15.0um

Figure 25. Selected area of Fig. 20 showing Silica particles in centre field surrounded by Calcium Hydroxide

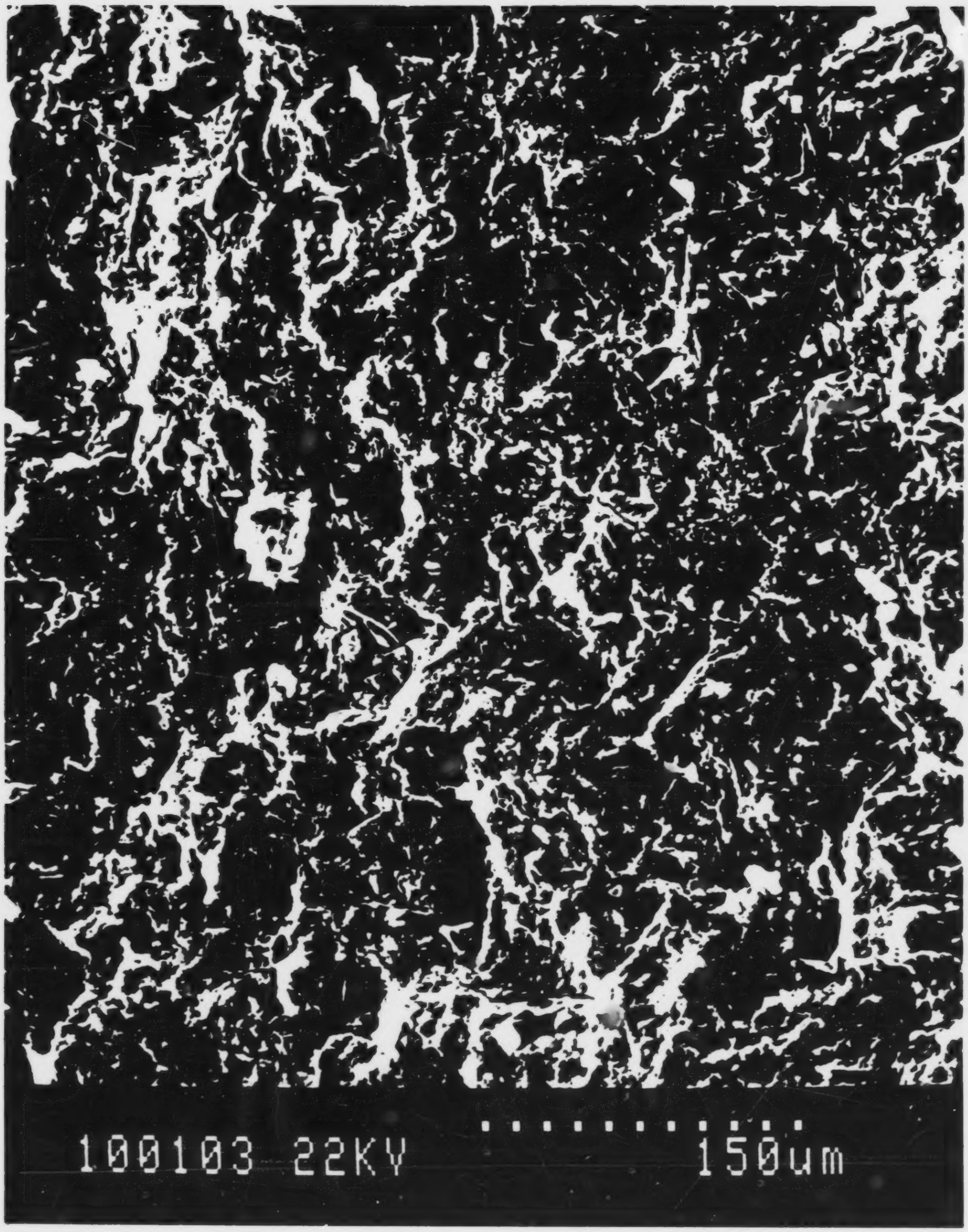

Figure 26. Low magnification view of fracture surface showing unhydrated Blastfurnace slag (BFS) particles. Note relatively porous nature of concrete and relatively small shrinkage cracks.

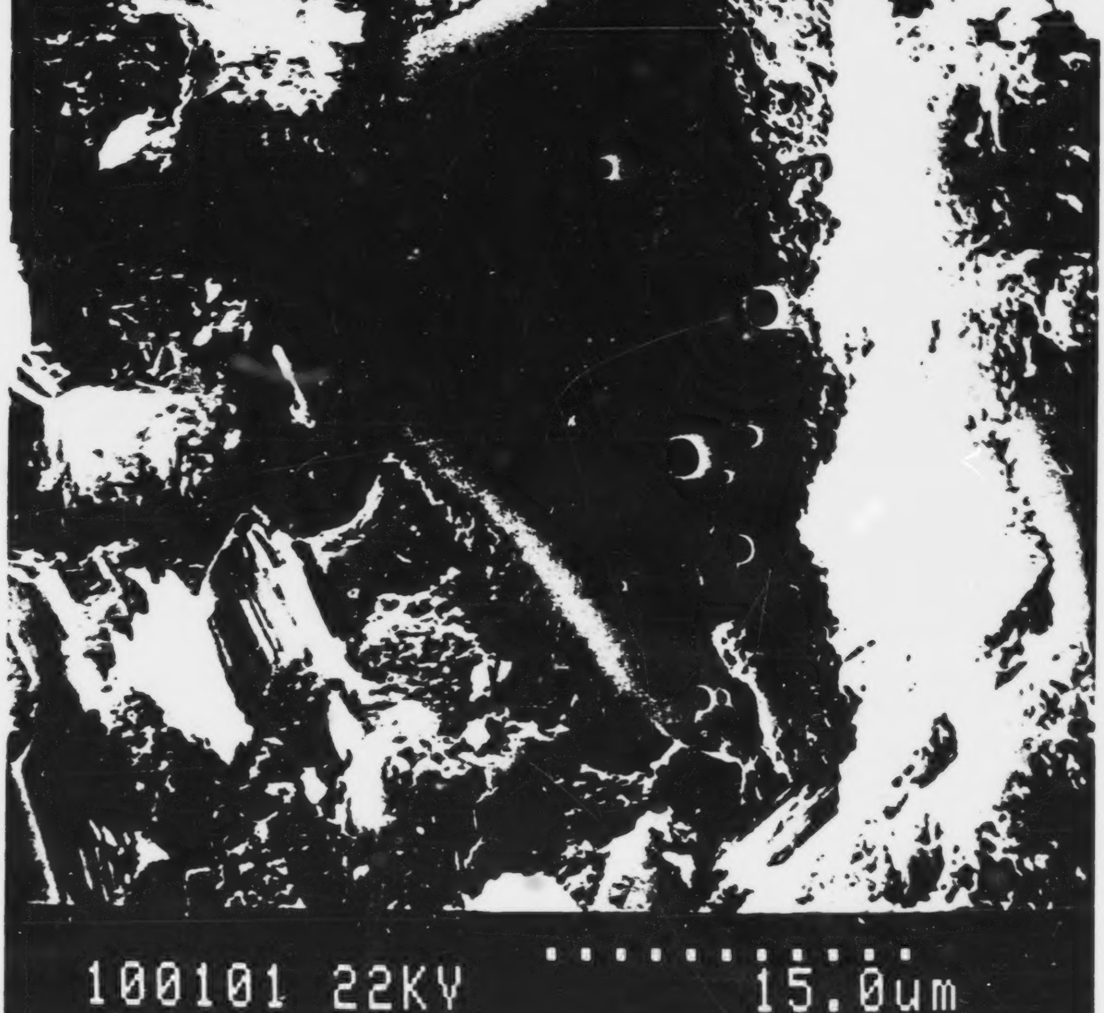
100101 22KV
15.0um

Figure 27. Vitreous Blastfurnace slag particle and surrounding matrix of
[illegible]

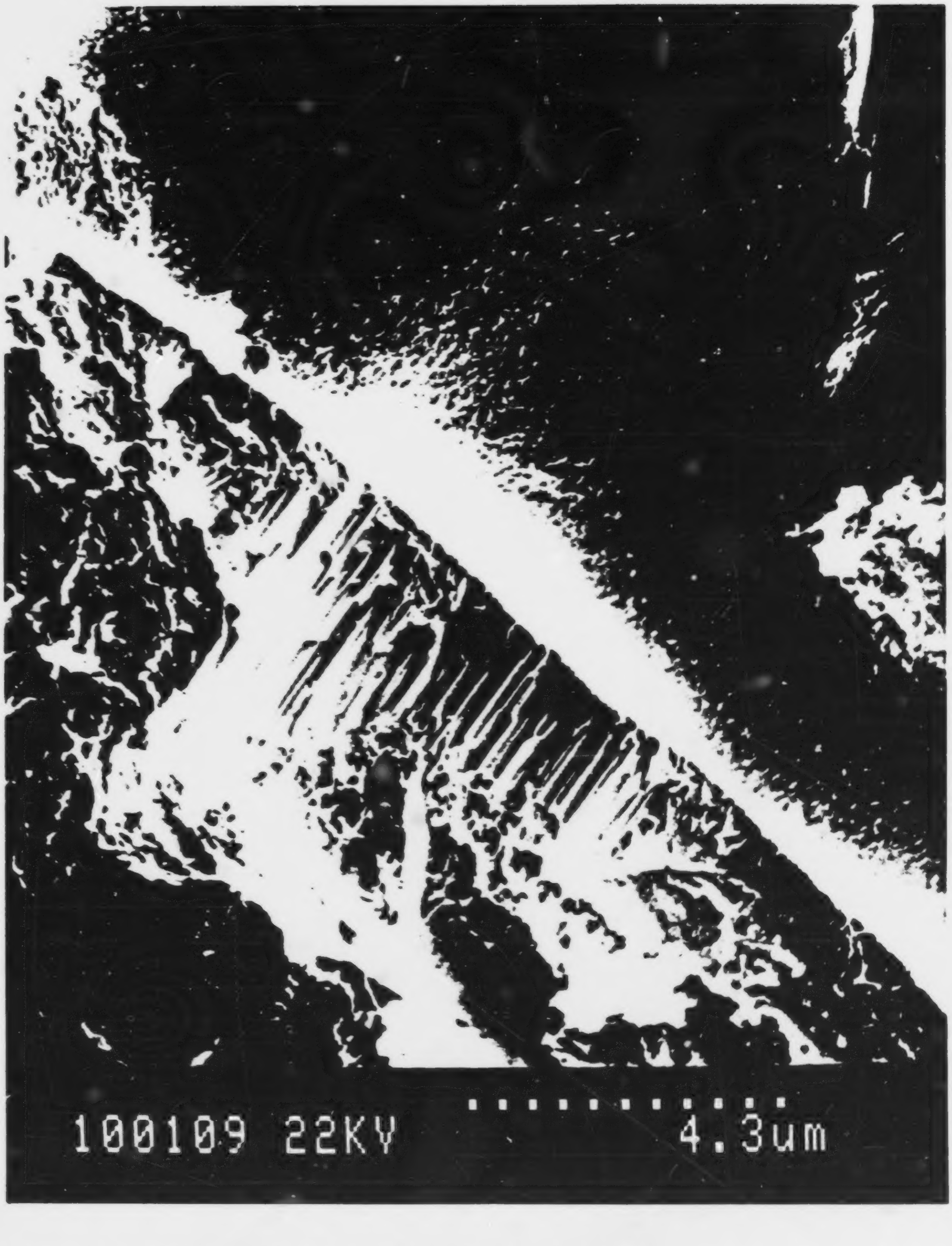
100109 22KV
4.3um

Figure 28. Interface of BFS particle and hydrate

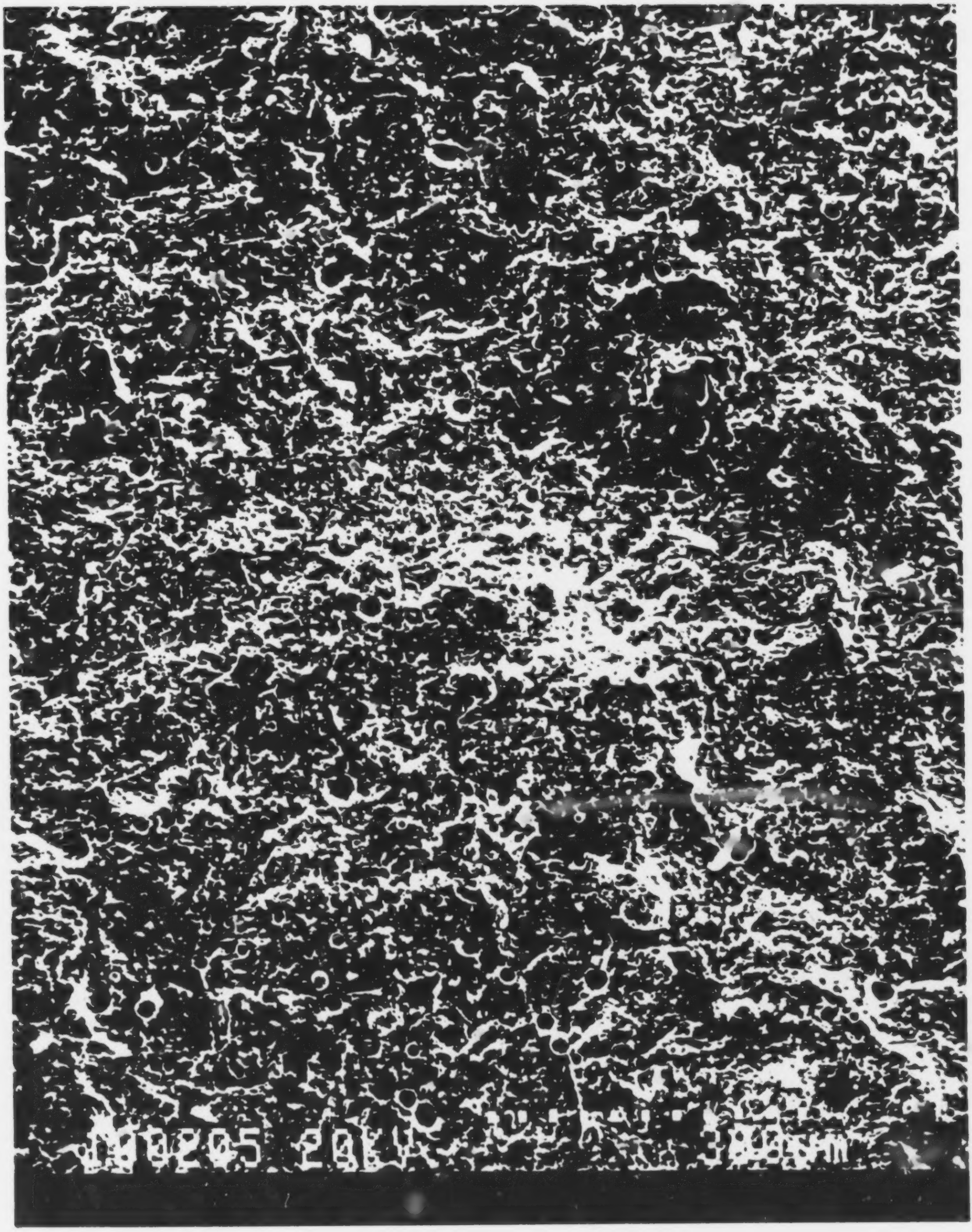

Figure 29. Low magnification view of work area. Note spherical Fly Ash particles and sockets left by such particles in fracture surface.

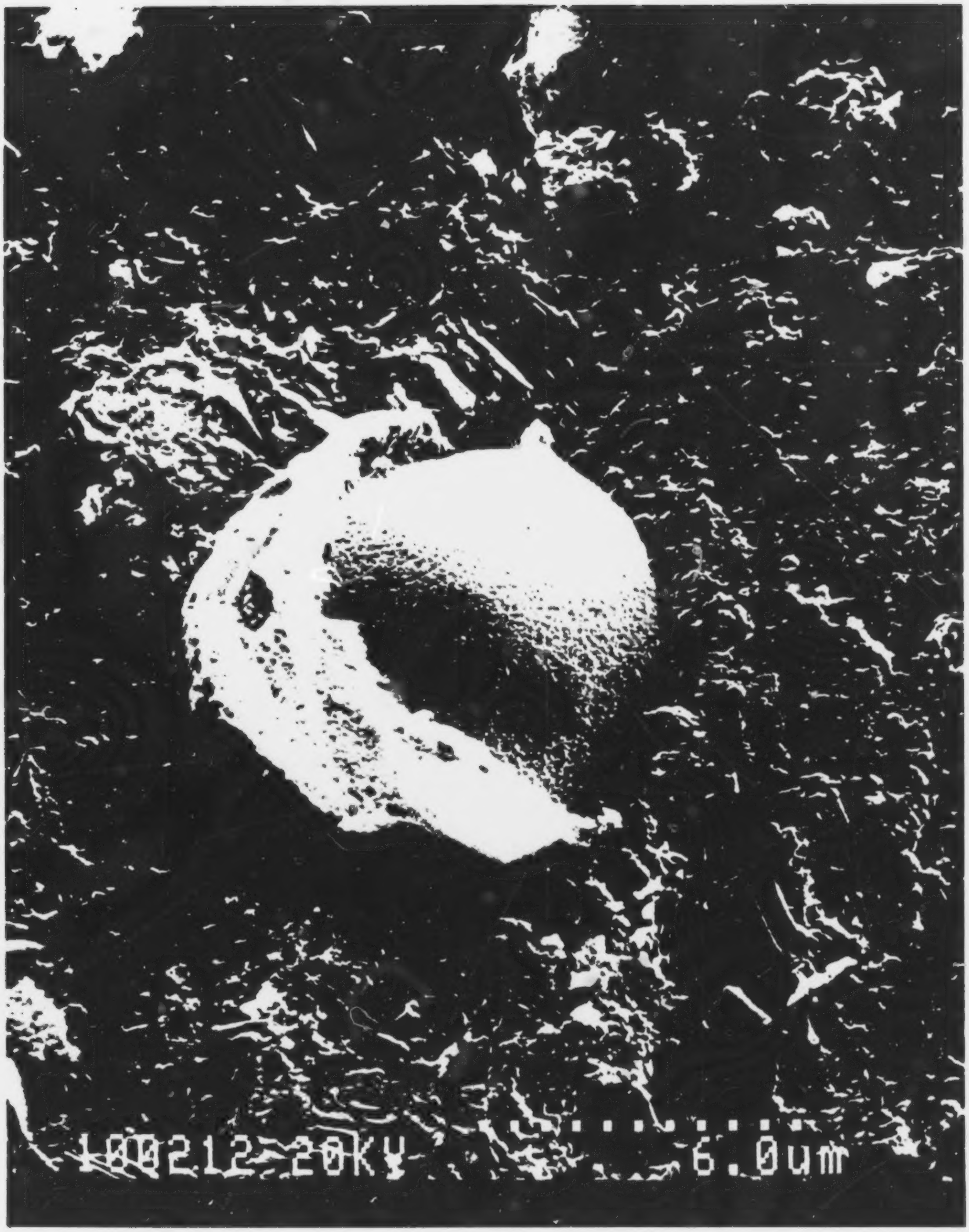
100212 20KV
6.0um

Figure 30. Siliceous Fly Ash particle with adhering shell of hydrated materials.

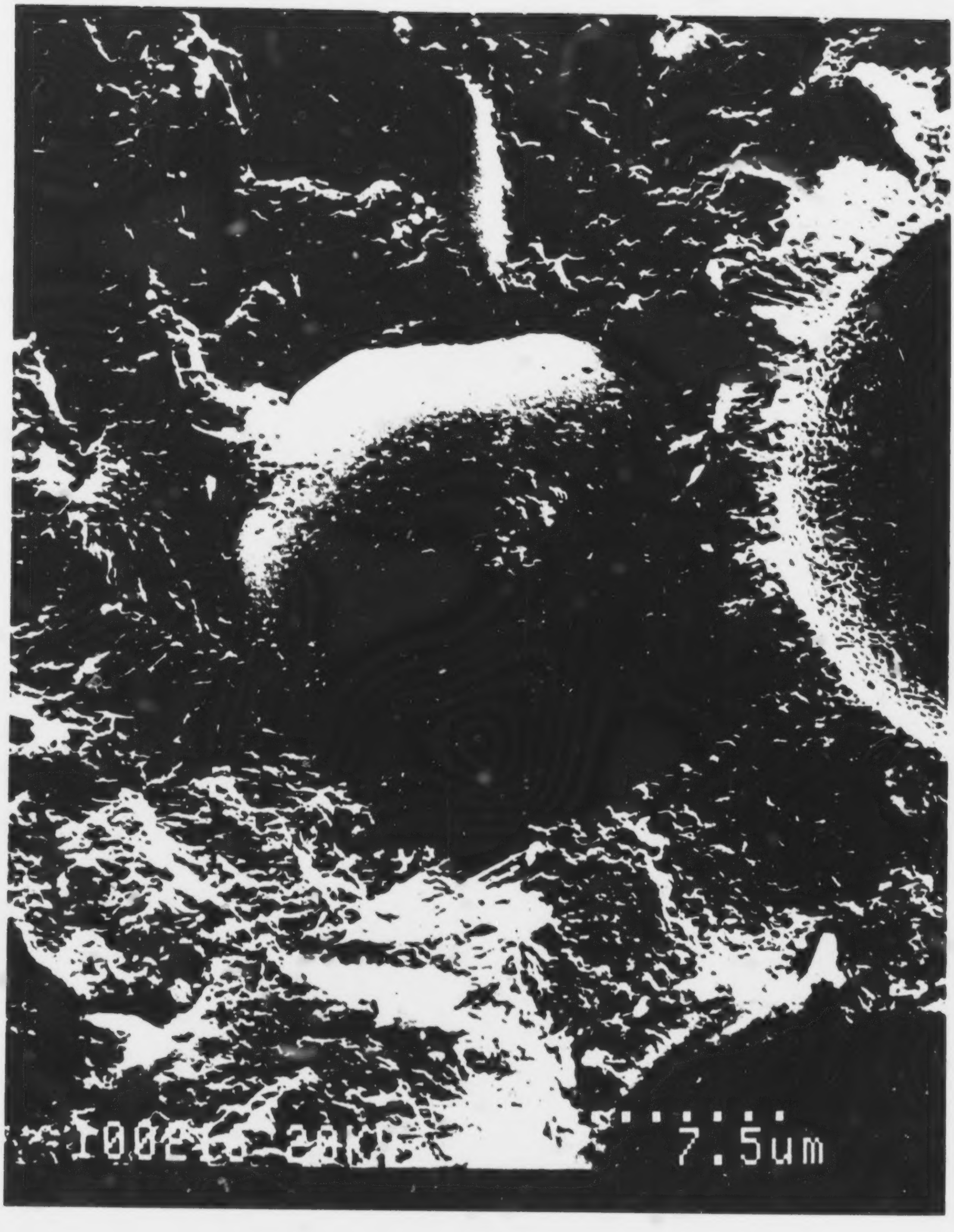

Figure 31. Siliceous (Si) Fly Ash particles (FAP) with Calcium Silicate Hydrate (CSH) and Calcium Hydroxide (CH) matrix. Note socket left by FAP on right.

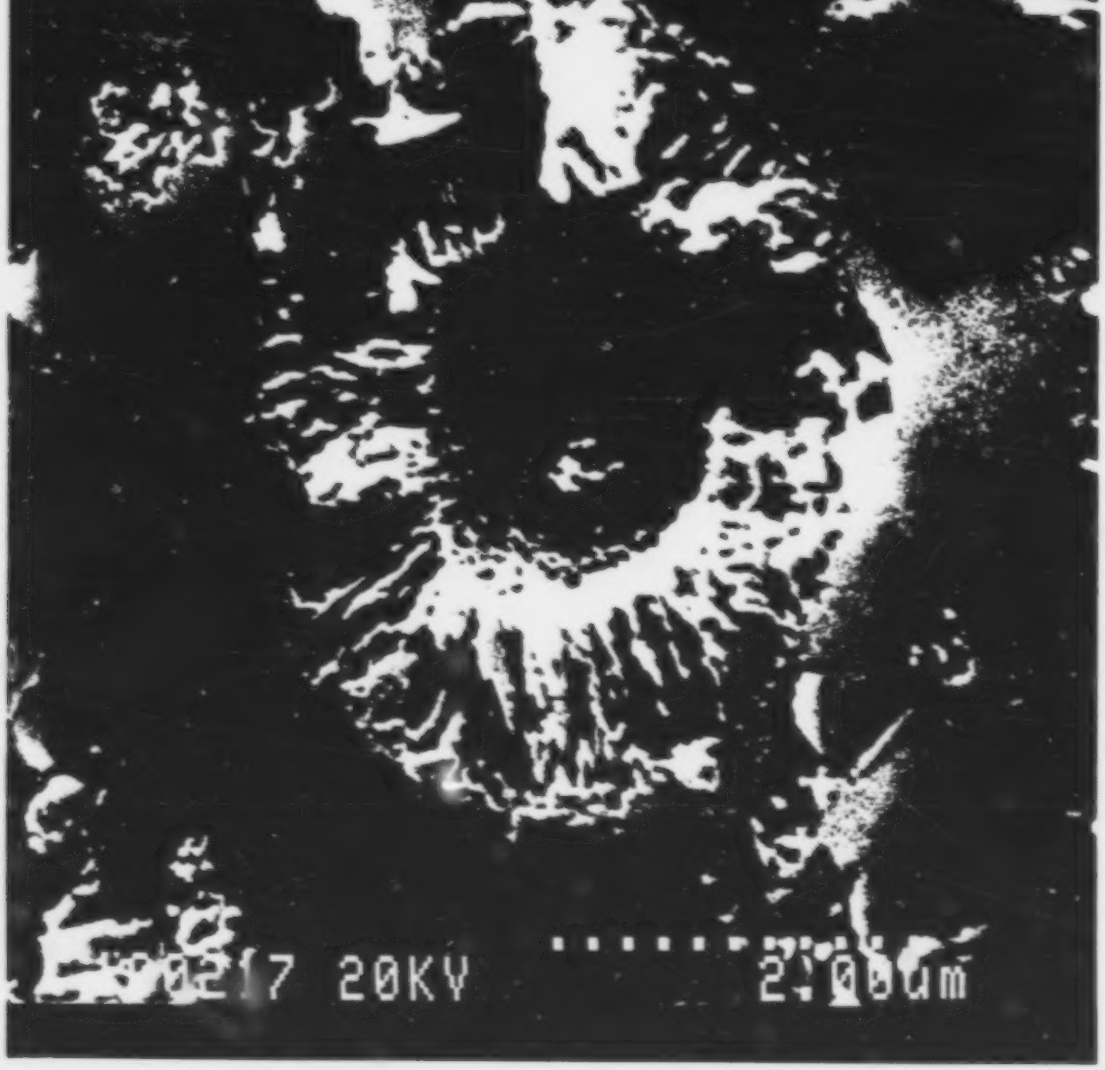
0217 20KV
2.00um

Figure 32. CH with hollow left by unhydrated nucleus of FAP and porous nature of surrounding shell of CSH hydrate.

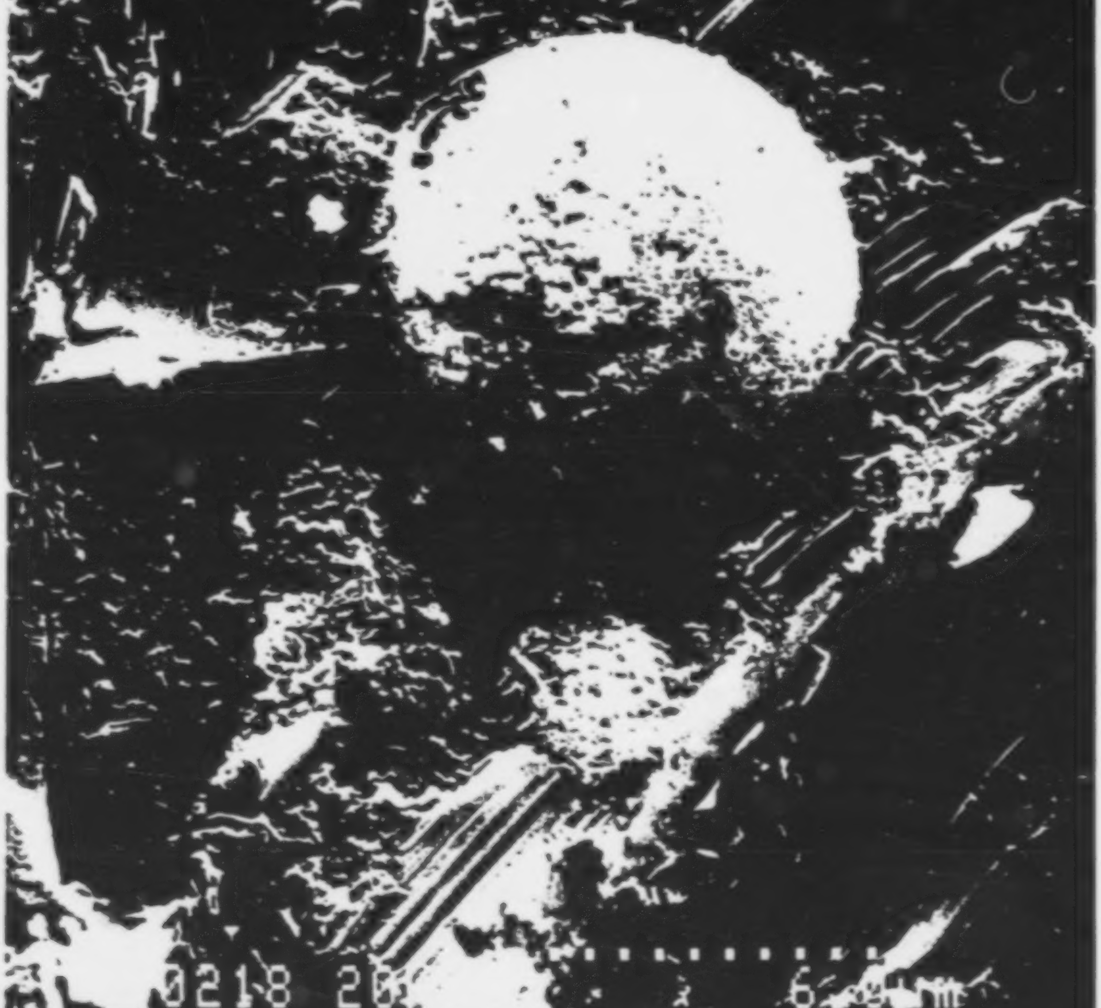

Figure 33. Hollow FAP with strongly oriented CH and with smaller FAP almost totally consumed in the reaction.

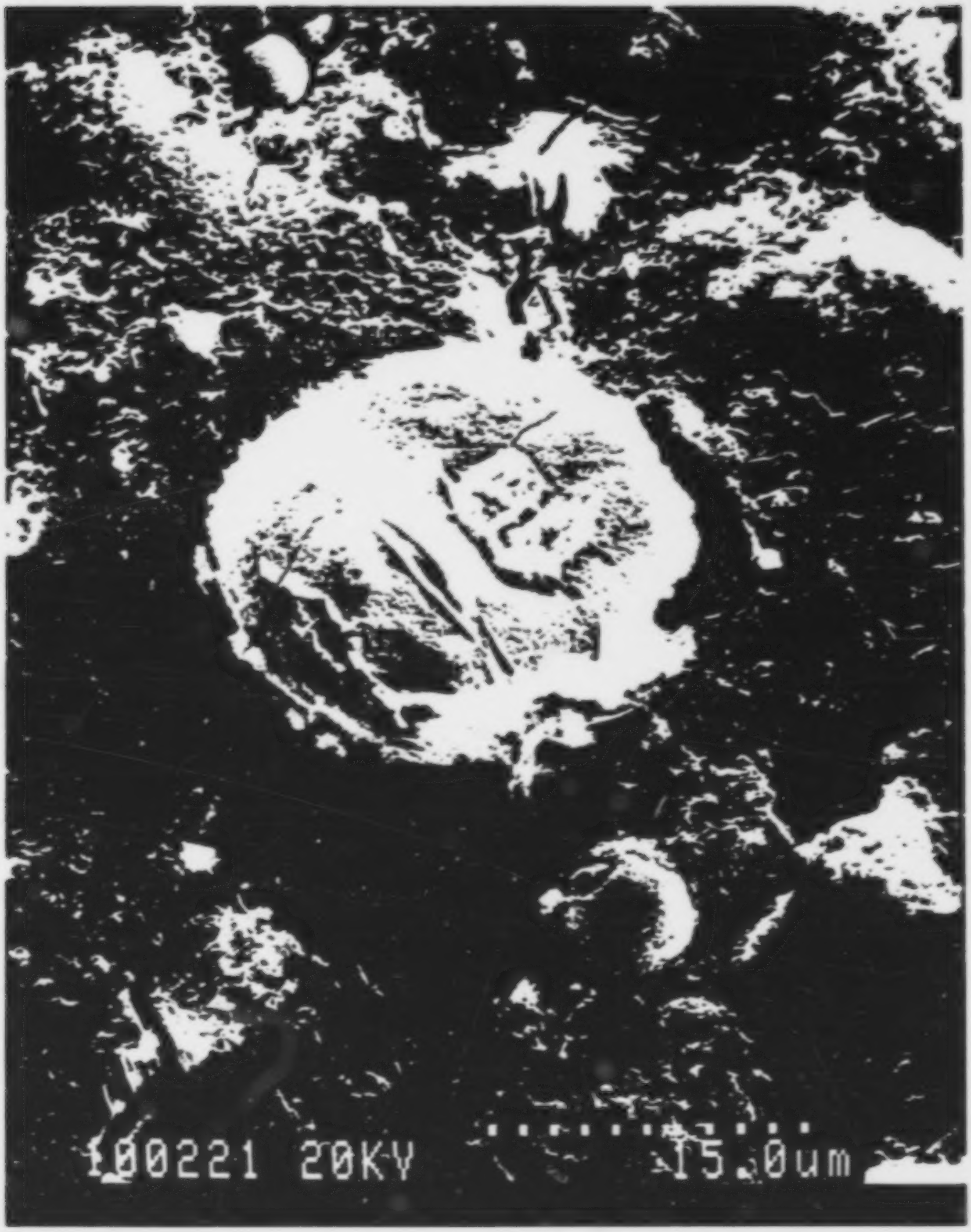
100221 20KV 15.0um

Figure 34. Large FAP with high Si and Al content, almost totally consumed in the reaction with CH and water. Note smaller FAP with shell of hydrate below and to right.

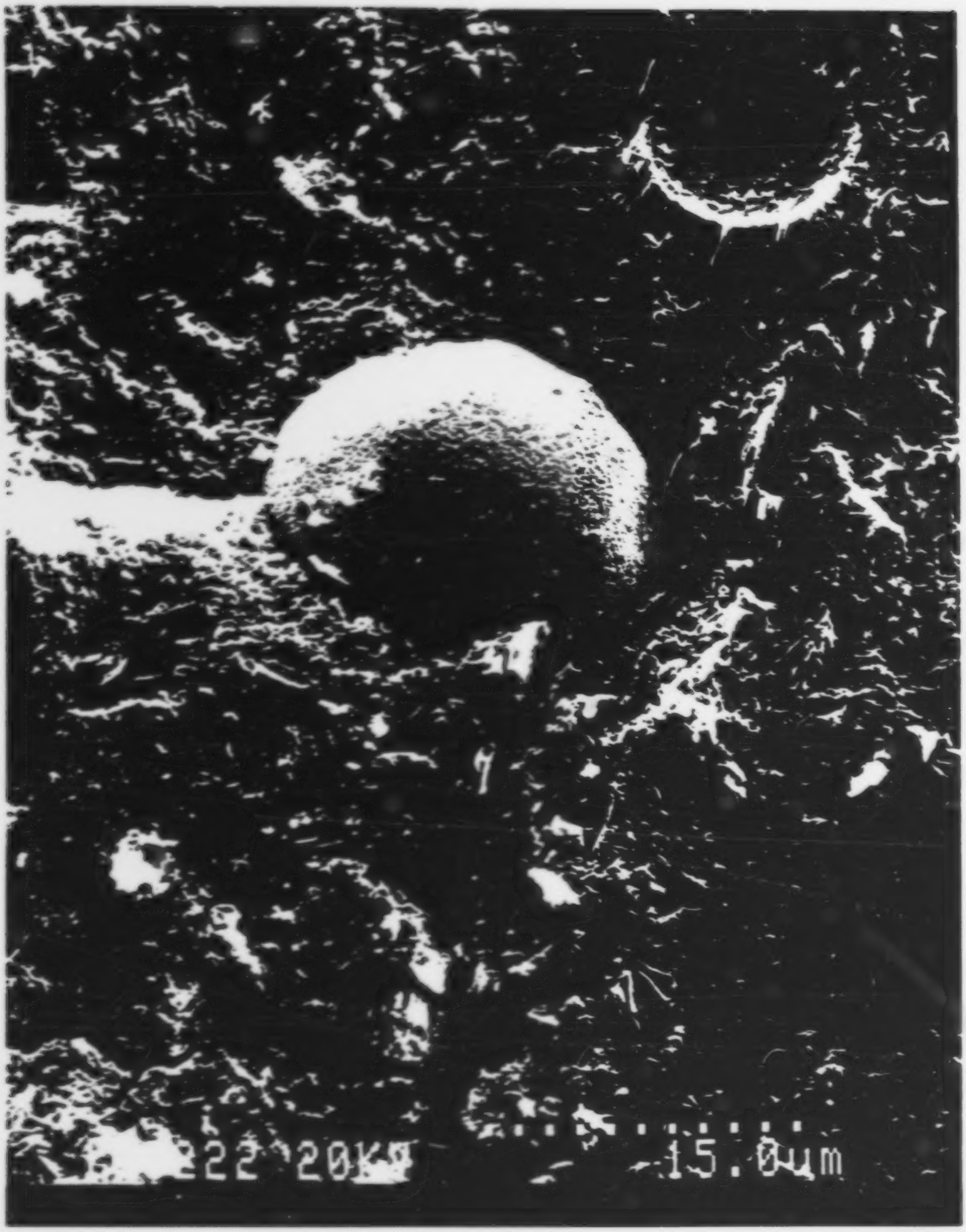
222 20KV
15.0µm

Figure 35. FAP with strongly oriented CH and shrinkage cracks.

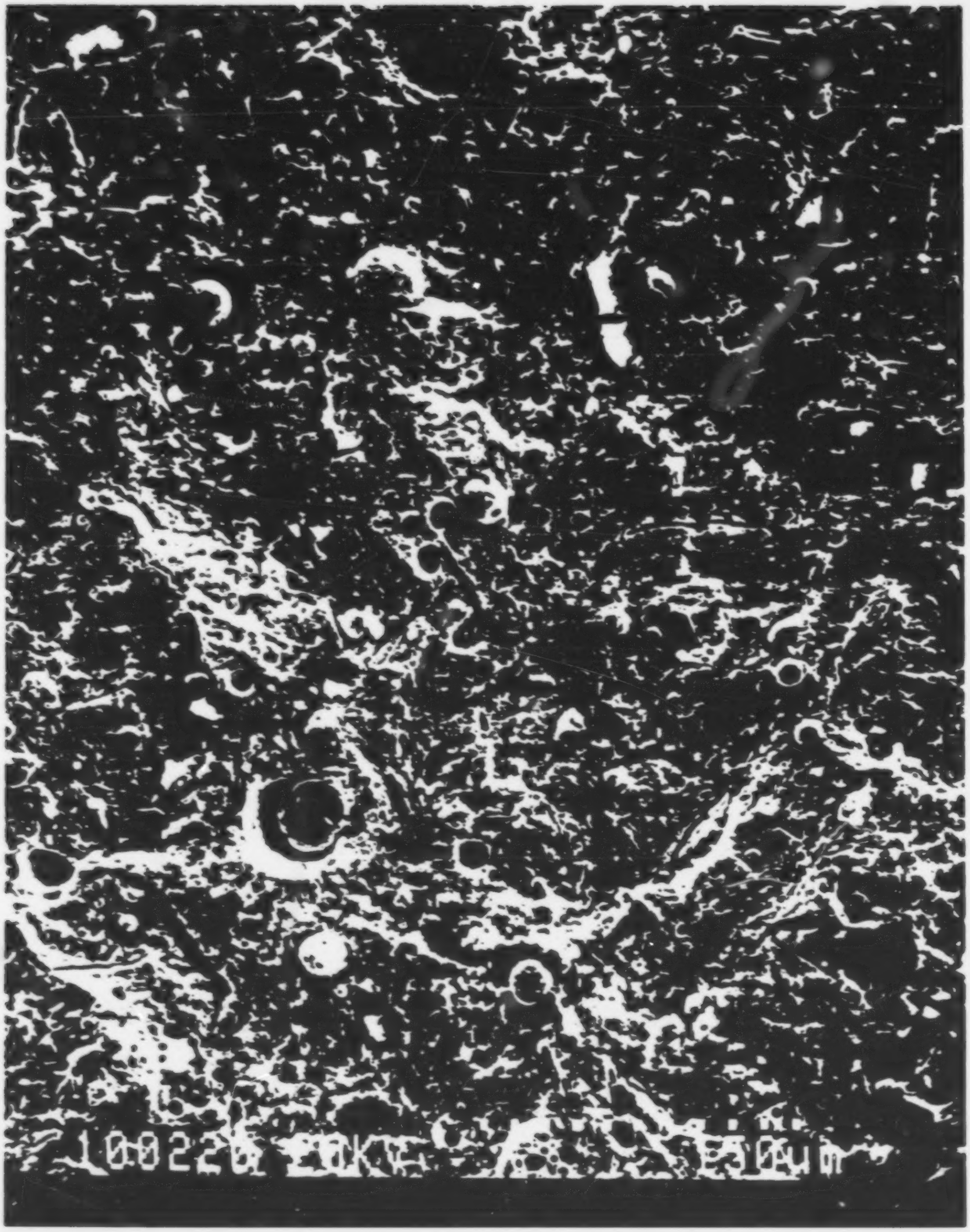
100220 20KV
10µm

Figure 36. Series D_1. General view of work area showing shrinkage cracks and Fly Ash particles.

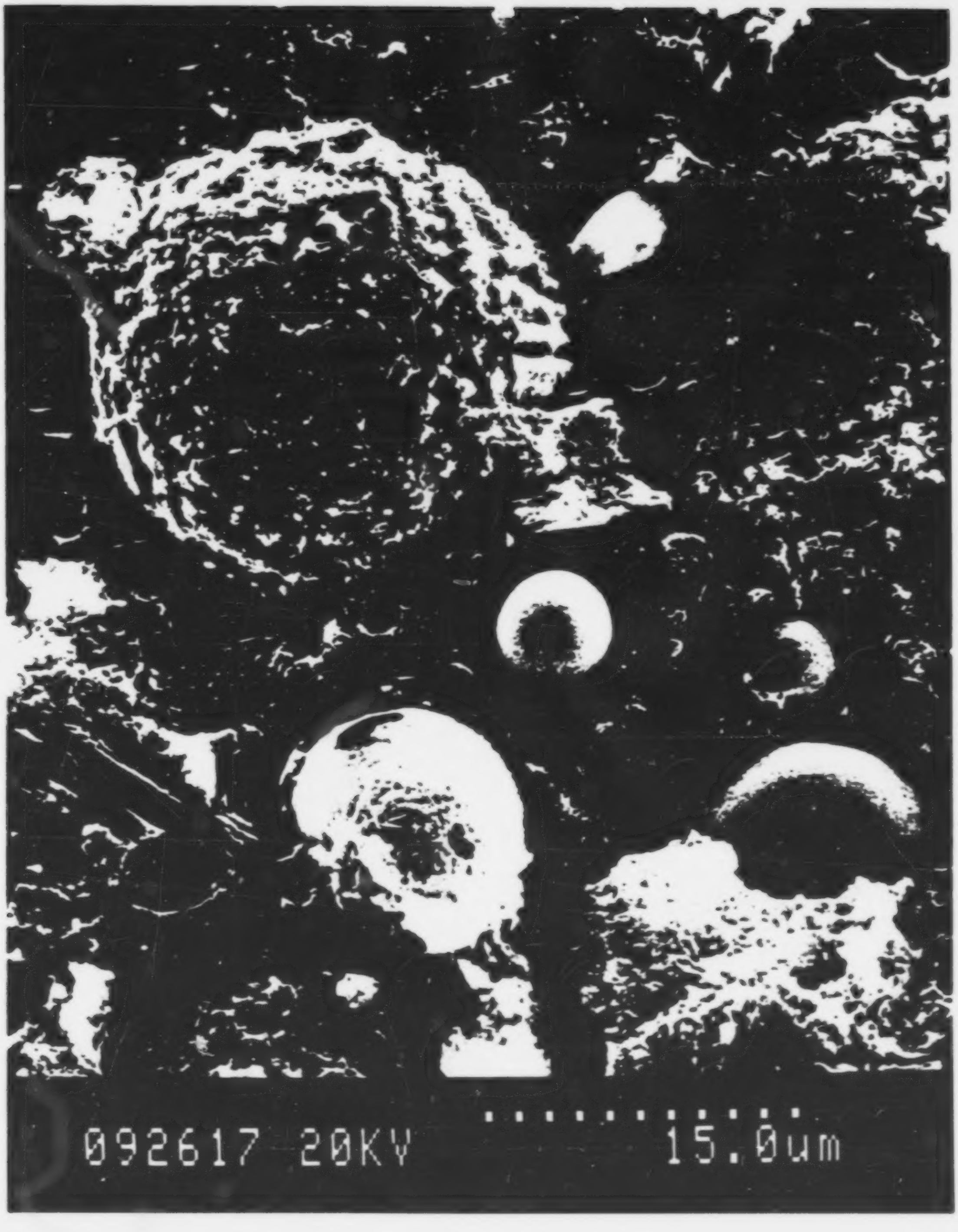
092617 20KV
15.0um

Figure 37. Typical Fe particle upper left with hollow Si-Al particle and 3 smooth particles which are almost pure Si.

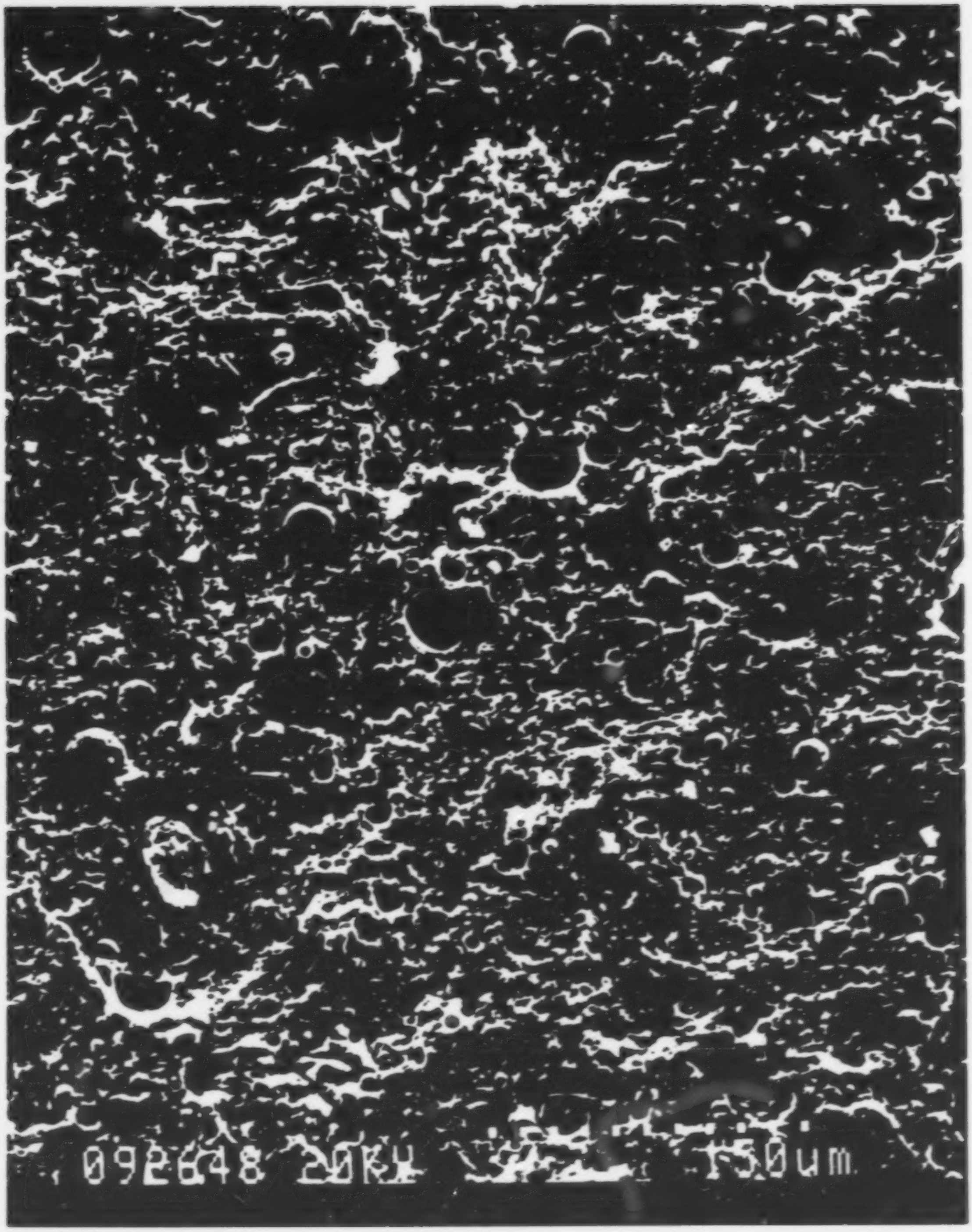
092648 20KV
150um

Figure 38. Series D_3. General view of work area showing rather more porous appearance relative to series D_1 - Figure 36.

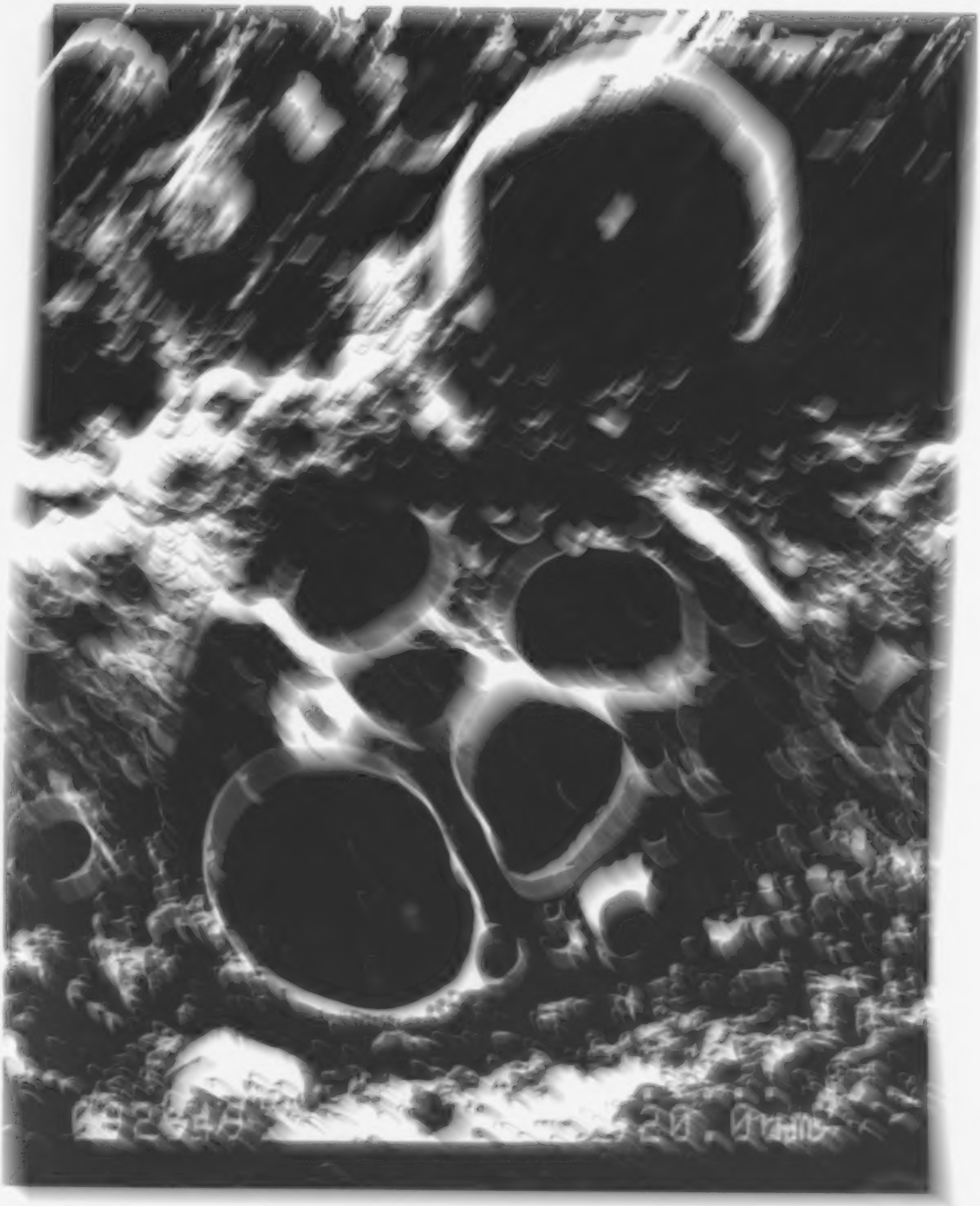
092648
20.0µm

Figure [illegible]. Nylon [illegible] split by fracture plane showing isolated internal [illegible]

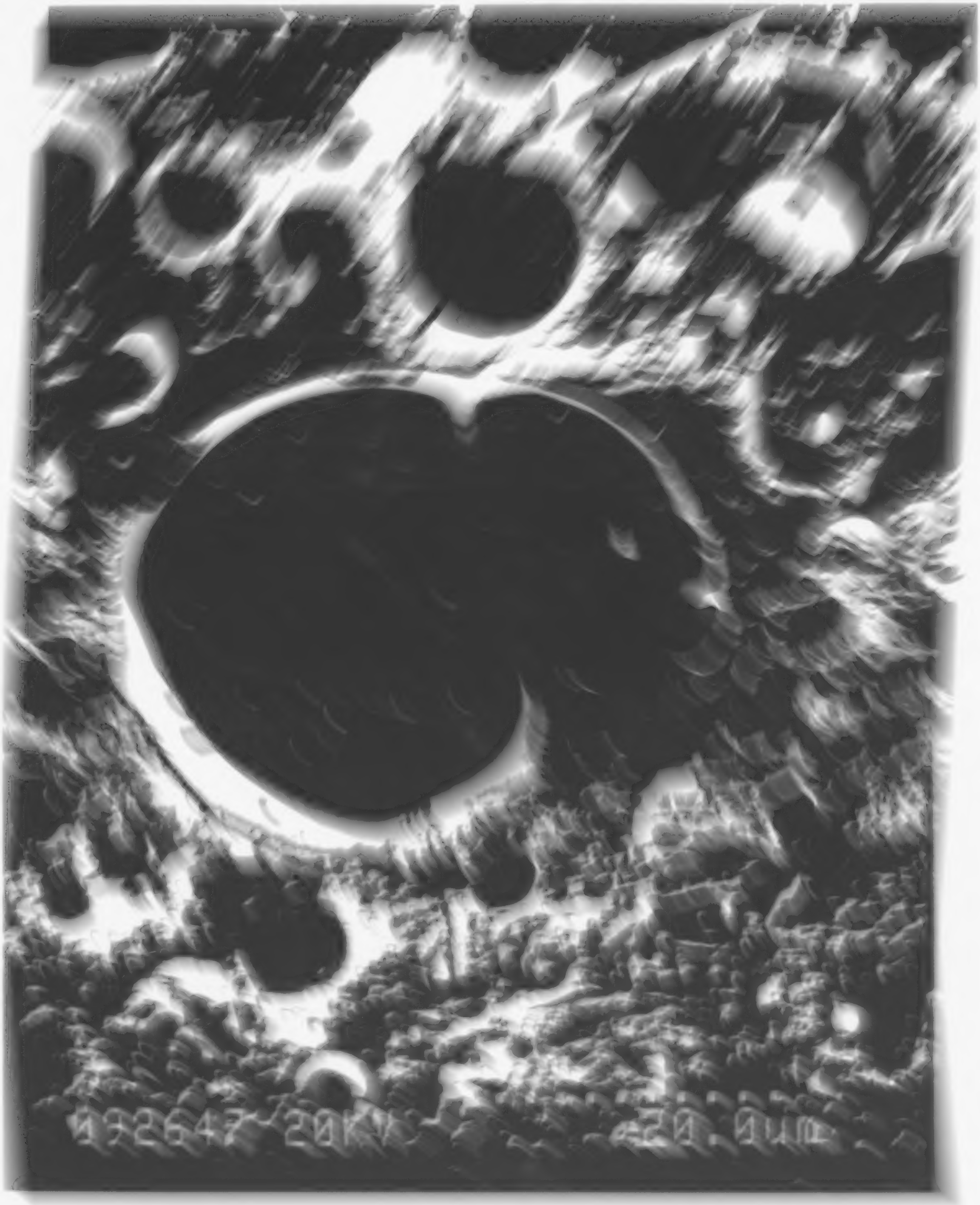
092647 20KV 20.0um

[illegible]

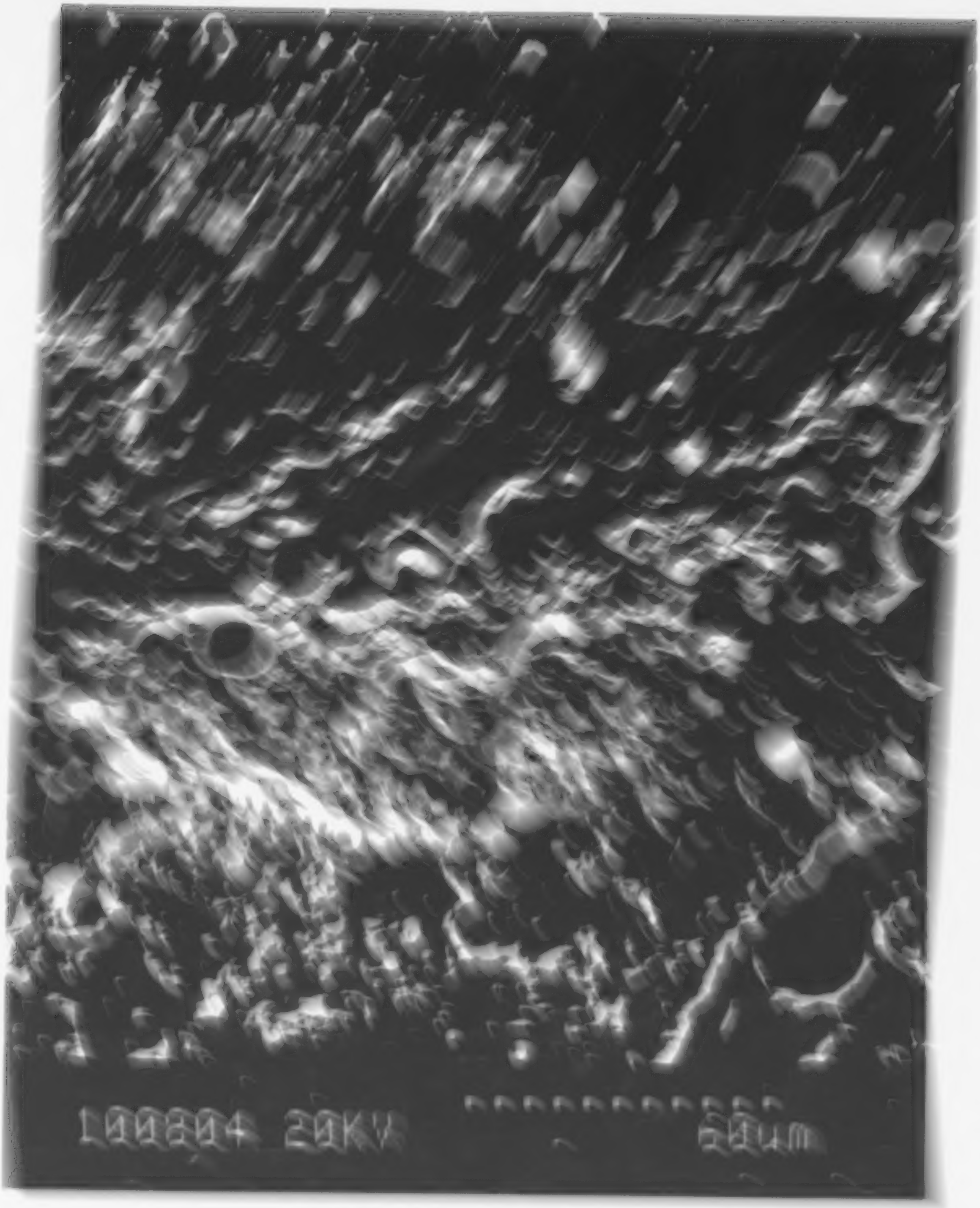
100804 20KV
50um

Figure 41. Series 3. General view of mesh area. Note relatively porous matrix.

100207 20KV
15.0um

[illegible]

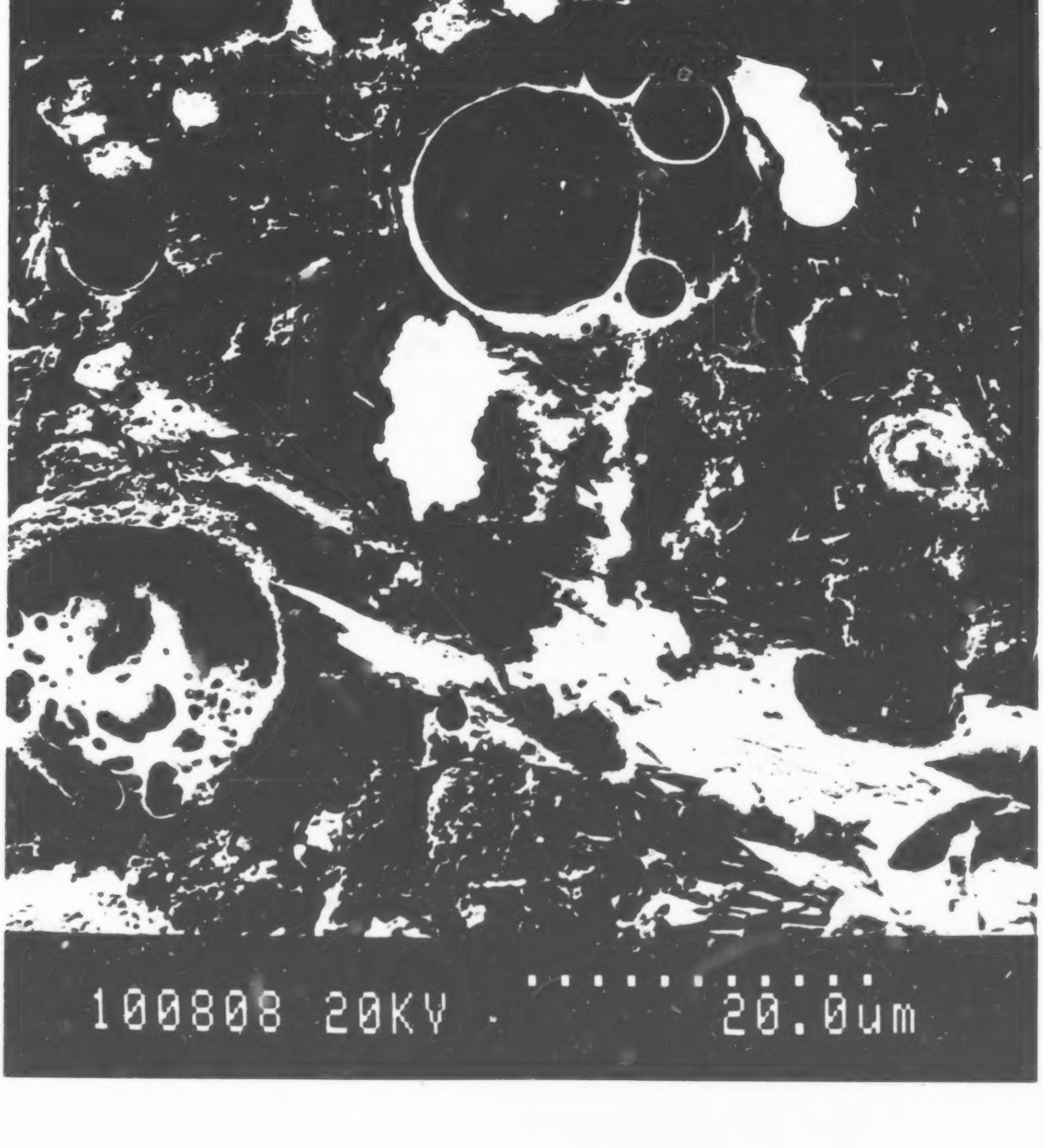
100808 20KV
20.0um

Figure 43. Hollow FAP's with porous matrix and Calcium Hydroxide sheets.

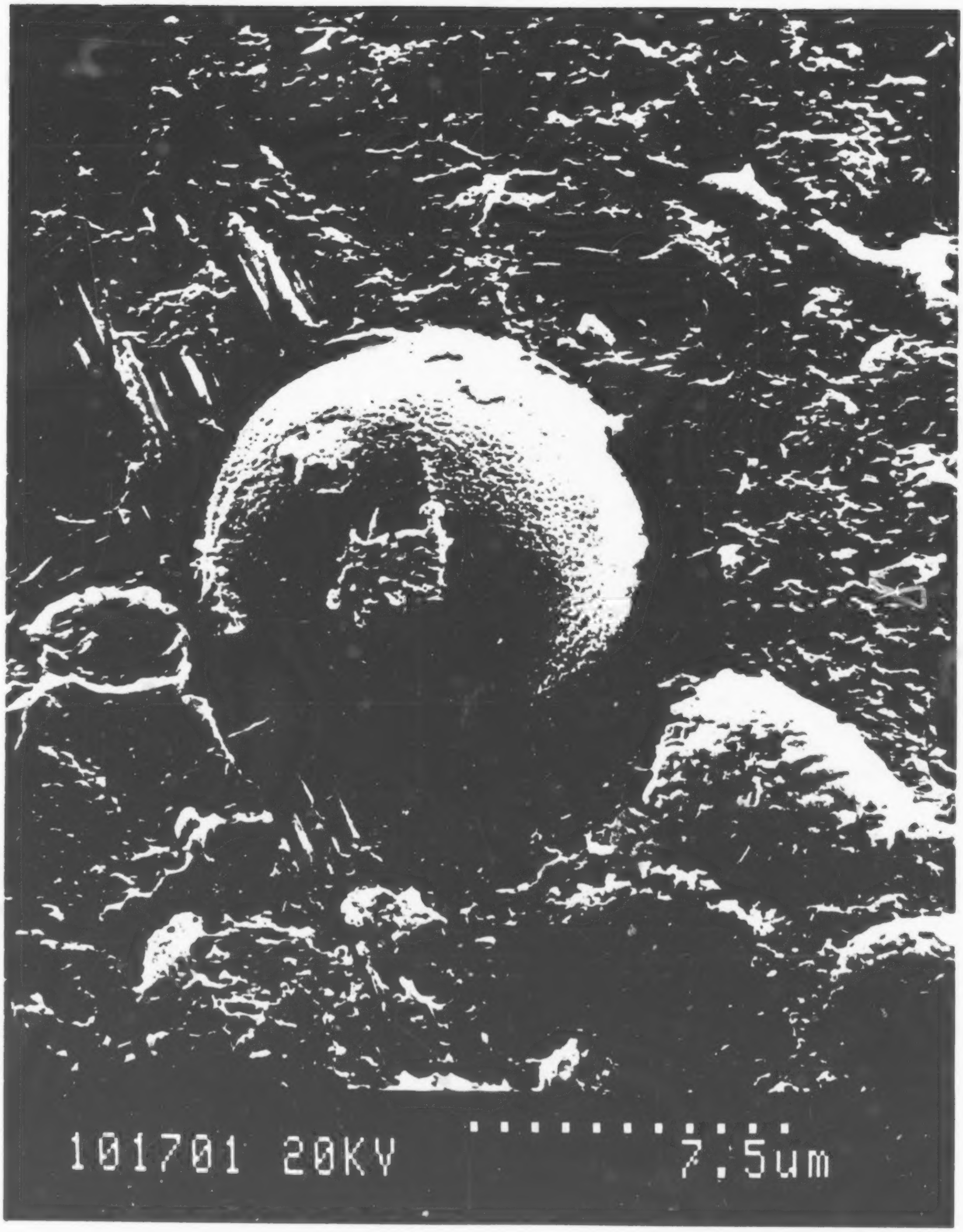
101701 20KV
7.5um

Figure 44. Siliceous FAP about 10 μm diameter with hydrate shell about 1 μm thick and diagonally oriented sheets of Calcium Hydroxide.

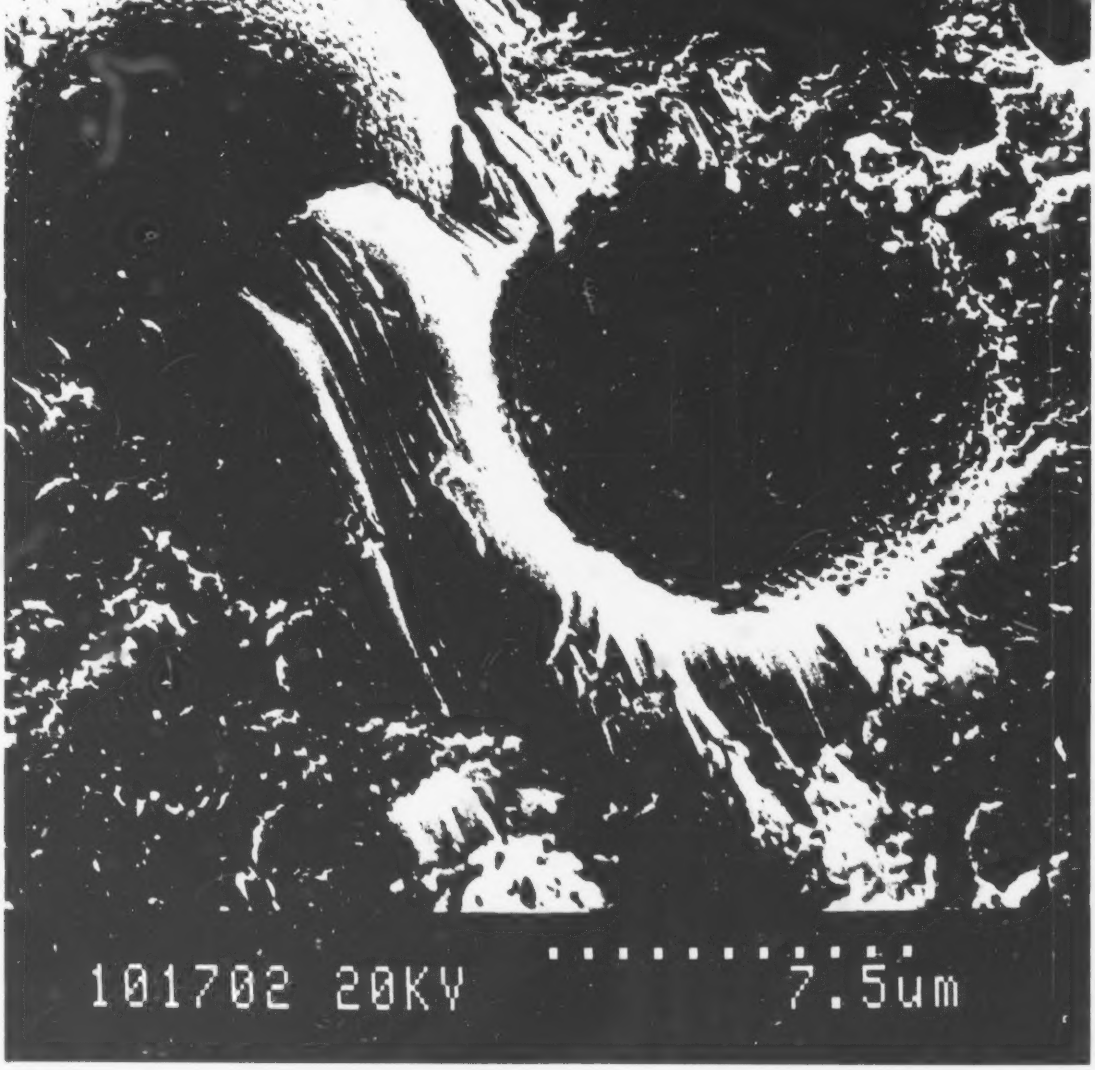
101702 20KV
7.5um

Figure 45. Strongly oriented CH matrix around socket with two siliceous FAP particles.

5. DISCUSSION AND CONCLUSIONS

5.1 General.

All of the concrete tested in this program was prepared with a degree of perfection which is unattainable in commercial concrete. It is clear that unavoidable defects in commercial concrete will have significant impact on the rate and magnitude of water vapour, gas and liquid water transport through concrete. Typical construction defects include: cavities due to incomplete compaction; thermally induced cracks; shrinkage cracks; bleeding cavities; slip forming cracks; and fissures at interfaces with reinforcing steel.

Additionally, aging effects [Ref. 15, 16] give rise to changes in pore size distribution, generally in the direction of increased permeability.

An important part of an appreciation of permeability in reactor buildings is an evaluation of the impact on permeability of unavoidable construction defects and fissurisation and changes of pore size distribution which result from service conditions.

5.2 Tentative Conclusions

5.2.1 Future work should be directed to defining the main performance criteria and devising field tests for evaluating concrete as placed in the actual structure.

5.2.2 The degree of prestress has a significant influence on permeance of concrete.

5.2.3 The water permeability test is easy to carry out and has potential as a quality assurance test.

5.2.4 The water vapour transmission test is useful for evaluating the effect of concrete mix parameters. It should be extended to include various pressure differences between source and sink. It is important to establish the equilibrium state of pore water at various distances from source and sink. The test is adaptable to evaluation of site concrete using drilled cores.

5.2.5 Gas diffusion tests as described by Figg [Ref. 9] show promise for quality assurance and for monitoring long range changes in the characteristics of concrete due to ageing.

5.2.6 Fly Ash appears to be a valuable substitute for Portland cement. Blastfurnace slag offers no advantage as a cement substitute.

5.2.7 SEM and EDX techniques are useful at the Research and Development stage but do not appear to be useful for characterising concrete as placed in the field.

5.2.8 The most important mix parameter affecting permeability is the total water demand. Water:cement ratio and strength have relatively little influence on permeability though they have obvious structural implications.

6. REFERENCES

1. Powers, T.C., Mann, H.M. and Copeland, L.E. The flow of water in hardened Portland cement paste. Highway Research Board, 309-323, 1959.

2. Loughborough, M.T. Permeability of concrete to air. Ontario Hydro Research Quarterly, 14-16, 1966.

3. Neville, A.M. Properties of concrete. Sir Isaac Pitman and Sons, Second Edition, 1972, p. 387.

4. Butler, J.E. The influence of pore pressure on concrete. Magazine of Conrete Research, Vol. 33, No. 114, March 1981, 3-17.

5. Ruettgers, A., Vidal, E.N. and Wing, S.P. An investigation of the permeability of mass concrete with particular reference to Boulder Dam. J. Amer. Concrete Institute, 382-416, 1935.

6. Mather, B., Callan, E.J., McCoy, E.E. and Carlson R.W. Permeability and triaxial tests of lean mass concrete. Vicksburg US Army Waterways Experimental Station, Technical Memorandum G-380, March 1954. (see also R.E. Davies. Same title. Berkeley, US Dept. of Army, 128, April 1950).

7. Griffin, D.F. and Henry, R.L. Integral sodium chloride effect on strength, water vapour transmission and efflorescence of concrete. J. Amer. Concrete Institute, 751-772, 1961.

8. Henry, R.L. and Korz, G.K. Water vapour transmission of concrete and of aggregates. U.S. Naval Engineering Laboratory, Port Hueneme, California, 1963.

9. Figg, J.M. Methods of measuring the air and water permeability of concrete. Magazine of Concrete Research, Vol. 25, No. 85, 213-219, Dec. 1973.

10. Rose, D.A. Water movement in unsaturated porous materials. RILEM Bulletin, Vol. 29, 119-123, Paris, Dec. 1965.

11. Feldman, R.F. The flow of helium into the Interlayer spaces of Hydrated Portland cement paste. Cement and Concrete Research, Vol. 1, No. 3, p. 285, May 1971.

12. Feldman, R.F. 3 papers on Helium inflow in cement paste. Cement and Concrete Research, Vol. 1, 285, Vol. 2, 123, Vol. 4, 1.

13. Lawrence, C.D. Private communication.

14. Leliavsky, S. Uplift in gravity dams. London, Constable and Co. Ltd. 267, 1958.

15. Garrett, W.S. and Campbell-Pitt, L.T. Tests on an experimental underground bulkhead for high pressures. J. of the S.A. Inst. of Min. and Metal. Sept. and October 1958.

16. Hunt, C.M., Tomes, L.A. and Blaine, R.L. Some effects of ageing on the surface area of cement paste. J. of Res. Nat. Bureau of Standards, Vol. 64A, No. 2, pp. 163-169.

17. Tomes, L.A., Hunt, C.M. and Blaine, R.L. Some factors affecting the surface area of Hydrated Portland cement as determined by Water-vapour and Nitrogen adsorption. J. of Res. N.B.S., Vol. 69, No. 6, pp. 357-364.

18. Powers, T.C. Properties of cement paste and concrete. 4th Int. Sym. Chem. Cem., Paper V-1, 5770613, Washington, 1960

19. Mills, R.H. Molecular sieve effect in concrete. Int. Sym. Chem. Cem., Vol. 111, 74-85, Tokyo, 1968.

20. Powers, T.C. The chemistry of cement. (Ed. H.F.W. Taylor) Academic Press, 1972, pp. 391-416.

21. Ramachandran, V.S., Feldman, R.F. and Beaudoin, J.J. Concrete Science Heyden, 1981, pp. 1-24.

22. Mills, R.H. Factors influencing cessation of hydration in water cured cement pastes. Structures of Portland Cement Paste and Concrete SR 90, Highway Res. Board, pp. 406-424.

23. Midgley, H.G. and Illston, J.M. Some comments on the microstructure of cement pastes. Cement and Concrete Research, Vol. 13, No. 12, pp. 197-206, March 1983.

24. Powers, T.C., Copeland, L.E. and Mann, H.M. Capillary continuity and discontinuity in cement paste. Journal of the Portland Cement Association Research and Development Laboratories, Vol. 1, No. 2, 38-48 (PCA Bulletin 110), May 1959.

25. Fagerlund, G. On the capillarity of concrete. Nordic Concrete Research VI, Oslo 1982.

26. Carman, P.C. Permeability of saturated sands, soils and clays, J. Agri. Sci. 29, 262 (1939).

27. McMillan, F.R. and Lyse I, Some permeability studies of concrete, Journal of the American Concrete Institute, Proceedings, Vol. 26, 101-142, Dec. 1928.

28. Haynes, J.M. Stereological analysis of pore structure, RILEM Journal, Vol. 6, No. 33, 175-179, May-June 1973.

29. Powers, T.C. and Brownyard, T.L. Studies of physical properties of hardened Portland cement paste. J.A.C.I. Vol. 18, No. 5, 596-602, Nov. 1947.

30. Pihlajavaara, S.E. Notes on the drying of concrete. State Inst. for Technical Research, Publication No. 100 Helsinki, 1965.

31. Mills, R.H. Dependence of drying shrinkage on dimensions of specimens. The Civil Engineer in South Africa, Nov. 1969, pp. 281-289.

32. Crank, J. The mathematics of diffusion. 2nd ed. p. 244. Clarendon Press, Oxford 1975.

APPENDIX A

Volume Distribution of Phases in Concrete

The entire quality spectrum of structural concrete is determined by mixing water W between 120 and 240 Kgm^{-3} and water:cement ratio, w_o between 0.28 and 0.75. Taking the density of anhydrous Portland cement = 3220 Kgm^{-3}, we obtain extreme values of cement paste content as follows.

		Mass Kgm^{-3}		Volume lm^{-3}			
Strength (MPa)	w_o	W	C	Water	Cement	Paste	Aggregate
90	0.28	250	857	240	266	506	494
20	0.75	120	160	120	50	170	830

In practice, for concrete in the strength range 30 to 50 MPa, w_o varies between 0.45 and 0.6 and W varies between 160 and 200 Kgm^{-3}, the aggregate volume varies between 660 and 770 lm^{-3}, the paste content between 340 and 230 lm^{-3} and initial porosity between 0.16 and 0.20.

When water reacts chemically with unit mass of Portland cement the amount of combined water is $w_m^o = 0.253$ and its volume is that of unit mass of Portland cement + 0.2530 mass of water - chemical shrinkage. The chemical shrinkage has been found to be $\Delta V = 0.2584 \times$ the volume of chemically combined water.

We may compute for completely hydrated cement:

For arbitrary volume		For 1 m^3 of hydrate	
Mass	Volume	Mass Kg	Volume l
1.000	0.3106	2007	623
0.253	0.1876	508	377
1.253	0.4982	2515	1000

In nature, cement is never completely hydrated and the ultimate degree of hydration may be determined [Ref. 22] by the empirical relationship

$$\alpha^* = \frac{1.031\ w_o}{0.194 + w_o}$$

Thus, at ultimate hydration we compute

		Arbitrary Units	
(a)	For unit mass cement	Mass	Units
	Unhydrated cement	$1-\alpha^*$	$\frac{1}{3.22}(1-\alpha^*)$
	Hydrated cement	$1.253\alpha^*$	$\frac{1}{2.515}(1.253\alpha^*)$
	Evaporable water	$w_o + 0.0654\alpha^*$	$w_o + 0.0654\alpha^*$
	TOTALS	$1 + w_o + 0.0654\alpha^*$	$\frac{1}{3.22} + w_o$

(b)	For $1m^3$ of cement paste	Mass	Volume 1
	Unhydrated cement	$\frac{3220(1-\alpha^*)}{1 + 3.22\ w_o}$	$\frac{1000(1-\alpha^*)}{1 + 3.22w_o}$
	Hydrated cement	$\frac{4036\alpha^*}{1 + 3.22w_o}$	$\frac{1604\alpha^*}{1 + 3.22w_o}$
	Evaporable water	$\frac{3220w_o + 604\alpha^*}{1 + 3.22w_o}$	$\frac{3220w_o + 604\alpha^*}{1 + 3.22w_o}$
	TOTALS	$\frac{3220(1+w_o) + 202\alpha^*}{1 + 3.22w_o}$	1000

Considering now 1 m^3 of paste and following Powers [Ref. 20, page 402] we assume the surface area of hydrated cement = 210 m^2g^{-1} and therefore, for $1m^3$:

$$\text{Surface area } \sigma = \frac{210{,}000\ .\ 4036\alpha^*}{1 + 3.22w_o}$$

$$= \frac{848 \times 10^6\alpha^*}{1 + 3.22w_o}\ m^{-1}$$

The monolayer capacity, V_m is approximately 0.261 (mass of non-evaporable water) [Ref. 29].

$$\text{i.e.} \qquad V_m \simeq \frac{(0.261)(0.253)(3220)\alpha^*}{1 + 3.22w_o}$$

$$\simeq (638\alpha^*)/(1 + 3.22w_o)$$

The quantity of immobile water ≃ 3 V_n [Ref. 20]. This is sometimes called gel water. We define

$$V_{gel} = 3V_n = (1916\alpha^*)/(1 + 3.22w_0)$$

The capillary water = the total evaporable water − the gel water

$$V_{cap} = (3.220w_0 - 1310\alpha^*)/(1 + 3.22w_0)$$

Three parameters are used in the Powers and Kozeny-Carman models for permeation through concrete:

Pore Ratio, $\quad \epsilon = \frac{V_{gel} + V_{cap}}{1000}$

$$= (3.220w_0 + 0.606\alpha^*)/(1 + 3.22w_0)$$

Effective pore space, $\epsilon_e = V_{cap}/1000$

$$= (3.22w_0 - 1.310\alpha^*)/(1 + 3.22w_0)$$

Surface area, $\quad \sigma = (8420\alpha^*)/(1 + 3.22w_0)$

Concrete

For concrete the values of ϵ, ϵ_e and σ are adjusted by multiplying the above values for paste by the volume ratio of cement paste in the concrete.

For example, suppose we have concrete with $W = 200\ \mathrm{Kgm^{-3}}$ and $w_0 = 0.5$.

We compute $C = 400\ \mathrm{Kgm^{-3}}$

$$V_c = \frac{400}{3.22} = 124.22\ l$$

$$W = \quad 200.00\ l$$

$$\text{TOTAL} = \quad 324.22\ l$$

The factor is 0.324.

Further, $\alpha = 0.54$

$\epsilon = 0.266$

$\epsilon_e = 0.059$

$\sigma = 78 \times 10^{-6}\ m^{-1}$

Sources of error. It is likely that the gel water is highly compressed and, contrary to our assumption, has a specific volume <1.

Estimation of Water Permeability of Concrete

At the time of final set of concrete water surrounds the solid phases - cement and aggregates - and the void spaces it occupies are interconnected. When hydration takes place the new solid, ≈ 1.6 x the volume of anhydrous cement, occupies space partly within the original grain boundaries of cement and partly in water-filled space between these boundaries. As hydration proceeds capillary pores become partially, or completely filled with reaction products and some pores become discontinuous.

After terminal hydration is reached, a self-[illegible]

For the present study it was decided to examine relationships developed by Powers [Ref. 18] and Carman [Ref. 26] in each case, permeability being thought of as a function of porosity at the age of interest.

Thus the first obstacle was to decide which of the infinite range of porosities to use. It was decided to invoke the concept of terminal hydration as a function of water cement ratio [Ref. 22] and use the relationships developed in Appendix A.

For a cement paste having water cement ratio = 0.5 the mass and volume ratios follow:

(a) For raw mix

	Mass per m^3	Volume m^3/m^3
Portland cement	1233.7	383.1
Mixing water	616.8	616.8

(b) At terminal hydration

For cement paste having w_0 = 0.5 at terminal hydration, α_t = 0.74, and we have:

	Mass Kg per m^3 paste	Volume (litres)
Unhydrated PC	[illegible]	[illegible]
Hydrated PC	[illegible]	[illegible]
Gel water	[illegible]	[illegible]
Capillary water	263	263

[illegible] = 241 x 10^{6} m^2/m^3

Hydraulic mean radius = 2.03 x 10^{6} μm

For (a) high workability concrete with a high water demand aggregate W = 240 Kgm^{-3} and C = 480 Kgm^{-3}.

For (b) low workability with low water demand aggregate W = 180 Kgm^{-3} and C = 280 Kgm^{-3}. The relevant parameters follow for concrete

Raw Mix	Mix (a)	Mix (b)
Cement Kgm^{-3}	490	280
Water Kgm^{-3}	280	180
In Hardened Concrete		
Gel Water Kgm^{-3}	70	51
Capillary Water Kgm^{-3}	202	70
[illegible]	[illegible]	[illegible]
[illegible]	[illegible]	[illegible]

It should be noted that both of these mixes would have approximately the same strength.

The permeabilities according to Powers (Eqn. 53), Kozeny-Carman (Eqn. 52) and modified Kozeny-Carman follow:

Equation	Calculated Permeability Coefficient m^{-2} Cement Paste	Mix (a)	Mix (b)
$K^{*} = 1.8 \times 10^{-12} \left(\frac{e^2}{1-e} \exp - 4.19 \left(\frac{1-e}{e}\right)\right)$	2.3×10^{-15}	73.2×10^{-26}	850.5×10^{-32}
$K^{**} = \frac{9.81 \times 10^6}{k_1 S^2} \cdot \frac{\epsilon_e^3}{(1-\epsilon_e)^2}$	1.4×10^{-12}	4.4×10^{-13}	3.3×10^{-13}
$K^{***} = \frac{9.81 \times 10^6 \cdot \epsilon^{1.1}}{k_1 S^2} \cdot \frac{\epsilon_e^3}{(1-\epsilon_e)^2}$	4.1×10^{-13}	3.1×10^{-14}	1.1×10^{-14}

We note that the Powers model K* displays undue sensitivity to mix design parameters.

APPENDIX C

DRYING AS A DIFFUSION CONTROLLED PROCESS

From Fick's second law, the equation for one-dimensional diffusion may be written

$$\frac{\partial c}{\partial t} = \frac{\partial}{\partial x} D \frac{\partial c}{\partial x} \qquad (1)$$

where c is the concentration at distance x from the exposed surface at time t, and D is the diffusion coefficient.

[illegible] loss of moisture on five [illegible] relative humidity on [illegible] of exposed surface, at [illegible]

$$1-a^* = [illegible] (1 - 2\pi^{-1/2} [illegible] - \exp z^2 \operatorname{erfc} z); \text{ where} \qquad (2)$$

1-a* = average moisture loss expressed as a fraction of the moisture loss at time of exposure = ∞;
h = the change of moisture concentration at the surface per unit concentration
$z^2 = h^2 D^* t$
D* = average coefficient of diffusivity; and
t = time of exposure to the drying influence.

The error function:

$$\operatorname{erfc} z = \frac{2}{\pi} \int_0^z e^{-u^2} du; \text{ where}$$

$\operatorname{erfc} \xi = 2/\pi \ \exp(-\xi^2)/4$; where
$\xi = x/2(D^* t)^{1/2}$; and
x = linear dimension representing flow path.

In most porous solids of high surface area D* is not constant and the solution to equation (1) is often based on assumptions that D* is a function of moisture concentration, length of drainage path, or time. In the case of cement paste, the structure itself changes with time due to hydration and drying, both processes taking place simultaneously. Since moisture concentration varies with the size of members, structure and hence the diffusion characteristics, also vary with dimensions. The cement paste system is therefore not amenable to rigorous mathematical treatment and an empirical approach must be adopted. We may note, in passing, that the co-ordinates: x representing distance from source or sink, and t enter into formal solutions of equation (1) in the combination

$$\frac{t}{x^2} \text{ or } \frac{t}{x}$$

Pihlajavaara had published curves in which u* is shown as a function of the Fourier number $Fo = kt/l^2$ where k is the effective diffusion coefficient. In some solutions he has assumed that the diffusion coefficient varies linearly and, in others, exponentially with the instantaneous value of moisture content u.

From a study of the literature there seemed little point in seeking an unattainable degree of precision in the theoretical approach and a suitable experimental technique was sought.

From Crank (32) equation 10.154 for a specimen drying from one side only we have:

$$\frac{M_T}{M_\infty} = \frac{4}{\pi^{1/2}} \left(\frac{DT}{2d}\right)^{1/2} \quad ; \text{ where}$$

M_T = the mass of water lost at time t
M_∞ = the mass of evaporable water
t = time; and
d = thickness of specimens

In this programme case, t is measured in hours, the thickness = 0.041 m and M_T and M_∞ are expressed as mass percentages and the above equation reduces to:

$$(D^*)^{1/2} = \frac{M_T}{60t^{1/2}} \cdot \frac{d}{M_\infty} \cdot \frac{\pi^{1/2}}{2}$$

$$= 147.7 \times 10^{-3} \left(\frac{b^* d}{M_\infty}\right) \quad ; \text{ where}$$

$$b^* = \frac{M_T}{t^{1/2}} = \text{the initial slope of the } M_T \text{ vs } t^{1/2} \text{ curve.}$$

MASS TRANSFER OF WATER VAPOUR UNDER STEADY STATE CONDTIIONS

The pseudo D'Arays coefficient is defined as:

$$K = \frac{Q}{Ai} \text{ ms}^{-1} \text{ where}$$

Q = the rate of mass transfer in $m^3 s^{-1}$
A = the cross sectional area in m^2
i = the dimensionless hydraulic gradient.

In our case the mass transfer $\frac{dw}{dt}$ is measured in grams per hour, therefore

$$Q = \frac{dw}{dw} \text{ x } \frac{1}{3.6 \text{ x } 10^9} \frac{m^3}{s}$$

$$= \frac{dw}{dt} \text{ x } 277.8 \text{ x } 10^{-12} \frac{m^3}{s}$$

APPENDIX D

PERMEABILITY OF CONCRETE BIBLIOGRAPHY

S.A. Abo-El-Enein, H. El-Didamony and H.A. Amer. Effect of admixtures on the physico-chemical properties of sea water cement: consistency and permeability studies. Tonindustrie Zeitung, 9, 641-643, 1981.

M. Akira and W. Hiroshi. A Hygrometer which utilizes an Anodic Oxide film of aluminum. Paper 40, Electric Hygrometry, 391-404.

American Society for Testing and Materials. Designation D1434-66. Standard methods of test for gas transmission rate of plastic film and sheeting. Annual Book of ASTM Standards. Part 27. Philadelphia, 461-473, 1973.

American Society for Testing and Materials. ANSI/ASTM C355-64. Standard test method for water vapour transmission of thick materials. Annual Book of ASTM Standards, Part 18, Philadelphia, 116-123, 1979.

Annais do Coloquio Permeabilidade do Concreto a Agua (Permeability of concrete to water). Instituto de Pesqnisas Technologicas, Instituto Brasileiro do Concreto, Sao Paul, 1971.

G. Ballivy, P.C. Aitcin, P. Niemants and P. Pinsonnault. Permeability of cement-based grouts and concrete. Geologists. Montreal, 1982.

H. Beck. Ermittellung der Gasdurchlassigkeit von fonerfesten Steinen. Archiv fur das Eisenhuttenwesen, 31, No. 10, 607-616, 1960.

L.E. Berlin, Yu. M. Butt and V.M. Kolhasov. Kinetics of the formation of the structural porosity of cement. Chem. Abstr. 68, 98362, 1968.

J. Binka and J. Novotny, A method of determining the medium gas permeability of concrete. Stavivo, 57, 197-198, 1979.

R.L. Blaine. A simplified air permeability fineness apparatus. ASTM Bull. No. 123, 51-55, 1943.

N. Bondarenko and S. Nerpin. Rheological properties of water in porous media. RILEM Bulletin, No. 29, 13-16, Dec. 1965.

J. Bonzel. The effect of cement, water/cement ratio, age and storage on the water-permeability of concrete. Beton 16, Nr 9, 379-383, 1966μ Beton 16, Nr 10, 417-421, 1966.

T. Bourbie and J. Walls. Pulse decay permeability analytical solution and experimental test. Society of Petroleum Engineers Journal, 719-721, 1982.

G. Brace, E. Balint and D.F. Orchard. The use of electrical resistance probes in tracking moisture permeation through concrete. University of New South Wales, Architecture and Building Research Laboratory, Report 7, Kensington, Australia, 1971.

British Standards Institution. Method 514A: Gas transmission rate ('permeability'). Methods of testing plastics BS 2782, Part 5, 318-322, 1970.

R.D. Browne, et.al. Concrete in the Oceans. Marine durability survey of the Tongue Sands Tower. Technical Report No. 5, 1980.

R.D. Browne and P.L. Domone. Permeability and fatigue properties of structural marine concrete at continental shelf depths. Underwater Construction Technology, Cardiff, 1975.

British Standard 4359. Part 2 1971. Methods for the determination of specific surface of powders. Part 2. Air Permeability Methods. May 1971.

J.E. Butler. The influence of pore pressure on concrete. Magazine of Concrete Research, Vol. 33, No. 114, March 1981, 3-17

R.W. Carlson and R.E. Davis. Discussion on the significance of pore pressures in hydraulic structures. Proceedings of the American Society of Civil Enginners. Vol. 74, 1532-1536, Nov. 1948.

P.C. Carman. Permeability of saturated sands, soils and clays, J. Agri. Sci. 29, 262 (1939).

D.A. Chapman. A study of the movement of water in and from concrete at elevated and non-uniform temperatures. Ph.D. Thesis, University of London, Jan. 1976.

L.C. Cheng and D.L. Katz. Diffusion of methane through concrete. American Concrete Institute, 75, No. 12, 673-679, 1978.

M. Collepardi, A. Marceialis and R. Turriziani. Penetration of Chloride ions into cement pastes. J. Amer. Ceramic Soc. 55, 534-535, 1972.

H.K. Cook. Permeability tests on lean mass concrete. Proceedings Amer. Soc. Test. Mat., 51, 1156-1165, 1951.

L.E. Copeland and R.H. Bragg. Self-desiccation in Portland cement pastes. Proc. Amer. Soc. for Testing Materials, No. 2-4, Feb. 1955 (PCA Bulletin 52).

L.E. Copeland and J.C. Hayes. The determination of non-evaporable water in hardened portland cement paste. Amer. Soc. Test. Mater. Bull., No. 194, 70, 1953.

Corps of Engineers. Permeability and Triaxial Tests of Lean Mass Concrete. Technical Memorandum No. 6-380, Waterways Experimental Station, Vicksburg, Miss. March 1954.

J.L. Costaz and J. Picant. Multiple-barrier concrete containment without steel liner. Int. Conf. on Experience in Design Construction and Operation of Pressure Vessels and Containments for Nuclear Reactors. York, 533-537, 1975.

C.L. Cutting, A.C. Jason and J.L. Wood. A Capacitance-resistance Hygrometer. J. Sci. Instr., 32, 423, 1955.

G.M. Darr and U. Ludwig. Determination of permeable porosity. RILEM Bulletin, Vol. 6, No. 33, 185-190, May-June 1973.

G.M. Darr and U. Ludwig. Determination of permeable porosity. Materiaux et Constructions, 6, Nr 33, 185-190, 1973.

R.E. Davies. Same title. Berkeley, US Dept. of Army, 128, April 1950).
N. Clayton. Fluid-pressure testing of concrete cylinders. Magazine of Concrete Research. Vol. 30, No. 102, 26-30, March 1978.

B. Derjaguin and S. Nerpin. Role of capillary and surface forces in moisture transfer in porous bodies. RILEM Bulletin, No. 27, 55-60, June 1965.

B. Derjaguin, S. Nerpin and N. Tchurayev. Effect of film transfer upon evaporation of liquids from capillaries. RILEM Bulletin, No. 29, 93-98, Dec. 1965.

B. Derjaguin and N. Zachavaeva. Physical properties of water and its mobility in fine pores. RILEM Bulletin, No. 27, 27-30, June 1965.

Deutsche Normen. Bestimmung der spezifischen Gasdurchlassigkeit fenerfester Stein. DIN 51088, 1963.

D.A. DeVries. Simultaneous transfer of heat and moisture in porous media. Transaction, Am. Geophys. Union, Vol. 39, No. 5, Oct. 1958.

M. Diamon, J. Akiba and R. Kondo. Thorugh pore size distribution and kinetics of carbonation reaction of Portland cement mortars. J. Amer. Cermaic Soc., 54, Nr 9, 423-438, 1971.

S. Diamond. A critical comparison of mercury porosimetry and capillary condensation pore size distributions of portland cement pastes. Cement Concr. Res. 1, 531, 1971.

S. Diamond and W.L. Dolch. Generalized log-normal distribution of pore sizes in hydrated cement paste. J. Coll. Interface Sci. 38, 234, 1972.

W.M. Dunagan and G.C. Ernst. A study of permeability of a few integrally water-proofed concretes. ASTM Proceedings, Vol. 34, 383-392, 1934.

H.T. Durgunoglu, S.S. Tezcan and Y. Acar. In situ permeability of fractured rock formation. Proceedings of the Tenth International Conference on Soil Mechanics and Foundation Engineering Stockholm, 15-19 June 1981, Edited A.A. Balkema, 1, 411-414, 1981.

L.I. Edel'man, D.S. Sominskii and N.V. Kopchikova. Pore size distribution in cement rocks. Colloid J. USSR. (Eng. Trans.), 23, 192, 1961.

D.H. Everett and J. Haynes. Capillary properties of some model pore systems. RILEM Bulletin, No. 27, 31-38, June 1965.

Fachbereich-Standard (DDR). Prufung des Erharteten Betons. Bestimmung der specifischen Gasdurchlassigkeit. TGL 21094/12, 1975.

G. Fagerlund. Determination of pore-size distribution from freezing-point depression. RILEM Bulletin, Vol. 6, No. 33, 227-231, May-June 1973.

G. Fagerlund. On the Capillarity of Concrete. Nordic Concrete Research VI, Oslo 1982.

R.F. Feldman. 3 papers on Helium inflow in cement paste. Cement and Concrete Research, Vol. 1, 285, Vol. 2, 123, Vol. 4, 1.

R.F. Feldman. The flow of helium into the interlayer spaces of hydrated portland cement paste. Cement and Concrete Research, Vol. 1, No. 3, p. 285, May 1971.

J.W. Figg. Methods of measuring the air and water permeability of concrete. Magazine of Concrete Research, Vol. 25, No. 85, 213-219, Dec. 1973.

J.A. Forrester and C.D. Lawrence. Self-diffusion of calcium ions in the equilibrium system calcium silicate hydrate - lime solution. J. Applied Chemistry, 11, 413-420, 1961.

H. Fritsche. Zum Einfuss des Gasruckes auf die spezifische Gasdurchlassigkeit von Beton nach TGL 21094/12 Betontechnik No. 1, 14-16, 1983.

W.R. Gardener. Mathematics of isothermal water conduction in unsaturated soils. Highway Res. Board, Special Rep. 40, Washington, D.C. 1958.

W.S. Garrett and L.T. Campbell-Pitt. Tests on an experimental underground bulkhead for high pressures. J. of the S.A. Inst. of Min. and Metal. Sept. and October 1958.

K. Gertis and W. Werner. Die Problematik der Porenanalyse von Baaustoffen. Deutscher Ausschuss fur Stahlbeton, 258, 1976.

O.E. Gjorv and K.E. Loland. Effect of air on the hydraulic conductivity of concrete. Durability of Building Materials and Components. ASTM 410-422, 1980.

O.E. Gjorv, O. Vennesland and A.H.S. El-Busaidy. Diffusion of dissolved oxygen through concrete. National Association of Corrosion Engineers, Corrosion 76 Houstor 17/2-17/3, 1976.

O.E. Gjorv, O. Vennesland and A.H.S. El-Busaidy. Electrical resistivity of concrete in the oceans. Offshore Technology Conference Houston, 581-584, 1977.

O.E. Gjorv and O. Vennesland. Diffusion of chloride ions from sea water into concrete. Cement and Concrete Research, 9, 229-238, 1979.

S.V. Giron and R.M. Martialay. Permeabilidad ol agna de tubos de hornigon (Water permeability in concrete piping liners). Instituto Eduardo Torroja Monografias No 344, Madrid, IET, 1977.

W.H. Glanville. The permeability of Portland cement concrete. Department of Scientific and Industrial Research, Building Research Technical Paper No. 3, 1931.

W.H. Glanville. The permeability of Portland cement concretes. London, H.M. Stationary Office, Building Research Technical Paper No. 3, 62, 1931.

C. Gohring and W. Riedel. Gasdurchlassigheit von Beton und ihr Einfluss auf die Korrosionsbetondigkeit in Salzlosungen WZ der Hockschule fur Architekfur und Bauwesen Weimar, 2, 143-149, 1974.

V.G. Golubov, E.N. Shcherbakov and O. Ya Bert. Effect of the stress condition of concrete under compression of its water permeability. Beton i Zhelezobeton, 23, No 10, 21-23, 1977.

S. Goto and D. Roy. The effect of w/c ratio and curing on the permeability of hardened cement paste. Cement and Concrete Research, 11, 575-579, 1981.

S. Goto and D.M. Roy. Diffusion of ions through hardened cement paste. Cement and Concrete Research, 11, 751-757, 1981.

D.F. Griffin and R.L. Henry. Integral sodium chloride effect on strength, water vapour transmission and efflorescence of concrete. J. Amer. Concrete Institute, 751-772, 1961.

A. Hanoar. Testing of concrete specimens for permeability at cryogenic temperatures. Mag. Concrete Research, 34, Nr 120, 155-162, 1982.

T.Z. Harmathy. Simultaneous moisture and heat transfer in porous systems with particular references to drying. Industrial and Engng. Chemistry Fundamentals, Vol. 8, 92-103, Feb. 1969. Amer. Chem. Soc.

L.F. Harza. Significance of pore pressure in hydraulic structures. Transactions of the American Society of Civil Engineers. Vol. 114, No. 2368, 193-214, 1949.

H.H. Haynes. Permeability of concrete in sea water. American Concrete Institute, Special Publication 65, 32-38, 1980.

H.H. Haynes and L.F. Kahn. Behaviour of 66 inch concrete spheres under short and long term hydrostatic loading. US Naval Civil Engineering Lab. TR R-774, 1972.

J.M. Haynes. Stereological analysis of pore structure, RILEM Journal, Vol. 6, No. 33, 175-179, 1973.

J.M. Haynes. Stereological analysis of pore structure, RILEM Bulletin, Vol. 6, No. 33, 175-179, May-June 1973.

J.M. Haynes. Pore size analysis according to the Kelvin equation. RILEM Bulletin, Vol. 6, No. 33, 209-213, May-June 1973.

R.L. Henry and G.K. Korz. Water vapour transmission of cocnrete and of aggreates. U.S. Naval Engineering Laboratory, Port Hueneme, California, 1963.

H.K. Hilsdorf. A method to estimate the water content of concrete shields. Nuclear Engineering and Design, Vol. 6, 251-263, 1967.

P. Hsieh et.al. A transient laboratory method for determining the hydraulic properties of tight rocks. International Journal of Rock Mechanics and Mining Science, 18, 245-258, 1981.

S. Hug. Beitrag zue klarung der permeations vorgauge in zementpasten und hochverdichteten zementkorpern Dissertation. Aachen, 1971.

B.P. Hughes, I.R.G. Lowe and J. Walker. The diffusion of water in concrete at temperatures between 50 and 95°C. British J. of Applied Physics, 17, 1545-1552, 1966.

C.M. Hunt, L.A. Tomes and R.L. Blaine. Some effects of ageing on the surface area of cement paste. J. of Res. Nat. Bureau of Standards, Vol. 64A, No. 2, pp. 163-169.

P. Huovinen. Air-permeability of concrete. Nordic Concrete Research 10.1-10.17, Oslo 1982.

G.W. Hyde and W.J. Smith. Permeability of cements and cement mortars. Journal of the Franklia Institute, Vol. 128, No. 3, 199-207, Sept. 1889.

S. Irmay. Theoretical models of flow through porous media. RILEM Bulletin, No. 29, 37-43, Dec. 1965.

D. Item. Etude de la capillarite des betons et mortier. These d'inginuer Docteur, Paris, 1967.

A. Jerglins. Air Leakage through Cracks in Concrete Elements. Nordic Concrete Research VI, Oslo 1982.

F.O. Jones and W.W. Owens. A laboratory study of low-permeability gas sands. Journal of Petroleum Technology, 163-1640, 1980.

M. Jung. Porosity and permeability of hydrated cement in concrete related to the concrete aggregate. Baustoffe Industrie, 13, No. 5, 154-157, 1970.

J.R. Keeton. Permeability studies of reinforced thin shell concrete. Technical report R-692, Naval Civil Engineering Laboratory, Port Hueneme, California, Aug. 1970.

A. Kjennerud. Permeability corrosion of mortar and water due to penetration of aggressive water. Nordisk Betong, 6, 21-26, 1974.

L.J. Klinkenberg. The permeability of porous media to liquids and gases. Drilling and Production Practice, 200-213, 1941.

C.E. Knot and R.C. Johnson. Permeability of grout seals surrounding thermoplastic well castings. Ground Water, 20, 415-419, 1982.

A.A. Langley. The air and water permeance of glass fibre reinforced concrete. Magazine of Concrete Research, Vol. 33, No. 114, 18-26, March 1981.

A.A. Langley. The air and water-vapour permeance of glass-fibre reinforced cement. Mag. Concrete Research, 33, No. 114, 18-26, 1981.

C.D. Lawrence. Private Communication.

C.D. Lawrence. Durability of concrete: molecular transport processes and test methods. Cement and Concrete Association. Technical Report No. 544, 1981.

F.M. Lea and R.W. Nurse. Permeability methods of fineness measurement: in Symposium on Particle Size Analysis. Suppl. to Trans. Inst. Chem. Eng., 25, 10 pp, 1947.

S. Leliavsky. Uplift in gravity dams. London, Constable and Co. Ltd. 267, 1958.

M. Levitt. The ISAT - a non-destructive tests for the durability of concrete. British J. of Non-destructive Testing. 106-112, 1971.

M.T. Loughborough. Permeability of concrete to air. Ontario hydro research quarterly, 14-16, 1966.

P.E.R. Lovelock. The laboratory measurement of soil and rock permeability. Institute of Geological Sciences, Water Supply Papers, Technical Communication, No. 2, London IGS, 1970.

Low flow low permeability measurements in largely impermeable rocks. Proceedings of the NEA/IAEA Workshop, 19-21 March 1979. Organised by OECD Nuclear Agency in cooperation with International Atomic Energy Agency, Paris OECD ISBN/ISSN 92-64-01955-3, 1979.

I.R.G. Lowe, B.P. Hughes and J. Walker. The diffusion of water in concrete at 30°C. Cement and Concrete Research, 1, 547-557, 1971.

U. Ludwig and H.E. Schwiete. Effect of open porosity on resistance of mortars and concretes to aggressive solutions. Baustoffind, 10, No. 9, 265-271, 1967.

A.W. Luikov. Heat and moisture transfer in capillary porous media. RILEM Bulletin, No. 29, 97-106, Dec. 1965.

H. Marion and G. Mahfouz. Design and construction of the Ekofisk artificial island. Proc. Inst. Civil Engineers, 56, 497-511, 1974.

A. Markestad. An investigation of concrete in regard to permeability problems and factors influencing the results of permeability tests. Forskningsinstituttet for Cement og Betong Ved Norges Tekniske Hogskole (Cement and Concrete Research Institute of Technology) Trondheim FCB, 1977.

C. Marle. Application of the methods of the thermodynamics of irreversible processus to the flow of a fluid through a porous medium. RILEM Bulletin, No. 29, 107-117, Dec. 1965.

B. Mather, E.J. Callan, E.E. McCoy and R.W. Carlson. Permeability and triaxial tests of lean mass concrete. Vicksburg US Army Waterways Experiment Station, Technical Memorandum G-380, March 1954. (See also

G. Matheron. Elements pour une theorie des milieux poreux. Masson et de Edileurs, 1967.

R.M. Martialay. Permeabilidad al aire del hurmigon (Permeability of air into Concrete). Insituto Eduardo Torroja de la Construccion ydel Cemento Monografias N 322 Madrid IET, 1975.

F.R. McMillan and I. Lyse. Some permeability studies of concrete. Journal of the American Concrete Institute. Proceedings, Vol. 26, 101-142, Dec. 1929.

P.K. Mehta and D. Manmohan. Pore size distribution and permeability of hardened cement pastes. 7th Congress Chemistry of Cement. Paris, 3, VII/1 = VII/5, 1980.

H.G. Midgley and J.M. Illston. Some comments on the microstructure of cement pastes. Cement and Concrete Research, Vol. 13, No. 12, pp. 197-206, March 1983.

R.H. Mills. Factors influencing Cessation of Hydration in Water cured cement pastes. Structure of Portland Cement Paste and Concrete SR 90, Highway Res. Board, pp. 406-424.

R.H. Mills. Curing of concrete at various depths from an exposed surface. Trans. S.A. Instn. Civ. Eng. 55-59, Dec. 1965.

R.H. Mills. Effects of water on dimensions, compressive strength and swelling pressure of hardened cement paste. Highway Res. Bd., Special Report No. 190, 84-111, Washington 1966.

R.H. Mills. Molecular sieve effect in concrete. Int. Sym. Chem. Cem., Vol. III, 74-85, Tokyo, 1968.

R. Munoz Martialay. Air permeability of concrete. RILEM/IUPAC Symposium Pore Structure and Properties of Materials Prague, E102-E121, 1973.

R. Munro. Permeability of hardened cement paste to water vapour. B.A.Sc. Thesis, University of Toronto, April 1982.

J. Murata. Studies on the permeability of concrete. RILEM Bulletin (Paris), No. 29, 47-54, Dec. 1965.

A.M. Neville. Properties of concrete. Sir Isaac Pitman and Sons, Second Edition, p. 387, 1972.

K. Niesel. Determination of the specific surface by measurement of permeability. RILEM Bulletin, Vol. 6, No. 33, 233-237, May-June 1973.

L-O. Nilsson. Moisture measurements in concrete by Hydrometric method. Studies in concrete techonology. Swedish Cement and Concrete Research Institute, Stockholm, Dec. 1979.

L.O. Nilsson. Hygroscopic moisture in concret - drying, measurement and related material properties. Report TVBM - 1003, 162 pp, Lund Sweden, 1980.

T. Nitta, Z. Terada and S. Hayakawa. Humidity-sensitive electrical conduction of $MgCr_4O_4$-TiO_2 porous ceramics. J.A. Ceram. Soc., Vol. 63, No. 5-6, 295-305.

B.K. Nyame and J.M. Illston. Capillary pore structure and permeability of concrete. 7th Int. Conf. Chem. Cem., Vol. III, VI - 181-186, Paris 1980.

B.K. Nyame and J.M. Illston. Capillary pore structure and permeability of hardened cement paste. 7th Congress Chemistry of Cement, Paris VI-181-VI-185, 1980.

B.K. Nyame and J.M. Illston. Relation between permeability and pore structure of hardened cement paste. Magazine of Concrete Research, No. 116, 139-146. Sept. 1981.

B.K. Nyame and J.M. Illston. Relationships between permeability and pore structure of hardened cement paste. Mag. Concrete Research, 33, No. 116, 139-146, 1981.

B. Ost and G.E. Monfore. Penetration of chloride into concrete. Journal of PCA R and D Laboratories, 8, 46-52, 1966.

A.M. Paillere and A. Attolou. Appareil de mesure de la permeabilite des betons et mortier hydraulique. Bull. Liason Labs Routiers, 43, 9-13, 1970.

L.J. Parrott, R.G. Patel and D.C. Killoh, Effect of age upon diffusion of hardened alite. Cement and Concrete Association DN/4043, 1982.

J.G. Patel, M.G. Hegde and J.C. Slattery. Further discussion of two-phase flow in porous media. AIChE Journal, 18, Nr 5, 1062-1063, 1972.

B. Perrin, J.C. Foures and R. Jayelas. Determination du coefficient de diffusion isothermie de l'humidite dans des materiaux de construction. Materiaux et Constructions, 16, 27-33, 1983.

J.R. Philip and D.A. DeVries. Moisture movement in porous materials under temperature gradients. Transactions, American Geophysical Union, Vol. 38, No. 2, 222-232, April 1957.

J.P. Philips. Physics of water movement in porous solids. Highway Res. Board, Special Rep. 40, Washington, D.C. 1958.

S.F. Pihlajavaara. Notes on the drying of concrete. The State Institute for Technical Research, Helsinki, 1963.

S.E. Pihlajavaara. Introductory bibliography for research on drying of concrete. State Institute for Technical Research, Laboratory of Concrete Technology. Duplicated, Second edition, Helsinki 1964.

S.E. Pihlajavaara and H. Paroll. On the correlation between permeability properties and strength of concrete. Cement and Concrete Research, 5, 321-328, 1975.

S.E. Pihlajavaara. Notes on the drying of concrete. The State Inst. for Technical Rewsearch, Publication No. 100, Helsinki, 1965.

T.C. Powers and T.L. Brownyard. Studies of physical properties of hardened Portland cement paste. J.A.C.I. Vol. 18, No. 5, 596-602, No.v 1947.

T.C. Powers, L.E. Copeland, J.C. Hayes and H.M. Mann. Permeability of Portland cement pastes. Journal of the American Concrete Institute. Proceedings, Vol. 51, No. 11, 285-300, Nov. 1954.

T.C. Powers. Hydraulic pressure in concrete. Proceedings of the American Society of Civil Engineers. Vol. 81, 1-7, 742, July 1955.

T.C. Powers, L.E. Copeland and H.M. Mann. Capillary continuity and discontunity in cement paste. Journal of the Portland Cement Association Research and Development Laboratories, Vol. 1, No. 2, 38-48 (PCA Bulletin 110), May 1959.

T.C. Powers, H.M. Mann and L.E. Copeland. The flow of water in hardened Portland cement paste. Highway Research Board, 309-323, 1959.

T.C. Powers. Properties of cement paste and concrete. 4th Int. Sym. Chem. Cem., Paper V-1, 577-613, Washington, 1960.

T.C. Powers. Physical properties of cement paste. Proc. 4th Int. Sym. Chem. Cem., p. 605, Washington 1960.

T.C. Powers. The chemistry of cement (Ed. H.F.W. Taylor) Academic Press 1972, pp. 399-400.

T.C. Powers, L.E. Copeland and H.M. Mann. Capillary continuity or discontinuity in cement pastes. Journal of PCA R and D Laboratories, 38-48, 1979.

R.D. Prangnell. The water pour resistivity of building materials. A literature survey. Materiaux et Constructions, 4, Nr 25, 399-405, 1971.

R.D. Prangnell. The water vapour resistivity of building materials. A literature survey. Materials and Structures: Research and Testing. Vol. 4, No. 24, 399-405, Nov.-Dec. 1971.

V.S. Ramachandran, R.F. Feldman and J.J. Beaudoin, Concrete Science Heyden 1981, 1-24.

J. Reekie and J. Aird. Flow of water through very narrow channels and attempts to measure thermomechanical effects in water. Nature, 156, 367-368, 1945.

P.W. Richards. A laboratory investigation into the water permeability and compressive strength properties of plain concrete produced with and without pulverised fuel ash as affected by curing temperature. Cement and Concrete Association ACT Project, 1982.

P.J. Ridgen. Flow of fluids through porous plugs and the measurement of specific surface. Nature, 157, 268, 1946.

RILEM Recommendation LC7. Water vapour permeability of autoclaved aerated concrete. Materials and Structures, 8, 1975.

RILEM, Tentative Recommendations. OPC 13.1 Tests for the penetration of water under pressure on hardened concrete. CPC 13.2 Tests for permeability of porous concrete. Materiaux et Constructions, 12, No. 69, 221-242, 1979.

A. Rio and R. Turriziani. The influence of superplasticizing agents on the penetration of aggressive ions into cement concretes and on their resistance to attack by aggressive solutions. Il Cemento 4, 171-181, 1981.

R.A. Robson. Mobility of water in porous media of high surface area. RILEM Bulletin, No. 27, June 1965, 65-72.

D.A. Rose. Water movement in porous materials, Part 1 - Isothermal vapour transfer. British Journal of Applied Physics, Vol. 14, 256-262, 1962.

D.A. Rose. Water movement in porous materials, Part 2 - The separation of the components of water movement. British Journal of Applied Physics, Vol. 14, 491-496, 1963.

D.A. Rose. Water movement in unsaturated porous materials. RILEM Bulletin, Vol. 29, 119-123, Paris, Dec. 1965.

P.P. Roussis, K. Tsimillis, C. Savvakis, S. Amarantos, N. Kanellopoulos and J.H. Petropoulos. On the measurement of desorption-permeation time lags. J. PhysE SCI Instrument, 13, 403-405, 1980.

A. Ruettgers, E.N. Vidal and S.P. Wing. An investigation of the permeability of mass concrete with particular reference to Boulder Dam. J. Amer. Concrete Institute, 382-416, 1935.

S.K. Sanyal, R.M. Pirnie, G.O. Ochen and S.S. Marsden. A novel liquid permeameter for measuring very low permeability. Society of Petroleum Engineers Journal, 206-210, 1972.

A.E. Scheidegger. The physics of flow through porous media. 2nd Edition, University of Toronto Press, 1960.

H.E. Schwiete and U. Ludwig. Uber die Bestummung der offerien Porositat im Zementstein. Tonindustrie Zeilung, 90 Nr12, 562-574, 1966.

H.E. Schwiete and L. Ludwig. Determination of open porosity in concrete. Tonind. Ztg. 90, 562, 1966, Chem. Abstr. 66, 48988, 1967.

H.E. Schwiete, H.J. Bohme and U. Ludwig. Measuring gas diffusion for the valuation of open porosity on mortars and concretes. Symposium Chemistry of Cement, Tokyo, III, 295-299, 1968.

K. Schwitzvebel and B.F. Jones. Mechanical strength development and permeability of fly ash-sludge-lime-mixtures. Morgantown Energy Technical Centre (Spec. Publ.) METC/SP US Dept. of Energy, 294-311, 1979.

F. Soeiro. Movement and equilibrium of moisture in porous media. RILEM Bulletin, No. 29, 137-143, Dec. 1965.

E.V. Sorensen and F. Radjy. Permeability of hardened cement paste in relation to pore structure. Hydraulic cement pastes, Sheffield, Cement and Concrete Association, 52-54, 1976.

J.W.T. Spinks, H.W. Baldwin and T. Thorvaldson, Tracer studies of diffusion in set Portland cement. Canadian J. of Technology, 30, 20-28, 1951.

H. Stamenkovic. High strength and water permeability of concrete as a function of surface area of aggregate. Materiaux et Constructions, 3, No. 14, 91-98, 1970.

R. Thenoz. Contribution a l'etude de la permeabilite des roches et de leur alterabilite - Application a des roches grantiques. These de doctorat es Science Toulouse, 1966.

L.A. Tomes, C.M. Hunt and R.L. Blaine. Some factors affecting the surface area of hydrated Portland cement as determined by water-vapour and nitrogen adsorption. J. of Res. N.B.S. Vol. 69, No. 6, 357-364.

K. Tuutti. The corrosion of steel in uncracked concrete - a hypothesis. Swedish Cement and Concrete Research Institute, 1977.

K. Tuutti. Corrosion of steel in concrete. Swedish Cement and Concrete Research Institute, 1982.

A. Tveit. Moisture and moisture transfer in porous materials. RILEM Bulletin, No. 29, 145-151, Dec. 1965.

I.L. Tyler and B. Erlin. A proposed simple test method for determining the permeability of concrete. Journal of PCA R and D Laboratories, 2-7, 1961.

W.O. Tynes. Laboratory investigation of 4 - half in aggregate concrete mixtures with high water-cement ratios. US Army Engineers Waterways Experiment Station Concrete Laboratory. Technical Report C-72-3, Vicksburg, Miss. 1972.

H. Ushiyama and S. Goto. Diffusion of various ions in hardened Portland cement paste. 6th Symposium Chemistry of Cement, Moscow, 1974.

O. Valenta. Durability of concrete. Materiau et Constructions, 3, Nr 17, 333-345, 1970.

G.J.R. van der Meulen and J. van Dijk. A permeability-testing apparatus for concrete. Mag. Concrete Research, 21, 121-123, 1969.

G. Verbeck. Pore structure. Amer. Soc. Test. Mater. Spec. Tech. Publ. 169-A, 211, 1966.

J. Vuorinen. One use of dilation factor and degree of saturation in testing concrete for frost resistance. Nordisk Betong, 37-64, 1970.

W.H. Wade and J.A. Wingrave. Macroscopic properties of fluids in micropores. RILEM/CNR Symposium Milan, 1983.

L.D. Wakeley and D.M. Roy. A method for testing the permeability between grout and rock. Cement and Concrete Research, 12, 533-534, 1982.

A.J. Watson and C.C. Oyeka. Oil permeability of hardened cement pastes and concretes. Mag. Concrete Research, 33, Nr 115, 85-95, 1981.

D.N. Winslow and S. Diamond. A mercury porosimetry study of the evolution of porosity in portland cement. J. Mater. 5, 564, 1970.

D. Whiting. Rapid measurment of the chloride permeability of concrete. Public Roads, 45, No. 3, 101-112, 1981.

L. Zagar. Die Grundlagen zur Ermittlung der Gasdurchlassigkeit von feuerfesten Baustoffen. Archiv fur des Eisenhuttenwesen, 26, 12, 777-782, 1955.

POOR

QUALITY

ORIGINAL